

ON-LINE PRECONCENTRATION TECHNIQUES FOR CAPILLARY
ELECTROPHORESIS OF DILUTE SAMPLES. FUNDAMENTAL
AND PRACTICAL STUDIES WITH PROTEINS
AND ENVIRONMENTAL POLLUTANTS

By

JIANYI CAI

Bachelor of Science

East China Institute of Chemical Technology

Shanghai, China

1985

Submitted to Faculty of the
Graduate College of the
Oklahoma State University
in partial fulfillment for
the requirements of
the degree of
MASTER OF SCIENCE
December, 1991


560210

1991

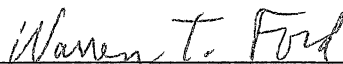
C1330

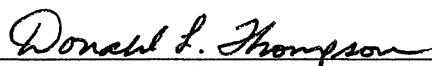
ON-LINE PRECONCENTRATION TECHNIQUES FOR CAPILLARY
ELECTROPHORESIS OF DILUTE SAMPLES. FUNDAMENTAL
AND PRACTICAL STUDIES WITH PROTEINS
AND ENVIRONMENTAL POLLUTANTS

Thesis Approved:

 Niall El Rami

Thesis Adviser

 Warren T. Ford

 Donald L. Thompson

 Thomas C. Collins

Dean of the Graduate College

ACKNOWLEDGEMENTS

I wish to express sincere appreciation to my advisor, Dr. Ziad El Rassi, for his guidance and advice throughout the course of my graduate studies. I would like to give special recognition to my committee members, Dr. Donald L. Thompson, Dr. Warren T. Ford for their support. Many thanks also go to Dr. Horacio Mottola for his suggestions and consultations.

My sincere gratitude also go to my colleagues and lab-mates, Maria Bacolod, Wassim Nashabeh, Jim Yu, Douglas Cheadle and Tim Smith, for their support and friendship, making life wonderful during the past two years. I would like to thank my fellow student, Chris Peeples, for his editorial assistance. Appreciation is also extended to all the faculty and staff members in the Department of Chemistry in Oklahoma State University for their kind assistance

I would say thanks to my husband for his understanding and support in all my endeavors. I also thank my parents, sisters and all the friends in China for their constant encouragement.

The financial supports from the Oklahoma Water Resources and Research Institute and in parts from the University Center of Water Research at OSU, from the College of Arts and Science-Dean Incentive Grant Program and from the University Center for Energy Research at OSU are gratefully acknowledged.

TABLE OF CONTENTS

Chapter	Page
I. BACKGROUND AND RATIONAL	1
Introduction	1
Historical	1
Merits of Capillary Electrophoresis (CE)	2
Instrumentation for Capillary Electrophoresis	3
Different Modes of Capillary Electrophoresis	5
Theory	9
Basic Principles of Capillary Zone Electrophoresis	9
Separation in MECC	16
Sample Introduction	20
Rationale of the Research	22
II. EVALUATION OF CZE WITH CHARGED POLLUTANTS. SEPARATION AND IONIZATION BEHAVIOR	24
Introduction	24
Experimental	25
Instruments	25
Reagents and Materials	25
Procedures	26
Results and Discussion	28
Determination of Strongly Basic Pollutants	28
Determination of Weakly Ionized Pollutants. Electrophoretic Determination of Dissociation Constants	33
Conclusions	40
III. MICELLAR ELECTROKINETIC CAPILLARY CHROMATOGRAPHY OF NEUTRAL SOLUTES WITH MICELLES OF ADJUSTABLE SURFACE CHARGE DENSITY. APPLICATIONS TO THE SEPARATION OF HERBICIDES	43
Introduction	43
Theory	44
Experimental	47
Instruments	47
Reagents and Materials	47
Procedures	48
Results and Discussion	51
Effect of Operational Parameters	51
Typical Separation	64

Chapter	Page
Limits of Detection	64
Conclusions	67
IV. ON-LINE PRECONCENTRATION OF NEURAL SPECIES WITH TANDEM OCTADECYL CAPILLARIES-CAPILLARY ZONE ELECTROPHORESIS	68
Introduction	68
Principles	69
Experimental	72
Instruments	72
Reagents and Materials	72
Procedures	73
Results and Discussion	75
Normal Detection Limits with CZE	75
Open-tubular Chromatography with Preconcentration Capillaries	75
Effect of Operational Parameters	77
Quantitative Determination of Dilute Samples with Octadecyl Preconcentration Capillaries	82
Conclusions	82
V. ON-LINE PRECONCENTRATION OF PROTEINS IN TANDEM METAL CHELATE CAPILLARIES-CAPILLARY ZONE ELECTROPHORESIS	84
Introduction	84
Principles	85
Experimental	86
Instruments	86
Reagents and Materials	86
Procedures	86
Results and Discussion	89
Electroosmotic Flow	89
Normal Detection Limit	90
Quantitative Determination of Dilute Samples with Metal-Chelate Preconcentration Capillaries	92
Effect of Operational Parameters	97
Preconcentration and Separation of Proteins	108
Restoration of Capillary Coating	108
Conclusions	110
BIBLIOGRAPHY	111

LIST OF TABLES

Table	Page
1. Maximum Wavelength and Molar Absorptivity	26
2. Limits of Detection	31
3. Determination of Dissociation Constant of Weak Bases	37
4. Determination of Dissociation Constant of p-Aminobenzoic acid	42
5. Limits of Detection	67
6. Electroosmotic Flow	89
7. Effect of Ionic Strength in the Debinding Electrolyte	100
8. Effect of pH of the Debinding Electrolyte	103
9. Sample Volume Introduced by Electromigration and Hydrodynamic Flow	105

LIST OF FIGURES

Figure	Page
1. Instrument Set-up for Capillary Electrophoresis	4
2. Schematic Representation of Electric Double Layer and Electroosmotic Flow (a), and Separation by CZE in Open Tubes (b)	13
3. Schematic Representation of MECC System (a), and Retention Window in MECC (b)	18
4. Spectra of Diquat (a), and Paraquat (b)	27
5. Typical Electropherogram Illustrating the Rapid Separation of Herbicides by CZE	29
6. Mobilities of Herbicides	30
7. Separation Efficiency of Herbicides	32
8. Determination of pK_a of Weak Bases (a), (b), and Selectivity of Aniline and p-Anisidine as a Function of pH (c)	38
9. Determination of pK_a of p-Aminobenzoic Acid	41
10. Schematic Representation of MECC System with Micelles of Adjustable Surface Charge	45
11. UV Spectra of the Herbicides	49
12. Effect of Borate Concentration on Retention Window and Peak Capacity	52
13. Effect of Borate Concentration on Retention Time of Herbicides	54
14. Effect of Borate Concentration on Efficiency and Selectivity	56
15. Effect of pH on Retention Window and Peak Capacity	58
16. Effect of pH on Retention Factor	59
17. Effect of pH on Efficiency and Selectivity	60

Figure	Page
18. Effect of Octylglucoside Concentration on Retention Window and Peak Capacity	62
19. Effect of Octylglucoside Concentration on Retention Factor	63
20. Effect of Octylglucoside Concentration on Efficiency and Selectivity	65
21. Typical Electropherogram Illustrating the Separation of Neutral Herbicides	66
22. Typical Shape of Langmuir Isotherm (a), and Schematic Illustration of the Idealized Structure of Octadecyl Preconcentration Capillary (b)	71
23. Retention Factor as a Function of Acetonitrile Concentration in Mobile Phase	76
24. Effect of Acetonitrile Concentration in Debinding Electrolyte	79
25. Effect of Feeding Time	80
26. Effect of Capillary Surface Concentration in Octadecyl Functions	81
27. Quantitative Determination of Dilute Samples with Octadecyl Preconcentration Capillaries	83
28. Schematic Illustration of the Idealized Structure of the Inner Surface of Metal Chelate Preconcentration Capillary	88
29. Normal Detection Limit of Albumin and Carbonic Anhydrase	91
30. Preconcentration of Dilute Human Albumin	93
31. Preconcentration of Dilute Carbonic Anhydrase.....	94
32. Typical Electropherograms Illustrating the Preconcentration of Human Albumin with Zn(II)-IDA-Cap-->CZE	95
33. Typical Electropherograms Illustrating the Preconcentration of Carbonic Anhydrase with Zn(II)-IDA-Cap-->CZE	96
34. Effect of Capillary Design on the Effectiveness of On-line Preconcentration with Zn(II)-IDA-Cap-->CZE	98
35. Effect of the Concentration of the Competing Agent in the Debinding Electrolyte	99
36. Effect of Ionic Strength in Binding (a), and Debinding (b) Electrolytes	101

Figure	Page
37. Comparison of Sample Introduction by Hydrodynamic and Electromigration Modes	104
38. Effect of Feeding Time on the Amount of Solute Accumulated	106
39. Preconcentration and Subsequent Separation with Tandem Zn(II)-IDA-Cap-->CZE	107
40. Restoration of Capillaries After Prolonged Use	109

NOMENCLATURE

I.S.	internal standard
u_{eo}	velocity of the electroosmotic flow
v	migration velocity
ζ	zeta potential
ζ_0	zeta potential of the solute
μ_{eo}	coefficient for electroosmotic flow
μ_e	electrophoretic mobility
μ	total mobility
t_r	retention time
ϵ	dielectric constant of the running electrolyte; molar absorptivity
η	viscosity of the solution
E	electric field strength
V	potential drop across the capillary
L	total length of the capillary
l	length of the capillary between the injection end and the detection point
v_e	sample volume introduced by electromigration
v_h	sample volume introduced by hydrodynamic flow
v	sample volume introduced
Q_e	amount of sample introduced by electromigration
Q_h	amount of sample introduced by hydrodynamic flow
Q	amount of sample introduced
t_i	injection time

r	inner radius of the capillary
C	concentration of sample
v_h	average hydrodynamic velocity
ρ	solution density
g	gravitational force constant
Δh	difference in height between the two ends of the capillary
R_s	resolution
N	number of theoretical plates
D	diffusion coefficient of solute
$W_{1/2}$	width of the peak at half maximum
Δv	difference in zone velocities
\bar{v}	average zone velocity
v_e	electrophoretic velocity
v_{eo}	electroosmotic flow
$\Delta\mu_e$	difference in electrophoretic mobilities of two adjacent solutes
$\bar{\mu}_e$	average electrophoretic mobility
μ_{mc}	net mobility of the micellar pseudostationary phase
$\mu_{mc,e}$	electrophoretic mobility of micelles
k'	retention factor
t_r	retention time of a retained species
t_o	retention time of an unretained marker
t_{mc}	retention time of micelle
α	relative retention or selectivity
n	peak capacity
K_{eq}	equilibrium constant
ρ_{mc}	overall charge density of the micelle

ρ_{complex}	charge density of the octylglucoside-borate complex
CE	capillary electrophoresis
CZE	capillary zone electrophoresis
MECC	micellar electrokinetic capillary electrophoresis
K_a , K_b	dissociation constant
μ_{ob}	electrophoretic mobility of the fully protonated species, BH^+ or BAH_2^+
μ_{oa}	electrophoretic mobility of the fully deprotonated species, A^- or BA^-
μ_o	electrophoretic mobility of the fully ionized species
λ_{max}	maximum wavelength
X_S , X_A	mole fractions of S, and A
K_x	distribution coefficient
θ	fractional coverage of sites by adsorbed solute
H	height equivalent to a theoretical plate

CHAPTER I

BACKGROUND AND RATIONALE

Introduction

Historical

High-performance capillary electrophoresis, using sophisticated instrumentation and advanced capillary technology, is becoming an important microseparation technique in the life science, biotechnology and environmental research.

Free zone electrophoresis in open tubes was first demonstrated by Hjerten in 1967 (1) in rotating tubes of 3 mm inner diameter. In 1974, Virtanen (2) reported the advantages of zone electrophoresis in glass tubes of smaller diameter (*i.e.* 200 μm to 500 μm). However, high separation efficiencies were not achieved due to the poor detection sensitivity and concomitantly large injection volumes. Twelve years later, Teflon tubes of 200 μm inner diameter were introduced, and separations with plate height of less than 10 μm were obtained (3). The breakthrough in capillary electrophoresis was brought about by Jorgenson and co-workers (4, 5), who provided the first demonstration of high separation efficiency with capillaries of inner diameter less than 100 μm . This work has become the landmark for capillary electrophoresis. Other workers followed the lead and demonstrated the high resolving power of capillary electrophoresis in important applications (6-12).

Another major development in HPCE was the pioneering work of Terabe (13) and co-workers, who introduced micellar electrokinetic capillary chromatography (MECC); a subdivision of capillary electrophoresis. MECC is an important approach to

the separation of neutral species under the influence of an electric field (14). The techniques of isoelectric focusing (15), isotachopheresis (16) and gel electrophoresis (17, 19) have also been adapted to capillary tubes.

Merits of Capillary Electrophoresis (CE)

Electrophoresis in capillaries offers numbers of advantages. The most important characteristic of capillary tubes is the effective heat dissipation. In electrophoresis, Joule heating, and consequently temperature gradient within the solution, is the major cause of zone broadening. With capillary tubes, the large ratio of inner surface area to volume greatly enhances the heat dissipation through the wall. Such heat removal can nearly eliminate convection so that as high as one million theoretical plates can be obtained (4). This also permits the use of very high electric field to speed the separations. The absence of a stationary phase eliminates the contribution of mass transfer resistances in the stationary phase to band broadening. Thus, the only significant factor that causes band spreading in CE is longitudinal molecular diffusion in the bulk of the running buffer.

Because very small sample volume is required, capillary electrophoresis is advantageous when the sample amount is extremely limited. The ultra-small sample requirement also permits the analysis of samples from single cells (20). Moreover, capillary electrophoresis is simple in instrumentation, since well developed detectors for high performance liquid chromatography (HPLC) can be used after slight modifications. Also, CE is readily automated, and the recently introduced prototype instruments by several companies have many of the features of HPLC instruments.

Compared with high performance liquid chromatography (HPLC), in which separation is due to the interaction of solutes with chromatographic surfaces, capillary electrophoresis exhibits different selectivities. Indeed, the elution orders in capillary

electrophoresis and HPLC often differ from each other. Hence, capillary electrophoresis can be a complementary tool to HPLC. The coupling of these two methods may become one of the most powerful approaches for the separation of multicomponent mixtures (21).

Instrumentation for Capillary Electrophoresis

Instrumental Set-Up. Figure 1 illustrates a typical instrument set-up for capillary electrophoresis. Essentially, a capillary electrophoresis instrument contains five basic elements: a high voltage source to apply a potential drop across the capillary, of *ca.* 20 to 30 kV; an on-column detector; two reservoirs for electrolytes with their corresponding electrodes; a capillary which spans between the reservoirs; a recorder, or an integrator or a computer. To prevent hydrodynamic flow, the two reservoirs are maintained at equal height. The capillaries are usually of fused-silica with inner diameters of 20 to 100 μm and lengths in the range of 10 to 100 cm. Optical windows for detection are made by burning out a short section of polyimide coating near one end of the capillary. In addition, the electrode at which high voltage is applied, is surrounded by a Plexiglass safety interlock box. When opening the box to gain access to the electrodes and reservoirs, the high voltage power supply is automatically turned off and in the meantime, its output is shorted to the ground through the voltage relay. Fig. 1 illustrates a typical instrument set-up for capillary electrophoresis.

Sample Introduction. Sample is introduced at one end of the capillary by either hydrodynamic flow or electromigration. In both cases, when the sample is being introduced, the electrolyte reservoir at the injection end is replaced by a sample reservoir. When hydrodynamic flow is used, a small pressure gradient between the inlet and outlet of the capillary is applied for a very short period of time to introduce a thin plug of sample. This can be made by gravity, vacuum, or pressure. When the sample

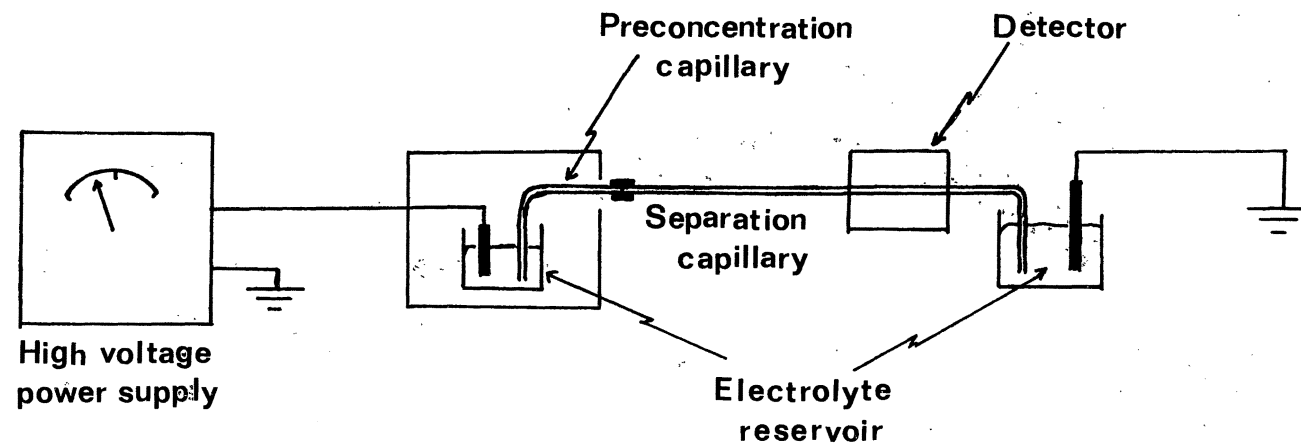


Figure 1. Instrument Set-up for Capillary Electrophoresis

is introduced by electromigration, the high voltage is applied for a few seconds to allow the electromigration of a small amount of sample into the capillary. Sample volumes are in the range of nanoliters.

Detection. Detection can be made by either on-line or off-line. The most widely used detection modes in capillary electrophoresis at present are UV absorption and fluorescence. Other detection methods have been described for capillary electrophoresis. These are laser-based detection (22), radioisotope detectors (23) and mass spectrometry (24). Derivatization (25, 26) and indirect detection method (27) are applied for non-fluorescent compounds. Each method has its own advantages and limitations. One of the major challenges in capillary electrophoresis is the detector sensitivity. In fact, the detection volumes are as small as 30 pL or less, depending on the inner diameter of the capillary. Because of the ultra-small sample volume involved, detectors must be of very high sensitivity. For example, the conductivity and refraction index detection modes, which can be used in HPLC, are not sufficiently sensitive for capillary electrophoresis.

Different Modes of Capillary Electrophoresis

The versatility and the wide scope of capillary electrophoresis stem from the various modes of separation, each of which has its own selectivity and utility.

Isotachophoresis. This mode is the electrophoretic analogue of displacement chromatography, whereby all sample components will migrate at the same velocity, a fact that gives the technique its name. In isotachophoresis, sample is introduced between a leading and terminating electrolyte. A steady-state condition is ultimately attained and each individual sample component is migrating as a "pure" band. Under this condition, each band is completely separated by sharp boundaries from the

preceding and the following zone. When sample cations are being determined, the leading electrolyte, which is on the side of the cathode, contains a cation of higher mobility than any of the sample cations, while the terminating electrolyte, which is on the side of the anode, contains a cation of lower mobility than any of the sample cations. In this mode, either cations or anions can be determined but not both at once.

Isoelectric Focusing. This mode involves separation of amphoteric compounds according to their isoelectric point. It has similarity to chromatofocusing. The key element to this method is the formation of a pH gradient in the separation channel, with low pH in the anodic reservoir and high pH at the cathodic reservoir. Sample components are thus focused in locations in the pH gradient that correspond to their isoelectric points and cease to move. Consequently, they are separated from each other. Isoelectric focusing in capillary tubes has been very useful for the separation of proteins according to their isoelectric points (28, 29).

Zone Electrophoresis. The most widely used mode is capillary zone electrophoresis (CZE). It is the electrophoretic analogue of elution chromatography. In this mode, sample is introduced as a narrow zone at one end of the capillary tube. Under the applied voltage, sample components migrate at different velocities and are eventually separated from each other as "pure zones". The separation is based on the difference in electrophoretic mobilities.

The most important application of CZE is in the area of proteins. Indeed, several reports have shown that peptides and proteins can be resolved by capillary zone electrophoresis (30-33). However, due to the solute-wall interactions, high molecular weight proteins can easily be adsorbed through multipoint attachment, which often leads to severe band broadening or no elution. This problem can be minimized by adjusting operational parameters such as the pH (30, 31, 34), salt concentration (35), and by the

capillary surface modification (10, 31, 36, 37). The capillary surface treatment, either by chemical reaction deactivation or by physical coating, is by far the most versatile. The high resolving power of CZE has been further exploited in the analysis of enzymatic digest of proteins with on-line MS. With this coupling, the analysis of protein digest can be routinely conducted (24, 38).

Gel Electrophoresis. This mode is the electrophoretic analogue of size exclusion chromatography. Gel columns provide unique selectivity. The porous nature of the gel, such as polyacrylamide, causes a sieving effect in which small molecules migrate faster than larger molecules. For this reason, this mode of capillary electrophoresis is also called gel-sieving electrophoresis.

Capillary gel electrophoresis with buffer containing sodium dodecyl sulfate (SDS) has been introduced for the separations of proteins and peptides (19). In the case of separation with SDS polyacrylamide gel electrophoresis (SDS-PAGE), proteins and peptides are denatured by SDS (39) and acquire approximately the same charge density, regardless of their identity. Because almost all the peptides bind with the negatively charged SDS in a constant weight ratio (1.4 g of SDS per gram of protein), the elution order is based solely on the molecular size or molecular weight. Non-denaturing polyacrylamide gel electrophoresis (PAGE) can also be employed whereby both size and charge will contribute to separation. It has been shown that PAGE is superior for the separation of large DNA fragments, RNAs, and synthetic oligonucleotides, since they have the same magnitude of charge/mass ratios. Besides the potential for sequencing, the gel columns provide a rapid means of purity assessment of synthesized oligonucleotides and micropreparative isolation of such species (18). PAGE can also be used with complexing agents to achieve unique selectivities. PAGE incorporated with inclusion compound, such as β -cyclodextrin, has been applied in the separation of D,L-dansylated amino acids (17).

Electrokinetic Chromatography. As mentioned earlier, separation in capillary electrophoresis can be modified by complexation. This approach led to the development of micellar electrokinetic capillary chromatography (MECC) (13, 40). The first separation with MECC was made with sodium dodecyl sulfate (SDS) micelles (13). The separations in MECC are based on the chromatographic partitioning between an aqueous phase and a micellar phase.

Surfactants other than SDS can also be used. These surfactants can either be anionic or cationic. Anionic surfactants are sodium decyl sulfate (41), sodium tetradecyl sulfate (42, 43), sodium N-lauroyl-N-methyltaurate (44), and sodium dodecyl salt (13, 42, 25, 45, 46). Cationic surfactants are dodecyltrimethylammonium salts (41), and cetyltrimethylammonium salts (41, 47). Changing anionic to cationic micellar system will change the sign of the zeta potential by the adsorption of the positively charged monomers to the solid surface, and reverse the electroosmotic flow (41).

MECC is particularly important in the analysis of neutral species and chiral racemates. Since neutral compounds have no electrophoretic mobility, they co-elute at the velocity of electroosmotic flow and can not be separated by CZE. Examples for the separations of neutral compounds with MECC are the separations of phenolic compounds and other substituted benzenes (13, 48), phenylthiohydantoin amino acids (45), metabolites of vitamin B₆ (46) and purines (49). Examples of the chiral separations with MECC are the separation of D, L-dansyl amino acids with Cu(II)-L-histidine complex (43) and Cu(II)-aspartame complex STS (50), the separation of D, L-dansyl-threonine, methionine and leucine with mixed micelles of didecyl-L-Ala and SDS (25). Many other chiral separations have been made with MECC (17, 51-55). MECC has also been applied to the separation of nucleotides, and oligonucleotides (49, 56). The selectivity of the separations can be manipulated by changing pH, or metal or surfactant concentrations.

MECC possesses several advantages over other separation techniques. When compared with HPLC, it has much higher separation efficiency, does not require the tedious procedures for the preparation of bonded stationary phases, and therefore is experimentally simple to use. While capillary zone electrophoresis is restricted to the separation of ionic compounds, MECC can be used effectively to separate neutral species. Moreover, MECC can provide enhanced selectivity for the separations of ionic compounds. However, it is limited by its elution range, the solute solubility, and the critical micelle concentration of surfactants.

Although it is also called MECC, polymer ions (57) and non-charged species such as crown-ethers, or charged species such as cyclodextrin derivatives (58) have also been employed as pseudostationary phases instead of micelles. In the case of polymer MECC, a polymer ion with an opposite charge to the analyte ions is added to the running buffer as the modifier. The analyte combines with polymer through ion-pair formation. The separation is based on the difference in the apparent velocities of the analytes, which is determined by the difference in the complex formation constants with the polymer ions. In the case of cyclodextrin MECC, cyclodextrin derivatives having ionizable groups served as pseudostationary phases. Solutes partition between the buffer phase and the interior of cyclodextrin derivatives. The separation is based on the inclusion-complex formation mechanism.

Theory

Since this study involved the investigation of some aspects of capillary zone electrophoresis (CZE) and micellar electrokinetic capillary chromatography (MECC), the theory part in this chapter will only cover CZE and MECC.

Basic Principles of Capillary Zone Electrophoresis

Electroosmosis. The most widely used capillaries are fused-silica tubes. Under normal aqueous conditions, the solid surface of fused-silica capillaries has an excess of negative charges, due to the ionization of the surface silanol groups. Electrolyte counterions form an electric double layer adjacent to the capillary walls. This electric double layer consists of a stagnant layer and a diffuse layer. As a result, a potential gradient arises at the solid-liquid interface. The potential across the layers is termed the zeta potential, ζ . When an electric field is applied, the electrostatic force will drive the cations in the diffuse layer to the cathode. Because the ions are solvated, the surrounding solvent will migrate to the cathode, and a bulk flow is formed, which is termed electroosmotic flow. The rate of this flow, u_{eo} , is determined primarily by the zeta potential. The relationship between ζ and u_{eo} can be expressed by the following equations (59):

$$\zeta = \frac{4\pi\eta\mu_{eo}}{\epsilon} \quad (1)$$

and

$$u_{eo} = \mu_{eo}E = \frac{\epsilon E \zeta}{4\pi\eta} \quad (2)$$

where μ_{eo} is the coefficient for electroosmotic flow, ϵ is the dielectric constant of the running buffer, η is the viscosity of the solution, and E is the electric field strength, which is given by

$$E = \frac{V}{L} \quad (3)$$

where V is the potential drop across the capillary, L is the total length of the capillary.

Because the flow originates in the diffuse region of the electric double layer (which has a thickness of around 3 to 300 nm for electrolyte concentrations of 10 mM to 1 μ M respectively), in practice, it is considered that the flow originates at the wall of the capillary. When the capillary radius is greater than seven times the double-layer

thickness, a flat profile is expected inside the capillary. Figure 2a illustrates the electric double layer and the flow profile of electroosmotic flow. According to Eqn 2, the electroosmotic flow can be manipulated by changing some operational parameters such as the electric field, the viscosity and/or the dielectric constant of the running electrolyte. Since the zeta potential is dependent on the nature and the ionic content at the capillary surface, the velocity of the electroosmotic flow will also change if there is a change in these parameters. For example, increasing the ionic strength of the running electrolyte will decrease the flow. It has been shown that the rate of electroosmotic flow is different in capillaries of different materials (e.g. glass, silica and Teflon).

Electroosmosis is advantageous for the separation of oppositely charged species in CZE. It allows their transport passing the detection point. Also, electroosmosis is the driving force for the differential migration of solutes in MECC. In CZE and MECC, the electroosmotic flow should not affect separation efficiencies (10). In fact, the plug-flow profile of this built-in "pump" causes less band spreading than hydrodynamic flow. While electroosmotic flow is suitable for separation in CZE and MECC, it must be eliminated or reduced in isotachopheresis or isoelectric focusing in capillaries.

Electrophoretic Mobility. When an electric field is applied to a capillary filled with an electrolyte, all charged species will move toward the electrode of opposite charge by electrostatic attraction forces. Without considering the electroosmotic flow, the migration velocity of charged species is proportional to the strength of the electric field. The proportionality constant is termed electrophoretic mobility, denoted μ_e . The magnitude of μ_e depends on the charge density (*i.e.* the overall valence) and the size of the solute, as well as the dielectric constant and the viscosity of the running buffer. Temperature also has some effect on the electrophoretic mobility. The relationship is given by

$$\mu_e = \frac{A\epsilon\zeta_0}{\eta} \quad (4)$$

where A is a constant whose value depends on the relative size of the solute and the electrical double layer surrounding the particle, which is termed the zeta potential, ζ_0 , of the solute. ζ_0 is directly related to the charge density, ρ , of the solute through Poisson's equation (61).

Separation Principle. In the presence of electroosmotic flow, the total mobility of the solute, μ , and the migration velocity, v , are given by

$$\mu = \mu_e + \mu_{eo} \quad (5)$$

and

$$v = v_e + v_{eo} = (\mu_e + \mu_{eo})E \quad (6)$$

where v_e and v_{eo} are the electrophoretic velocity and electroosmotic flow, respectively. The retention time, t_r , *i.e.* the time for a solute to migrate from the injection end of the capillary to the detection point, is given by

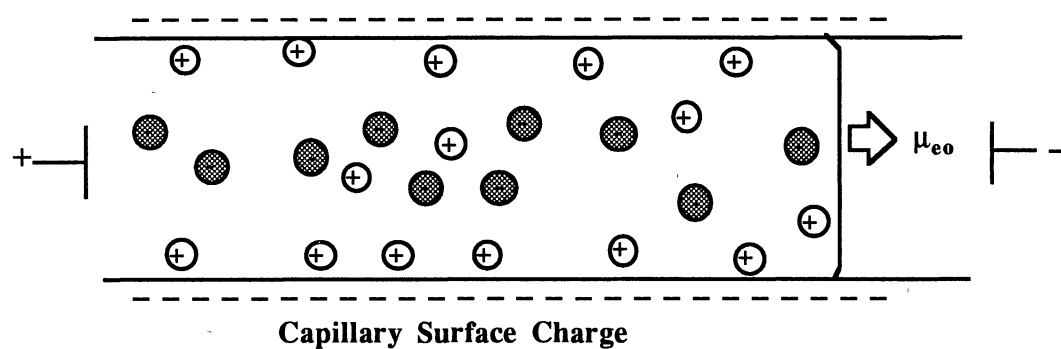
$$t_r = \frac{l}{v} = \frac{lL}{(\mu_e + \mu_{eo})V} \quad (7)$$

where l is the length of the capillary between the injection end and the detection point. It should be noted that l and L are usually not of the same value ($l < L$). From this equation, the total mobility of solute can be determined experimentally:

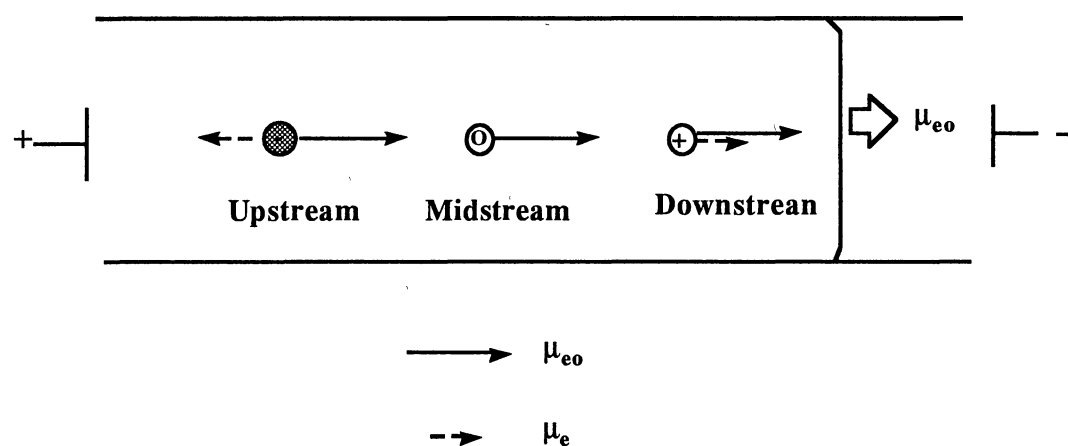
$$\mu = \mu_e + \mu_{eo} = \frac{lL}{t_r V} \quad (8)$$

Since the electroosmotic flow can be determined by an electrically neutral species,

$$\mu_{eo} = \frac{lL}{t_0 V} \quad (9)$$



(a)



(b)

Figure 2 Schematic Representation of Electric Double Layer and Electroosmotic Flow (a), and Separation by CZE in Open Tubes (b)

where t_0 is the retention time of a neutral species, the magnitude of electrophoretic mobility of a charged species can be obtained from Eqn 10:

$$\mu_e = \mu - \mu_{eo} = \frac{IL}{V} \left(\frac{1}{t_r} - \frac{1}{t_0} \right) \quad (10)$$

In most cases, the electroosmotic flow is greater than the migration velocity of charged species under electrostatic force, that is $|\mu_{eo}| > |\mu_e|$. Thus, all ions, regardless of their charges will migrate in the same direction toward the cathode. The separation in free solution electrophoresis is based on difference in electrophoretic mobility of the species. The electrophoretic mobility of positively charged species is in the same direction as the electroosmotic flow, but that of the negatively charged species is in the opposite direction. The electrophoretic mobility of non-ionic species is zero. So, under these conditions, positively charged species elute first, followed by neutral species and then the negatively charged species. Fig. 2b shows the separation of charged and uncharged species by CZE in open tubes.

Separation Efficiency. There are several factors that cause band broadening in capillary electrophoresis. If the conditions are optimized, that is, in the absence of solute-wall interaction and Joule heating, the major cause of band spreading will be longitudinal molecular diffusion. Under these conditions, the separation efficiency in terms of the total number of theoretical plates, N , is expressed as the standard molecular diffusion term (62):

$$N = \frac{(\mu_e + \mu_{eo})V}{2D} = \frac{(v_e + v_{eo})L}{2D} \quad (11)$$

Since

$$H = \frac{L}{N}$$

therefore,

$$H = \frac{2D}{v_e + v_{eo}} \quad (11a)$$

where D is the diffusion coefficient of the solute and H is the height equivalent to a theoretical plate. It is interesting to note that according to this equation, keeping all the other parameters unchanged, the higher the field the better the separation efficiency will be. However, there are practical limits to this approach. At some point, Joule heating generated from the applied field will ultimately form a temperature gradient inside the capillary. This temperature gradient will result in a viscosity gradient across the tube diameter, which lead to perturbation in the overall velocity profile. This perturbation will result in mass transfer resistance causing band spreading.

Similar to chromatography, in capillary electrophoresis, N can also be calculated from the half width of the peak using the equation:

$$N = 5.54 \left(\frac{t_r}{W_{1/2}} \right)^2 \quad (12)$$

where $W_{1/2}$ is the width of the peak at half height.

Resolution and Selectivity. The selectivity, α , and the resolution, R_s , of two adjacent zones in electrophoresis can be given by the following equations (4, 63):

$$\alpha = \frac{\Delta v}{\bar{v}} = \frac{\Delta \mu_e}{\bar{\mu}_e} \quad (13)$$

$$R_s = \frac{1}{4} \sqrt{N} \frac{\Delta v}{\bar{v}} = \frac{1}{4\sqrt{2}} \Delta \mu_e \sqrt{\frac{V}{D(\bar{\mu}_e + \mu_{eo})}} \quad (14)$$

where Δv is the difference in zone velocities, \bar{v} is the average zone velocity, $\Delta \mu_e$ is the difference in electrophoretic mobilities of the two adjacent solutes, $\bar{\mu}_e$ is the average electrophoretic mobility. According to this equation, high resolution can be obtained with high fields and low diffusion coefficient of the solute. Moreover, the best

resolution is obtained when the magnitude of μ_{eo} is close to that of $-\overline{\mu}_e$, however, the analysis time will be greatly increased.

Separation in MECC

Pseudostationary Phase. When a surfactant is added to the running buffer above its critical micelle concentration, it will form micelles with hydrophobic center and highly charged outer surface. Upon application of electric field, these micelles will gain a large electrophoretic mobility toward the electrode of opposite charge. However, under normal condition in capillary electrophoresis, there is a strong electroosmotic flow in the opposite direction to the electrophoretic flow of the micelles and is of greater magnitude. As a result, two distinct phases, aqueous (mobile) and micellar (pseudostationary), exist within the capillary and migrate at different velocities toward the electrode with the same charge as the micelles. Unlike conventional chromatography, where the stationary phase is immobilized on the support, the "stationary" phase in MECC is moving in the same direction with the mobile phase but at a much lower velocity. The net mobility of the micellar pseudostationary phase, μ_{mc} , can be determined according to Eqn 4:

$$\mu_{mc} = \mu_{eo} + \mu_{mc,e} \quad (15)$$

where $\mu_{mc,e}$ is the electrophoretic mobility of micelles. The time required for the electrophoretically retarded micelles to reach the detection point, t_{mc} , is given by

$$t_{mc} = \frac{L}{(\mu_{eo} + \mu_{mc,e})V} \quad (16)$$

The value of t_{mc} is measured experimentally with a solute such as Sudan III or any uncharged and hydrophobic solute that is fully solubilized by the micelles (13, 42).

Note that μ_{eo} and $\mu_{mc,e}$ are of opposite sign and the absolute magnitude of μ_{eo} is greater

than that of $\mu_{mc,e}$ (*i.e.* $|\mu_{eo}| > |\mu_{mc,e}|$). Thus, reduction in $|\mu_{eo}|$ or increase in $|\mu_{mc,e}|$ can result in a dramatic increase in t_{mc} as $|\mu_{eo}|$ and $|\mu_{mc,e}|$ approach the same value.

Retention Parameters. In MECC, the selective retention arises from the differential partitioning of solutes between the faster-moving aqueous phase and the slower-moving hydrophobic interior of the micellar phase. This partitioning requires solubilization by the micelles through surface interactions or through penetration of the solute into the micelle core. Thus, electrically neutral species are separated based on their relative hydrophobicities. The more hydrophobic the solute, the longer time it will spend in the micellar phase and consequently it will be more retarded. A schematic representation of a system for MECC is shown in Fig. 3a. Terabe *et al.* (13) have derived equations for the retention time, t_r , and retention factor, k' , of non-ionic solutes in MECC:

$$t_r = \frac{(1 + k')t_0}{1 + (t_0/t_{mc})k'} \quad (17)$$

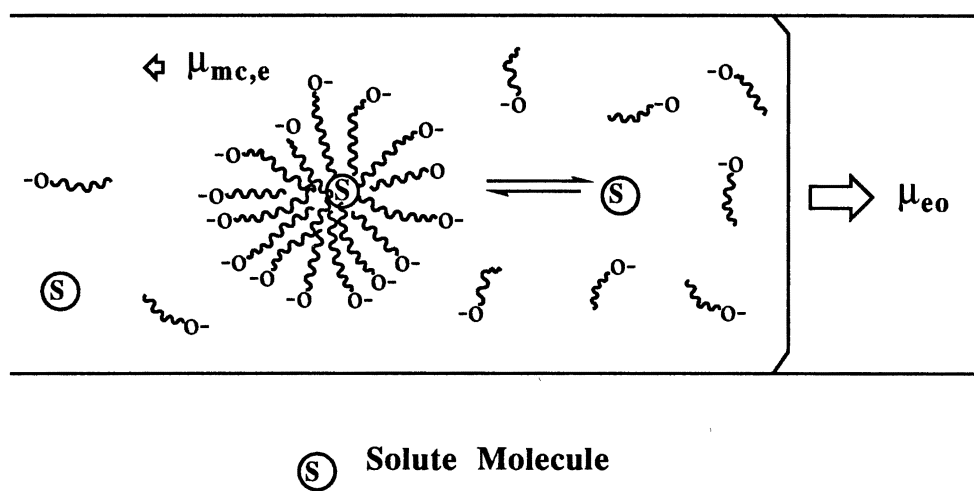
and

$$k' = \frac{t_r - t_0}{t_0(1 - t_r/t_{mc})} \quad (18)$$

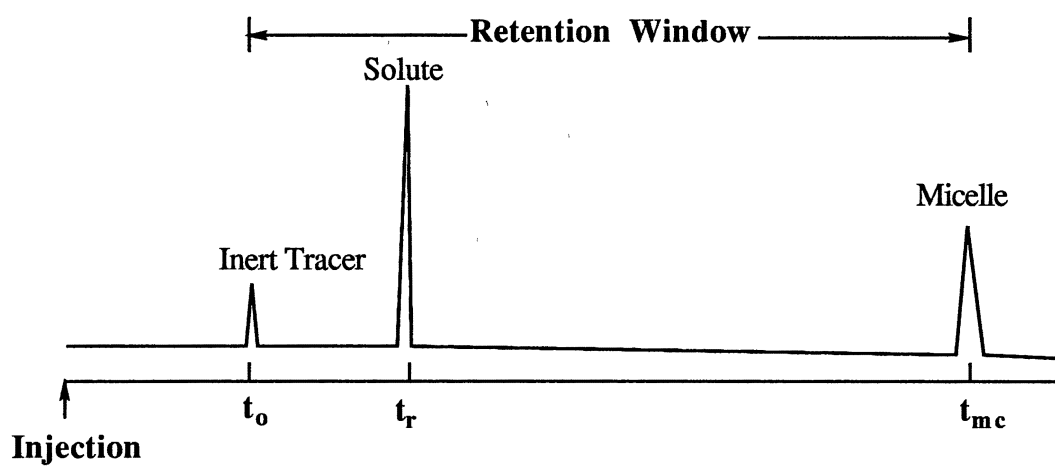
where t_0 is the retention time of an unretained marker, such as that of water or methanol which has no interaction with the micelles. The value of t_0 is determined only by the magnitude of the electroosmotic flow velocity. Since the retention factor k' is proportional to the volume ratio of the micellar phase to the aqueous phase, the k' values can be easily adjusted by changing the nature and/or the concentration of the surfactant, and therefore the volume of the micellar phase.

Selectivity. As in chromatography, the relative retention or selectivity, α , is given by:

$$\alpha = \frac{k_2'}{k_1'} \quad (19)$$



(a)



(b)

Figure 3. Schematic Representation of MECC System (a), and Retention Window in MECC (b)

where k_1' and k_2' are the retention factors of solute 1 and 2, respectively. One of the major advantages of MECC is its versatility in the manipulation of selectivity. The selectivity in MECC can be altered by changing a number of parameters such as the composition of both the aqueous and the pseudostationary phases. For example, the composition of the aqueous phase can be adjusted by adding organic modifiers. Micellar composition can be modified by using different surfactants in order to produce micelles of different sizes, aggregation numbers, and geometries. Also, the nature of micelles can be altered by the addition of divalent metal ions to the running buffer to produce metal-micelle complexes. All these adjustments will in turn affect the selectivity of MECC.

Resolution and Peak Capacity. Resolution, R_s , in MECC is given by the following equation:

$$R_s = \underbrace{\frac{\sqrt{N}}{4}}_{\text{efficiency}} \cdot \underbrace{\frac{\alpha - 1}{\alpha}}_{\text{selectivity}} \cdot \underbrace{\frac{k_2'}{k_2' + 1} \cdot \frac{1 - t_0/t_{mc}}{1 + (t_0/t_{mc})k_1'}}_{\text{retention}} \quad (20)$$

Peak capacity is defined as the maximum number of peaks that can be separated with an $R_s = 1.0$ within a specified range of retention time. According to Giddings (64), for cases in which peaks are separated with 4σ resolution, where σ is the standard deviation of the peak, under a constant plate number N , peak capacity, n , is given by

$$n = 1 + \frac{\sqrt{N}}{4} \ln \frac{t_{\text{last}}}{t_{\text{first}}} \quad (21)$$

where t_{first} and t_{last} are the retention time of the first and the last eluting peaks, respectively. In MECC, neutral solutes that interact with the micelles will elute within the "retention window". This "retention window" is defined as the time window

between the retention time of an unretained marker, t_0 , and the retention time of the micelles, t_{mc} , as shown in Fig. 3b. Therefore, peak capacity in MECC is expressed as

$$n = 1 + \frac{\sqrt{N}}{4} \ln \frac{t_{mc}}{t_0} \quad (22)$$

The above equation shows that the peak capacity in MECC is limited by the ratio, t_{mc}/t_0 , which is determined by the specific MECC system. The limited "retention window" is the major obstacle in the application of MECC to complex sample analysis.

Sample Introduction

In capillary electrophoresis, sample can be injected either by hydrodynamic flow or by electromigration. From Eqn 6, the sample volume injected by electromigration, v_e , can be determined by:

$$v_e = \frac{(\mu_e + \mu_{eo})V_i\pi r^2 t_i}{L} \quad (23)$$

where t_i is the injection time, r is the inner radius of the capillary. The amount of solute injected by electromigration, Q_e , is:

$$Q_e = \frac{(\mu_e + \mu_{eo})V_i\pi r^2 C t_i}{L} \quad (24)$$

where C is the concentration of the sample.

For hydrodynamic flow, the average hydrodynamic velocity, v_h , can be calculated by Poiseuille equation:

$$v_h = \frac{\rho g r^2 \Delta h}{8\eta L}$$

where ρ is the solution density, g is the gravitational force constant, Δh is the difference in height between the two ends of the capillary. The volume and the amount of sample introduced by hydrodynamic flow, v_h and Q_h , can be determined by

$$v_h = \frac{\pi \rho g r^4 \Delta h t_i}{8 \eta L} \quad (25)$$

and

$$Q_h = \frac{\pi \rho g r^4 \Delta h C t_i}{8 \eta L} \quad (26)$$

In both cases, the volume and the amount of sample introduced, v and Q , can be determined by experimental measurement and calculated as follows:

$$v = \frac{\pi r^2 L t_i}{t_r} \quad (27)$$

and

$$Q = \frac{\pi r^2 L C t_i}{t_r} \quad (28)$$

It should be noted that in the case of hydrodynamic sample introduction, t_r is the time it takes for the sample zone to migrate from the injection end to the detection point under the gravity force. There are two conditions which must be met for this equation to be valid. First, the analytes must be dissolved in the running buffer. Second, the injection voltage must be equal to that of the voltage applied during the separation process.

Hydrodynamic injection mode is not dependent on electrophoretic mobility and the amount of sample introduced into the capillary is a slug with a composition similar to that of the sample. Conversely, in electromigration, the amount of each component of the sample is dependent on their relative electrophoretic mobilities as well as the ionic strength of the sample buffer.

Rationale of the Research

Capillary electrophoresis uses high voltage to carry out separations. The technique has many advantages such as high efficiency, high resolution, small sample requirement, rapid separation, and simple instrumentation. As a microseparation and micropreparative technique, capillary electrophoresis is a complementary tool to HPLC. Capillary electrophoresis has been used for the separations of small molecules, as well as large molecules, such as biopolymers. With the introduction of complexation and electrokinetic chromatography, neutral compounds can be separated readily by capillary electrophoresis. Chiral separation is also an important application of capillary electrophoresis.

Although capillary electrophoresis has been shown as a powerful separation technique, many aspects of the capillary electrophoresis system require further development. As discussed above, the limited retention window is an obstacle in the application of micellar electrokinetic chromatography to the analysis of multicomponent samples. Another problem with capillary electrophoresis is its inadequacy for dilute samples. Since very small sample volume (*ca.* 1-5 nL) should be used to avoid band broadening, the minimum detectable sample concentration is limited.

In order to provide ways by which the retention window of MECC can be modified, and to facilitate the separation and elution in this mode of capillary electrophoresis, we introduced a new MECC system with micelles of controlled surface charge density and degree of ionization. The retention window of the MECC system was readily manipulated by changing operational parameters such as pH, concentration of the surfactant, and concentration of the surface charge density modifier of the micelles.

We also attempted to improve the concentration detectability of CZE. In this study, capillaries coated with metal chelating ligands or octadecyl functions were

developed for on-line preconcentration of dilute samples. This approach allowed the use of large sample volumes without sacrificing the separation efficiency.

To further advance the field of capillary electrophoresis and enlarge the scope of its applications, we have developed novel methodologies that are useful for the rapid determination of dissociation constants of weak bases, acids and ampholytes.

CHAPTER II

EVALUATION OF CZE WITH CHARGED POLLUTANTS. SEPARATION AND IONIZATION BEHAVIOR

Introduction

Capillary zone electrophoresis (CZE) is a powerful technique for the analysis of charged species. The electroosmotic flow as a built-in pump allows the transport of positively and negatively charged species passing the detection point. The difference in electrophoretic mobility permits the separation. The use of free zone electrophoresis in open-tubular format in conjunction with novel electrolyte systems permits high separation efficiencies, low mass detection limit and rapid separations.

Currently, the separation and determination of non-volatile pollutants is mainly carried out by HPLC, whereas gas chromatography (GC) is the chief technique for the determination of volatile compounds. For CZE to become widely accepted and complement HPLC and GC, its scope of applications needs to be enlarged.

Capillary zone electrophoresis holds a lot of promise in this area, not only for the separation but also for the characterization of charged solutes, *i.e.*, the determination of their ionization behavior. This chapter will discuss the capability of CZE in the separation and the determination of ionization behavior of some species of environmental interest. The methodologies developed in this study can be applied for a wide range of organics.

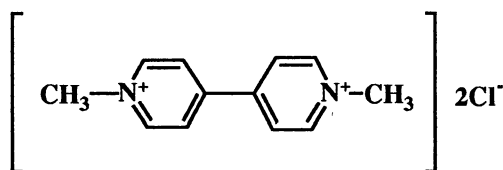
Experimental

Instruments

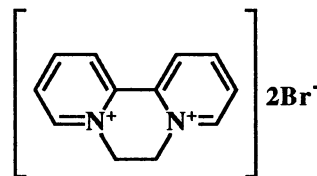
The instrument used in this study for electrophoresis was the same as that described in the first chapter. It consists of a 30-kV dc power supply (Glassman High Voltage, Whitehouse Station, NJ, U.S.A.) Model HP30P3 of positive polarity and a Linear (Reno, NV, U.S.A.) Model 200 UV-Vis variable wavelength detector equipped with a cell for on-column detection. Platinum wires were used as the electrodes in this study. The electropherograms were recorded with a computing integrator from Shimadzu (Columbia, MD, U.S.A.). Fused-silica capillaries having an inner diameter of 50 μm and outer diameter of 375 μm were obtained from Polymicro Technology (Phoenix, AZ, U.S.A.). The untreated fused-silica capillary used in this study has 80 cm total length with a separation distance of 50 cm (*i.e.*, from the injection end to the detection point). The instrument for the UV spectrometry measurement was a UV-Visible Recording Spectrophotometer, Model UV-160 from Shimadzu.

Reagents and Materials

Aniline was from Fisher Scientific Company (Fair Lawn, NJ). Anisidine, 2-aminopyridine and p-aminobenzoic acid were purchased from Aldrich (Milwaukee, WI). The herbicides, *i.e.*, paraquat and diquat, were purchased from Chem Service (West Chester, PA, U.S.A.). Their structures are as follows:



Paraquat



Diquat

Phenol was from J. T. Baker Inc. (Phillipsburg, NJ). Sodium phosphate, phosphoric acid, sodium borate, boric acid, sodium acetate, and sodium hydroxide were from Fisher Scientific (Pittsburgh, PA, U.S.A.). Deionized water was used to prepare the running electrolyte. All solutions were filtered with 0.2 μm Uniprep Syringeless filters from Genex Corp., (Gaithersburg, MD, U.S.A.) to avoid capillary plugging.

Procedures

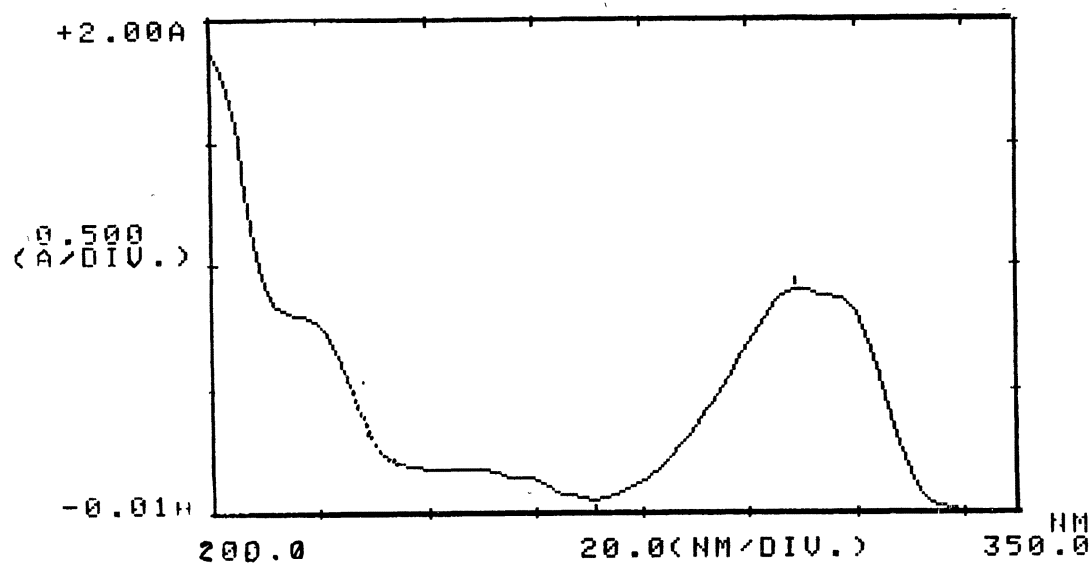
UV Spectrophotometry. Sample solutions were made by dissolving a small amount of paraquat and diquat in distilled water. Absorption spectra of the herbicides were obtained by scanning from 200 to 350 nm.

Figure 4 shows the UV spectra of the two herbicides. The maximum wavelengths, λ_{max} , the molar absorptivities, ϵ , and the correlation coefficient of the plots of absorbance versus concentration, for paraquat and diquat are listed in table 1.

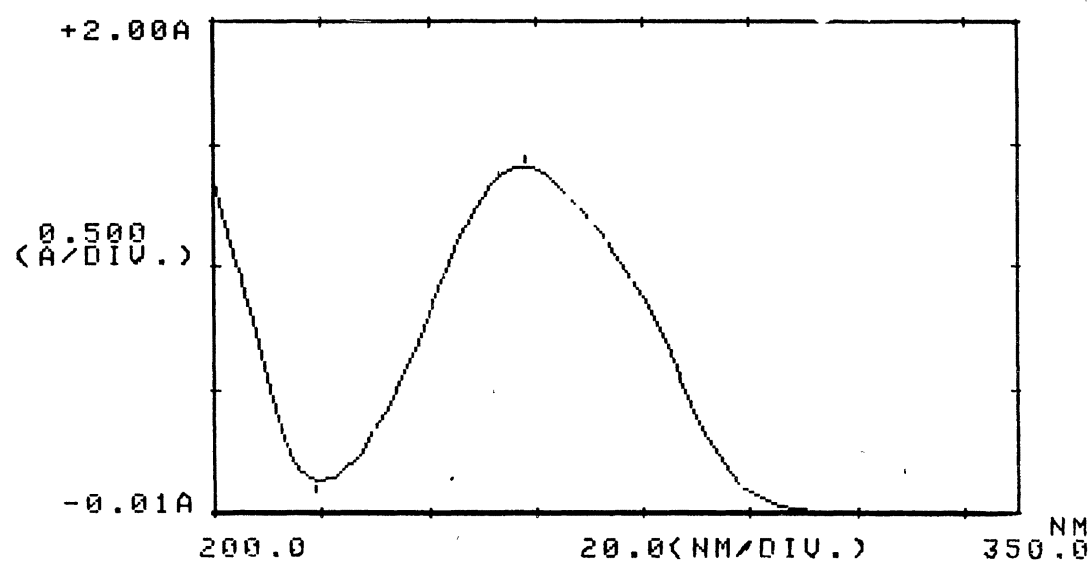
TABLE 1
MAXIMUM WAVELENGTH AND MOLAR ABSORPTIVITY

Sample	λ_{max} (nm)	ϵ ($\text{cm}^{-1}\text{M}^{-1}$)	Correlation Coefficient
Paraquat	258	1.72×10^4	0.9996
Diquat	308	1.62×10^4	0.9979

Capillary Electrophoresis. The running electrolyte was prepared by dissolving



(a)



(b)

Figure 4. Spectra of Diquat (a) and Paraquat (b)

proper amount of sodium salt in deionized water and adjusting the pH to the desired value. Sample solutions were prepared by dissolving pure compounds in the running electrolyte. All injections were made by electromigration for 2-5 seconds, at an applied voltage that was the same as that for separation. The running voltage used for all the measurements was 15 kV. Electroosmotic flow was determined by measuring the migration time of phenol, which was considered as neutral under the experimental conditions.

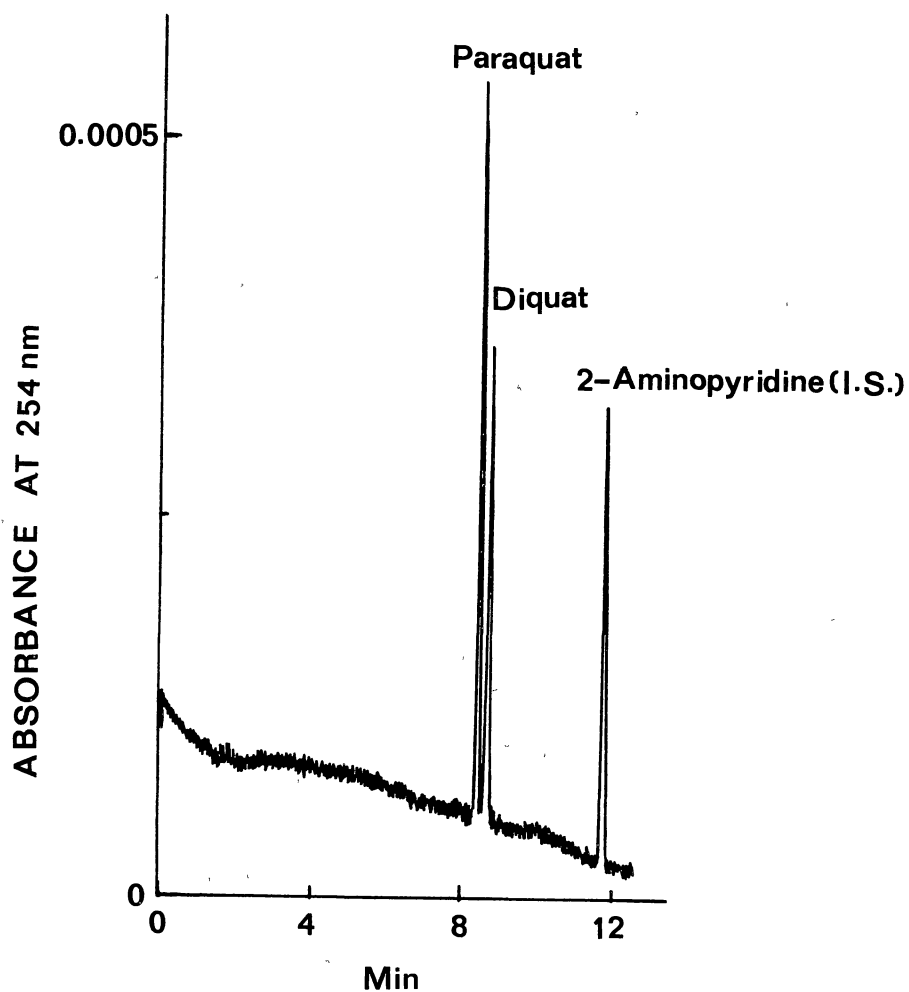
Results and Discussion

Determination of Strongly Basic Pollutants

In this study, paraquat and diquat were chosen as examples of fully ionized pollutants. Paraquat and diquat are effective aquatic herbicides and are used at low concentrations (1-5 $\mu\text{g/mL}$). Residues cause problems in soil and subsequent rotational crops may be affected. They can also contaminate the water-table which may pose serious health problems. The analysis of these herbicides at such low concentrations with conventional bioassay was time consuming and laborious (65). The precision instrumentation of CZE makes the determinations of these species easier and faster.

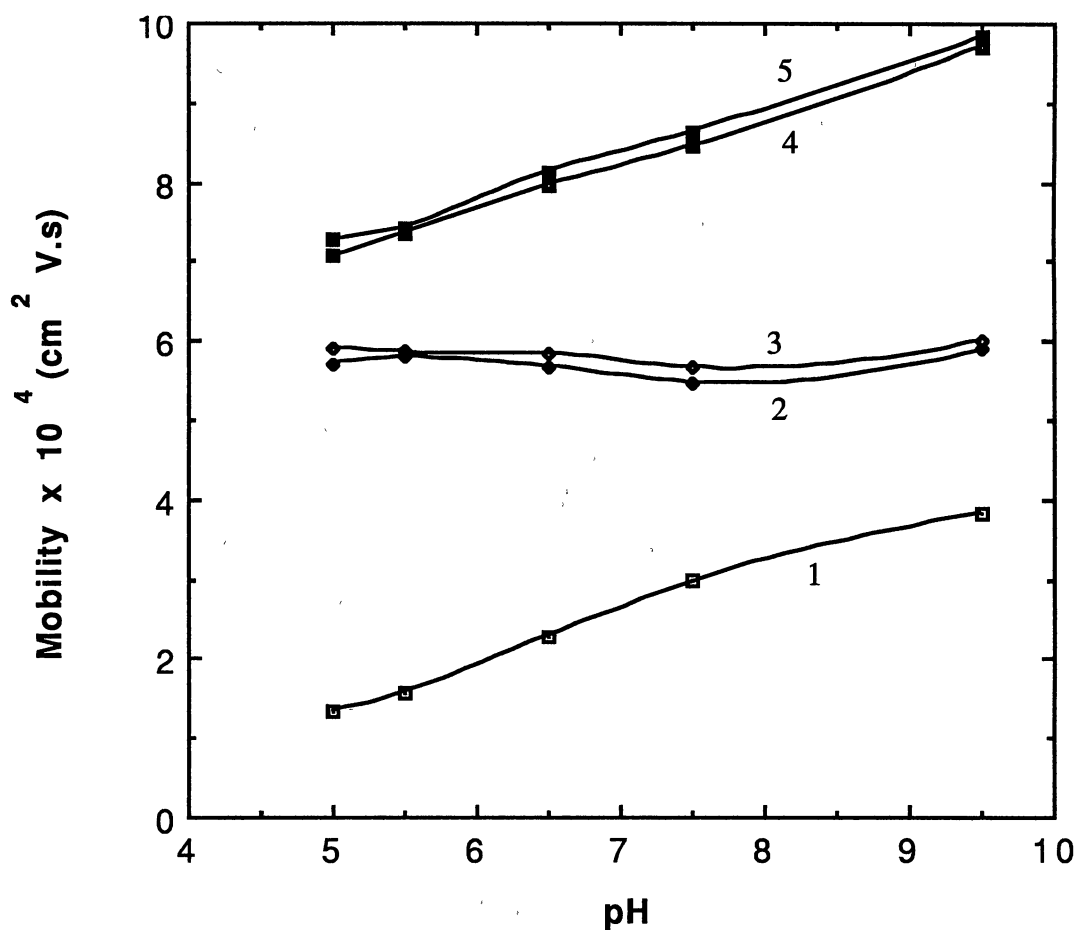
Figure 5 is a typical electropherogram of the separation of the two herbicides. As shown in Fig. 5, the separation was achieved in 10 minutes with high separation efficiency. The two herbicides are quaternary ammonium ions having the same net charges (*i.e.*, +2) and slightly different molecular weights (184 for diquat, 186 for paraquat). The separation is based on the difference in the shape of the two species.

The electrophoretic and the overall mobilities of the two herbicides as well as the electroosmotic flow are shown in Fig. 6. They were calculated according to Eqns 10, 8 and 9, respectively. The measurements of electroosmotic flow and the overall mobility are necessary for the determination of electrophoretic mobility (see Eqn 10).



Separation capillary: untreated fused-silica, 50 cm (to the detection point), 80 cm (total length) x 50 μ m I.D.; Running electrolyte: 0.10 M sodium phosphate, pH 3.5; Sample injection: electromigration, 5 seconds; Running voltage: 15 kV; Internal standard: 2-aminopyridine; Detection: 254 nm.

Figure 5 Typical Electropherogram Illustrating the Rapid Separation of Herbicides by CZE



1, Electroosmotic flow;
 2 and 3, Electrophoretic mobilities of diquat and paraquat, respectively;
 4 and 5, Overall mobilities of diquat and paraquat, respectively

Separation capillary: same as in Figure 5; Sample injection: electromigration, 2 seconds; Running voltage: 15 kV; Detection: 254 nm;
 Running electrolytes: pH 4.0-5.5, 5 mM acetate + 0.2 M sodium chloride;
 pH 6.0-8.0, 5 mM phosphate + 0.2 M sodium chloride;
 pH 8.5-9.5, 5 mM borate + 0.2 M sodium chloride;
 The experimental data points are the average of two measurements.

Figure 6 Mobilities of Herbicides

Since the two herbicides have constant charge density over the pH range studied, their electrophoretic mobilities remained unchanged regardless of the change in pH.

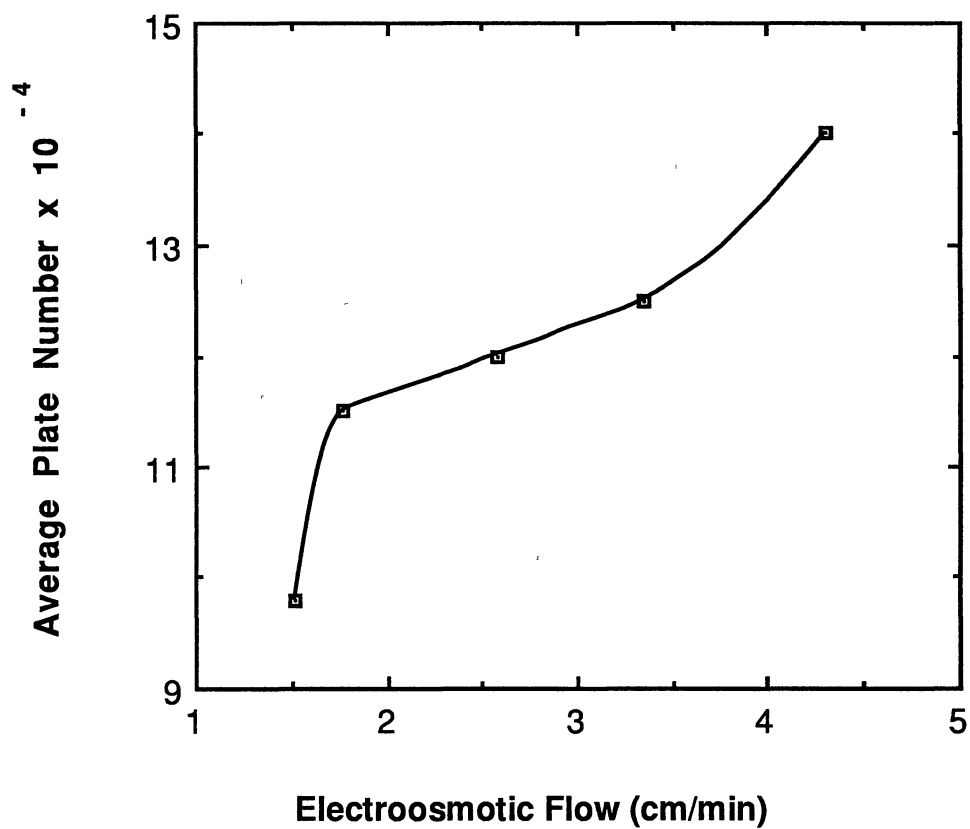
High efficiency was obtained in the separation of paraquat and diquat. Figure 7 illustrates the separation efficiency of paraquat and diquat as a function of electroosmotic flow (*i.e.*, at various pH). The theoretical plate number, N , was calculated according to Eqn 12. As shown in Fig. 7, the average theoretical plate number was above 100,000 (or 200,000) plates/meter. The fact that N increases with the magnitude of electroosmotic flow may be due to diminishing longitudinal molecular diffusion.

The detection limits of CZE in terms of concentration and absolute amount were also determined and the results are listed in Table 2.

TABLE 2
LIMITS OF DETECTION*

Sample	<u>Limits of Detection</u>				Correlation Coefficient
	<u>Concentration</u>		<u>Injected Quantity</u>		
	(μg/mL)	(μM)	(pg)	(femtomole)	
Paraquat	0.40	1.55	3.97	15.4	0.996
Diquat	0.50	1.45	5.78	16.8	0.996

* Detection: 308 nm for diquat, 254 nm for paraquat; other experimental conditions are as in Fig. 5. The data are the average of two measurements.



Experimental conditions are as in Figure 6. The experimental data points are the average of two measurements.

Figure 7 Separation Efficiency of Herbicides

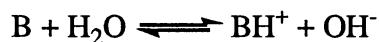
In order to obtain these detection limits, calibration curves for paraquat and diquat were made by injecting several dilutions of stock solutions. In these measurements, 2-aminopyridine was used as an internal standard to minimize errors in sample injection. For both paraquat and diquat, the linearity was quite satisfactory in the concentration range studied. The data show that CZE is suitable for quantitative analysis of femtomole quantities.

Determination of Weakly Ionized Pollutants.

Electrophoretic Determination

of Dissociation Constants

Principles. Electrophoretic mobility of many charged species can be adjusted by changing parameters such as pH of the running electrolyte to alter their charge densities. This renders CZE adequate for the determination of dissociation constants of weak acids and bases. For the protonation of a base, B,



the equilibrium constant, K_b , can be expressed as

$$K_b = \frac{[BH^+][OH^-]}{[B]}$$

Since the ion-product constant of water, K_w , is given by

$$K_w = K_a K_b = [H^+][OH^-]$$

the acid dissociation constant, K_a , is then

$$K_a = \frac{[B][H^+]}{[BH^+]}$$

where B and BH^+ denote the deprotonated and protonated species, respectively.

If μ_{ob} is the electrophoretic mobility of the fully protonated species, BH^+ , the net electrophoretic mobility, μ_e , of the charged species is the product of its mole fraction and μ_{ob} (66, 67):

$$\mu_e = \frac{[BH^+]}{[BH^+] + [B]} \mu_{ob} \quad (29)$$

Rearranging the above equations lead to the following fundamental relationship:

$$\mu_e = \frac{[H^+]}{[H^+] + K_a} \mu_{ob} \quad (30)$$

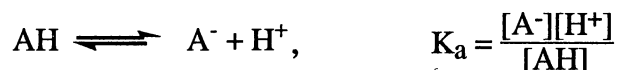
or

$$pH = pK_a - \log \frac{\mu_e}{\mu_{ob} - \mu_e} \quad (31)$$

A plot of pH versus $\log \frac{\mu_e}{\mu_{ob} - \mu_e}$ will result in a straight line with a slope equal to -1

and an intercept equal to pK_a .

In an analogous way, for the dissociation of an acid, AH,



the following equations can be obtained:

$$\mu_e = \frac{[A^-]}{[AH] + [A^-]} \mu_{oa} \quad (32a)$$

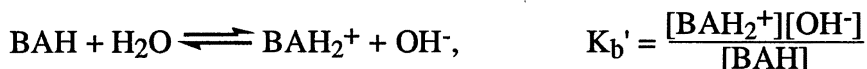
$$\mu_e = \frac{K_a}{[H^+] + K_a} \mu_{oa} \quad (32b)$$

$$pH = pK_a + \log \frac{\mu_e}{\mu_{oa} - \mu_e} \quad (32c)$$

where AH and A^- denote the protonated and fully deprotonated species, respectively, and μ_{oa} is the electrophoretic mobility of A^- . Similar to that of a base, plot of pH versus

$\log \frac{\mu_e}{\mu_{oa} - \mu_e}$ will result in a straight line with a slope equal to 1, and an intercept equal to pK_a .

For the dissociation of an ampholyte species, BAH,



where the base dissociation constant, K_b' , can be expressed as acid dissociation constant, K_a' , through the ion-product constant of water, K_w :

$$K_a' = \frac{K_w}{K_b'} = \frac{[BAH][H^+]}{[BAH_2^+]}$$

If μ_{ob} is the electrophoretic mobility of the fully protonated form, BAH_2^+ , and μ_{oa} is that of the deprotonated form, BA^- , the net electrophoretic mobility of the charged species, μ_e , is the sum of the products of μ_{ob} , μ_{oa} and the mole fractions of their respective species:

$$\mu_e = \frac{[BAH_2^+]\mu_{ob}}{[BAH_2^+] + [BAH] + [BA^-]} + \frac{[BA^-]\mu_{oa}}{[BAH_2^+] + [BAH] + [BA^-]} \quad (33)$$

Since the fully protonated and deprotonated species have the same magnitude of charge densities except that they are of opposite sign, *i.e.*:

$$\mu_{ob} = -\mu_{oa} = \mu_o$$

Combining the above equations yields the following expression:

$$\mu_e = \frac{[H^+]^2 - K_a K_a'}{K_a' [H^+] + [H^+]^2 + K_a K_a'} \mu_o \quad (34)$$

or

$$(\mu_e + \mu_o)K_a K_a' + \mu_e [H^+] K_a' + (\mu_e - \mu_o)[H^+]^2 = 0 \quad (35)$$

Solving Eqn 35 yields:

$$K_a = \frac{\begin{vmatrix} \mu_{e1}[H^+]_1 & (\mu_{e1}-\mu_o)[H^+]_1^2 \\ \mu_{e2}[H^+]_2 & (\mu_{e2}-\mu_o)[H^+]_2^2 \end{vmatrix}}{\begin{vmatrix} (\mu_{e1}-\mu_o)[H^+]_1^2 & \mu_{e1}+\mu_o \\ (\mu_{e2}-\mu_o)[H^+]_2^2 & \mu_{e2}+\mu_o \end{vmatrix}} \quad (36a)$$

and

$$K_a' = \frac{\begin{vmatrix} (\mu_{e1}-\mu_o)[H^+]_1^2 & \mu_{e1}+\mu_o \\ (\mu_{e2}-\mu_o)[H^+]_2^2 & \mu_{e2}+\mu_o \end{vmatrix}}{\begin{vmatrix} \mu_{e1}+\mu_o & \mu_{e1}[H^+]_1 \\ \mu_{e2}+\mu_o & \mu_{e2}[H^+]_2 \end{vmatrix}} \quad (36b)$$

From Eqns 36a and 36b, we can determine K_a and K_a' , provided that values of electrophoretic mobility of the ampholyte at two or more different pH values are available.

Applicability to Pollutants. To demonstrate the capability of CZE in the determination of dissociation constants of pollutants, aniline, p-anisidine and p-aminobenzoic acid were chosen as model solutes, since they represent a class of priority pollutants; the aromatic amines (68).

Aniline and anisidine were examples of weak bases. Figure 8a shows the plots of electrophoretic mobilities of aniline and p-anisidine versus pH. They were determined as indicated above using Eqn 10. The sigmoidal curves obtained are similar to that of the titration curves and can be used for the measurement of ionization constants of these two weak bases. However, according to Eqn 31, a more direct determination

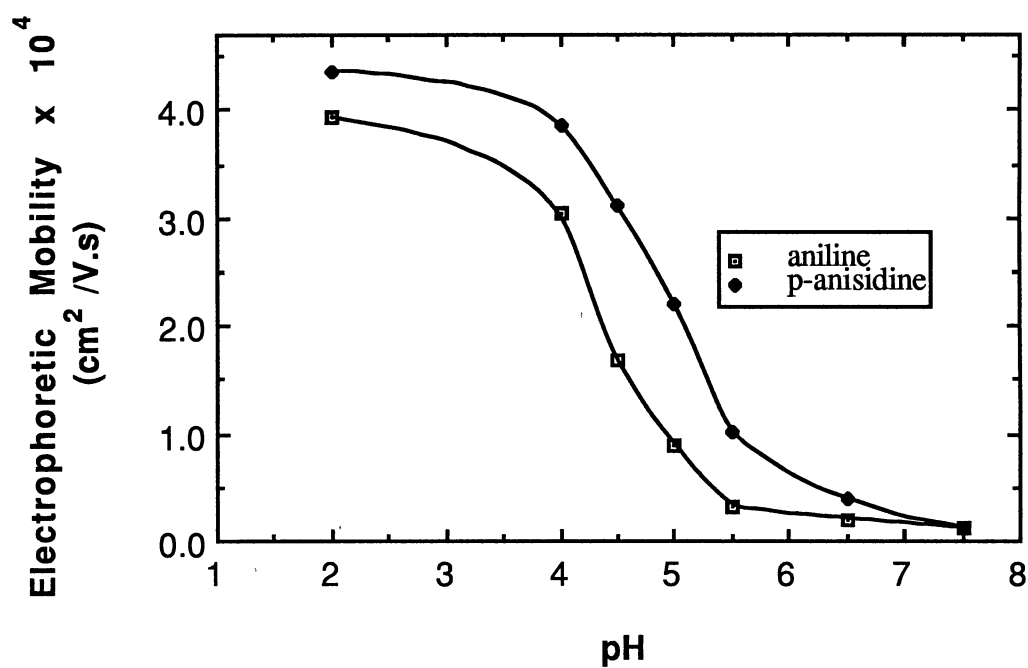
of the dissociation constants can be made by the plots of pH versus $\log \frac{\mu}{\mu_{ob} - \mu}$.

Figure 8b is the illustration of such plots. In these plots, only the points in the pH domain where small changes in the electrolyte pH cause large changes in the electrophoretic mobilities are used. μ_{ob} for each sample was approximated as the value of the net mobility at low pH (*i.e.*, pH 2) where the species are considered as fully protonated, and the electroosmotic flow is negligible. The pK_a values can be determined from the y-intercept of these straight lines. The results together with the reported values for pK_a are listed in Table 3.

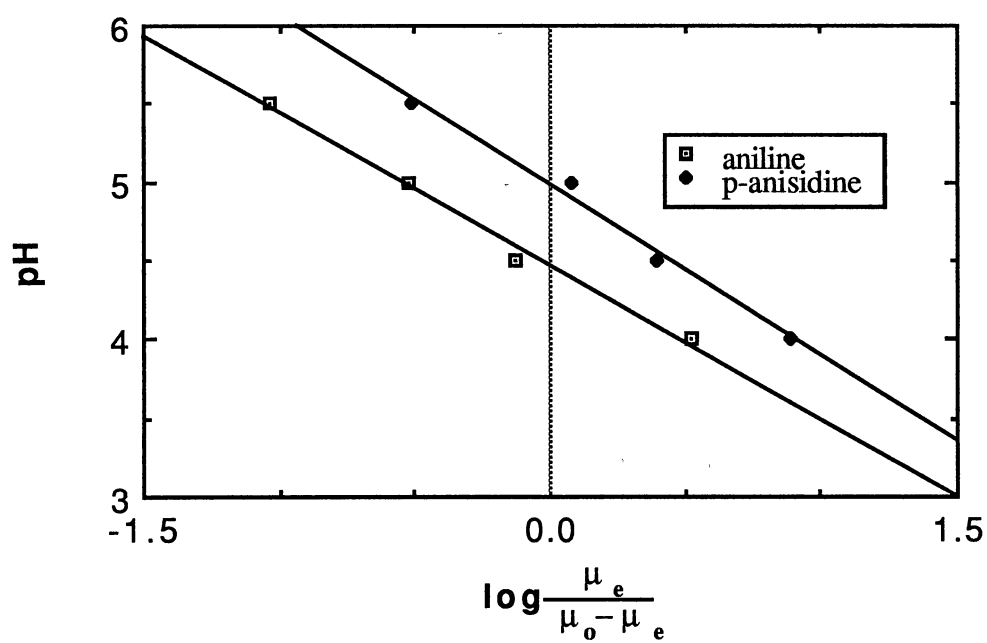
TABLE 3
DETERMINATION OF DISSOCIATION CONSTANT OF WEAK BASES

Sample	pK_a		Slope	Correlation Coefficient
	Measured Value	Reported Value*		
Aniline	4.45 (~0.2)	4.60 \pm 0.005 (0)	-0.98	0.996
	4.46 (~0.2)	4.82 (0.1)		
		4.71 (0.5)		
		4.65 \pm 0.03 (1.0)		
p-Anisidine	4.98 (~0.2)	5.01 (0.3)	-1.09	0.994
	5.10 (~0.2)	5.36 (0)		

* Taken from reference 69. The numbers in parentheses indicate the ionic strength. The temperature of the reported values was 25 °C.



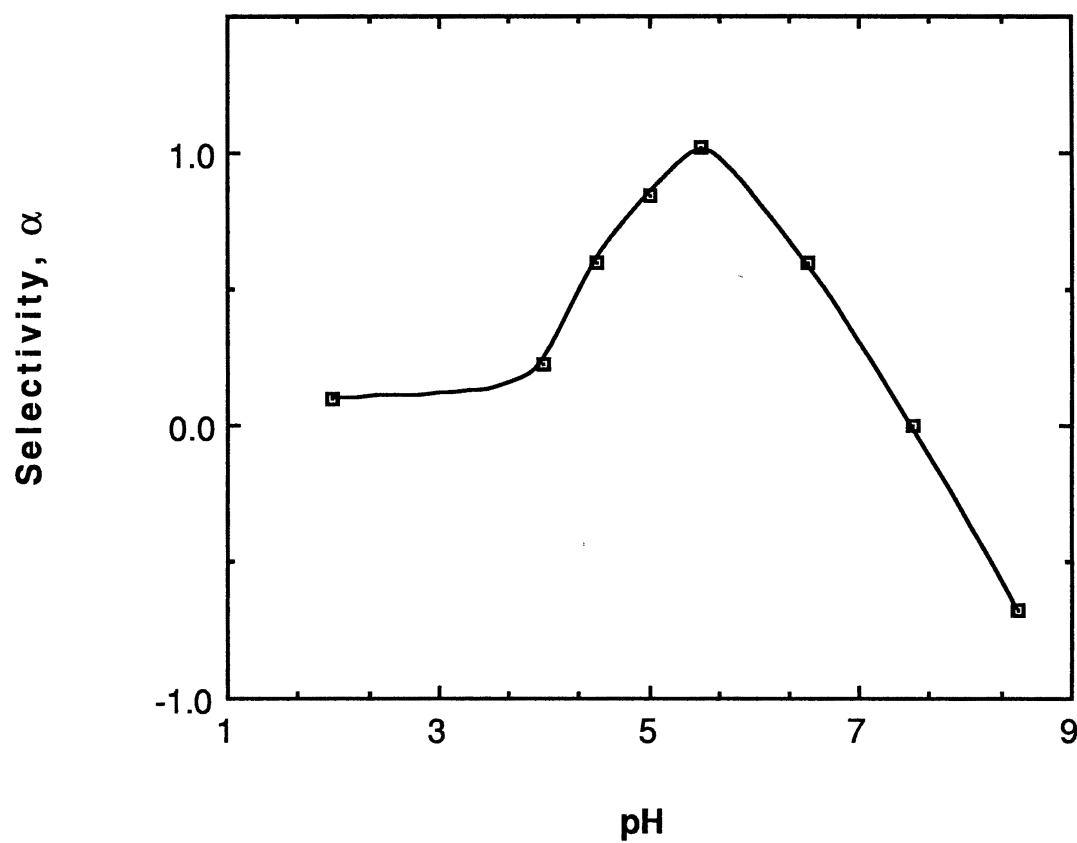
(a)



(b)

Sample: aniline and anisidine; Inert tracer: phenol; Other experimental conditions are as in Figure 6. The experimental data points are the average of two measurements.

Figure 8a, b Determination of pK_a of Weak Bases



Solutes: aniline and anisidine; Other experimental conditions are as in Figure 6. The experimental data points are the average of two measurements.

Figure 8c Selectivity of Aniline and p-Anisidine as a Function of pH

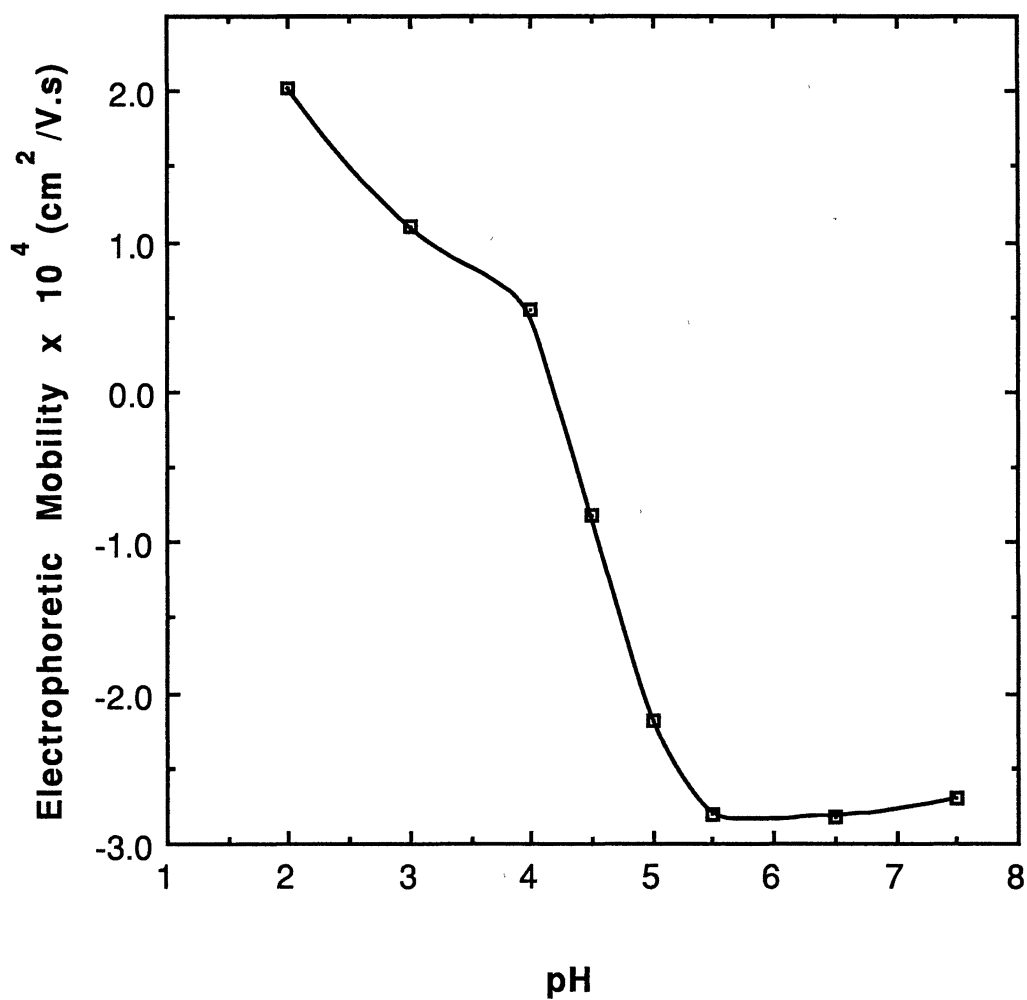
These data shows that the dissociation constant can be determined from electrophoretic mobility measurements. The measured values were close to those obtained by potentiometric measurements. In a similar way, we project that pK_a of weak acids can also be determined by CZE.

The selectivity α , for aniline and anisidine at different pH is illustrated in Fig. 8c. They are calculated using Eqn 13. As expected, the maximum selectivity was obtained near the average value of pK_a 's of the two weak bases.

P-aminobenzoic acid was an example of ampholytes. Fig. 9 is the plot of electrophoretic mobility of p-aminobenzoic acid as a function of pH. From the curve, one of the pK_a value can be measured directly. Although the first ionization constant is difficult to determine in this curve, it was calculated using Eqns 36a and 36b. In this calculation, the values of the electrophoretic mobilities at six different pH values (*i.e.*, pH 2.0, 3.0, 4.0, 4.5, 5.0 and 5.5) were used to obtain an average value. Table 4 presents the calculated and reported values for p-aminobenzoic acid. The difference between the calculated and the reported values may due to the difference in temperature and in ionic strength of the media.

Conclusions

The above studies have proved that CZE is suitable for the determination of charged pollutants. High theoretical plate number can be obtained, which allowed the separation of closely related herbicides. In addition, the precision instrumentation of CZE permitted the determination of the ionization behavior of weak bases and acids. This study developed a general methodology for the determination of dissociation constant by CZE.



Solute: p-aminobenzoic acid; Other experimental conditions are as in Figure 6.
The experimental data points are the average of two measurements.

Figure 9 Determination of pK_a of p-Aminobenzoic Acid

TABLE 4
DETERMINATION OF DISSOCIATION CONSTANT OF P-AMINOBENZOIC ACID

pK _a		pK _a '	
Calculated	Reported*	Calculated	Reported*
4.47 ± 0.28 (~0.2)	4.87 ± 0.02 (0)	2.82 ± 0.69 (~0.2)	2.41 ± 0.04 (0)

* Taken from reference 69. The numbers in parentheses indicate the ionic strength. The temperature of the reported values was 25 °C.

CZE has several advantages as a tool in the determination of ionization behavior over titrimetric method. CZE requires small amount of samples and permits the determination of several species simultaneously. In fact, samples do not need to be pure, since CZE can separate the impurities from the solutes of interest.

However, since the separation in CZE is based on the differences in the electrophoretic mobilities, CZE is inadequate for the analysis of neutral species, which have zero electrophoretic mobility and migrate with the bulk flow. The separations of neutral species can be achieved with the use of micellar electrokinetic capillary chromatography. The following chapter will cover this part of the work.

CHAPTER III

MICELLAR ELECTROKINETIC CAPILLARY CHROMATOGRAPHY OF NEUTRAL SOLUTES WITH MICELLES OF ADJUSTABLE SURFACE CHARGE DENSITY. APPLICATIONS TO THE SEPARATION OF HERBICIDES

Introduction

Micellar electrokinetic capillary chromatography (MECC) is increasingly used for the separation of neutral species (13, 49, 45, 46, 48). To date most applications of MECC have used sodium dodecyl sulfate (SDS) in a neutral pH buffer as the micellar phase. However, MECC with SDS suffers from limited elution range which limits peak capacity and resolution. In addition, hydrophobic compounds all partition completely into the micelles and are not resolved. Several attempts have been made to extend the elution range of the technique (70, 71). In one approach, surfactants having shorter alkyl chains (e.g., sodium decyl sulfate) have been introduced. The smaller micelles thus obtained exhibited higher electrophoretic mobility. Since this modification did not affect the electroosmotic flow appreciably, the net result was a decrease in the total mobility of the micelles. However, the relatively high critical micelle concentration (CMC) of short chain-length surfactants dictated the use of high concentration (*i.e.*, high ionic strength), which posed problems of high current and therefore system overheating. Another approach was to decrease the electroosmotic flow. This was achieved by coating the capillary inner surfaces (72, 73), or adding organic modifiers (74). Under these conditions, both t_{mc} and t_0 increased. Such methods lead to long analysis time,

and as a result, species which are strongly retained by the micelles may not pass the detection point.

In this work, we have introduced a novel micellar system that allows the adjustment of the elution range to the desired value in order to suit a wide range of applications. Also, the new micellar system investigated here has a decreased shade of hydrophobicity.

This new approach exploited the complexation between octylglucoside (surfactant) and borate (complexing agent). This method provided several advantages over traditionally used micelles. First, octylglucoside has a relatively short non-polar chain and a large polar head moiety. This balance in hydrophobicity-hydrophilicity is advantageous for the separations of highly nonpolar species. Due to their relatively high hydrophobicity, previously described micelles have been inadequate for the separation of strongly non-polar compounds, which associated avidly with the slow-moving micelles and could not be separated. Furthermore, in the octylglucoside-borate micelles, the surface charge can be varied conveniently by changing the borate concentration in the running electrolyte and/or by varying the pH of the aqueous phase. These readily tuned features provided a means to manipulate the separation efficiencies, peak capacity and selectivity.

Theory

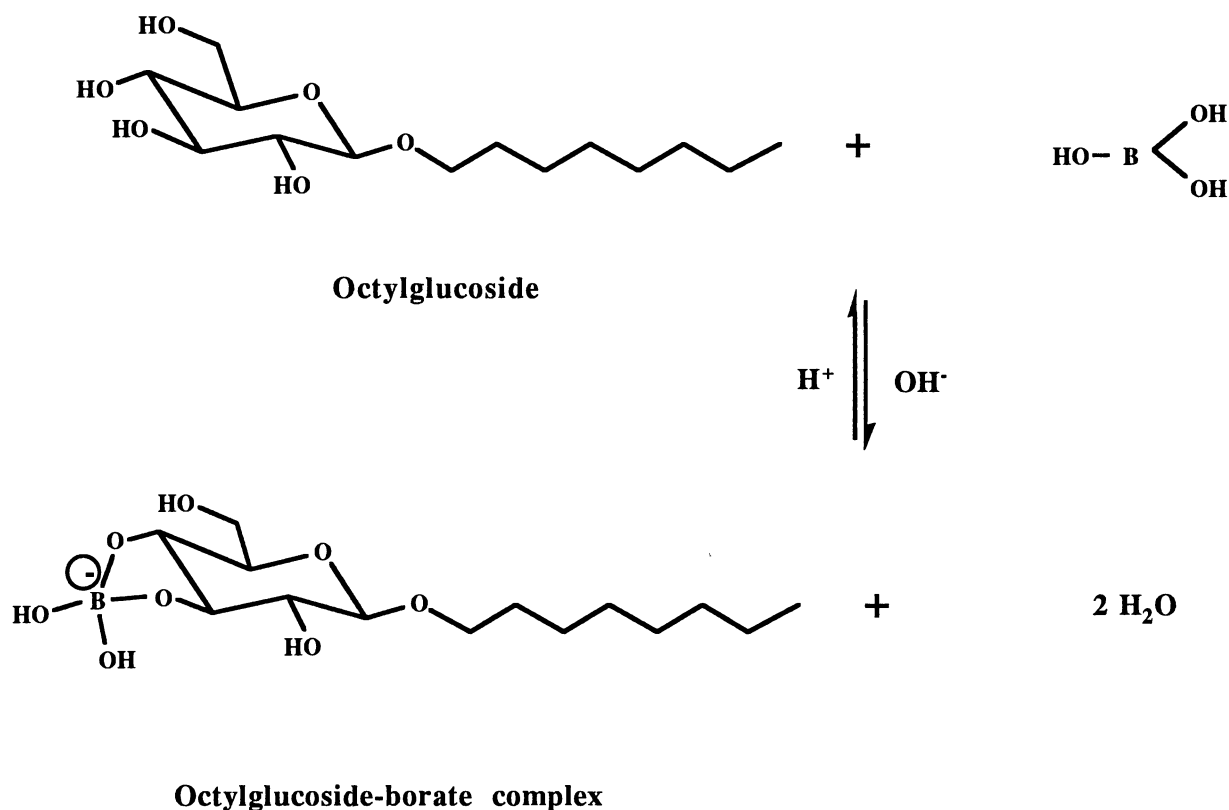
The manipulation of the surface charge density of the micelles under investigation is based on varying the extent of complexation between octylglucoside and borate. Figure 10 is a schematic illustration of the novel MECC system developed and evaluated in this work. It shows the mechanism of retention of neutral solutes and the control of the surface charge of the micelles through complexation with borate.

Octylglucoside which is a non-ionic surfactant, can acquire a negative charge upon complexing with borate. The process of octylglucoside-borate complexation has an equilibrium constant, K_{eq} , given by

$$K_{eq} = \frac{[C_8-Glc][Borate][OH^-]}{[C_8-Glc-Borate]} \quad (37)$$

where $[C_8-Glc]$, $[Borate]$, $[OH^-]$, and $[C_8-Glc-Borate]$ stand for the concentrations of octylglucoside, borate, hydroxide ions and octylglucoside-borate complex, respectively.

The reaction is as follows:



As a result of the complexation, the overall charge density of the micelles, ρ_{mc} , can be expressed as

$$\rho_{mc} = \frac{[C_8-Glc-Borate]}{[C_8-Glc] + [C_8-Glc-Borate]} \cdot \rho_{complex} \quad (38)$$

where ρ_{complex} is the charge density of the octylglucoside-borate complex. The change in the overall charge density will alter the electrophoretic mobility of the micelles $\mu_{\text{mc},e}$ (see Eqn 4). According to Eqn 16, without changing the electroosmotic flow, this process will lead to a change in t_{mc} . This is particularly important in the manipulation of "retention window" and separation behavior in MECC system.

Experimental

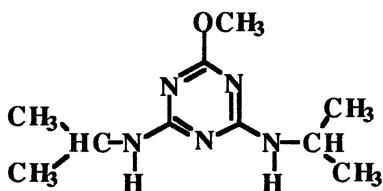
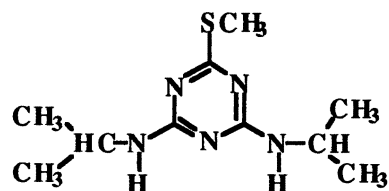
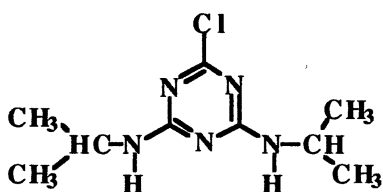
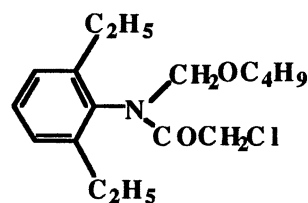
Instruments

The instruments used in this study for UV spectrophotometry and capillary electrophoresis measurements were the same as those described in the previous chapter. The untreated capillaries were rinsed successively with methanol, 0.1 M HCl, and water, and then filled with the running buffer. In order to maintain reproducibility, the capillary was rinsed with the running electrolyte between runs. In all the measurements, the running voltage was 15 kV.

Reagents and Materials

Octylglucoside was obtained from Sigma Chemical Co (St. Louis, MO, U.S.A.). Sodium borate, boric acid, sodium hydroxide, and hydrochloric acid were from Fisher Scientific (Pittsburgh, PA, U.S.A.). Deionized water was used to prepare the running electrolyte. All solutions were filtered with 0.2 μm Uniprep Syringeless filters from Genex Corp. (Gaithersburg, MD, U.S.A.) to avoid capillary plugging.

The herbicides, *i.e.*, prometon, prometryne, butachlor and propazine, were purchased from Chem Service (West Chester, PA, U.S.A.). The structures of the four herbicides are shown below:

**Prometon****Prometryne****Propazine****Butachlor**

Procedures

UV Spectrophotometry Measurements. Sample solutions were made by dissolving a small amount of prometon, prometryne, butachlor and propazine in distilled water containing a small amount of acetonitrile to enhance the solubility of the herbicides. After calibration of the instrument with the solvent (blank), absorption spectra were obtained for each of the above herbicides by scanning from 200 to 350 nm.

Figure 11 shows the UV spectra of the four herbicides. The maximum wavelengths, λ_{\max} , for prometon, prometryne, and propazine were found at 220, 223, and 223 nm respectively, while that of butachlor was at lower wavelength but with reasonable absorption at 220 nm. For this reason, the UV detector for capillary electrophoresis was set at 220 nm.

Sample and Micellar Solution Preparation. Due to the low solubility of the prometon and prometryne, the stock solutions of each herbicide were prepared by adding an excess amount of the pure compound to water. After stirring overnight, the

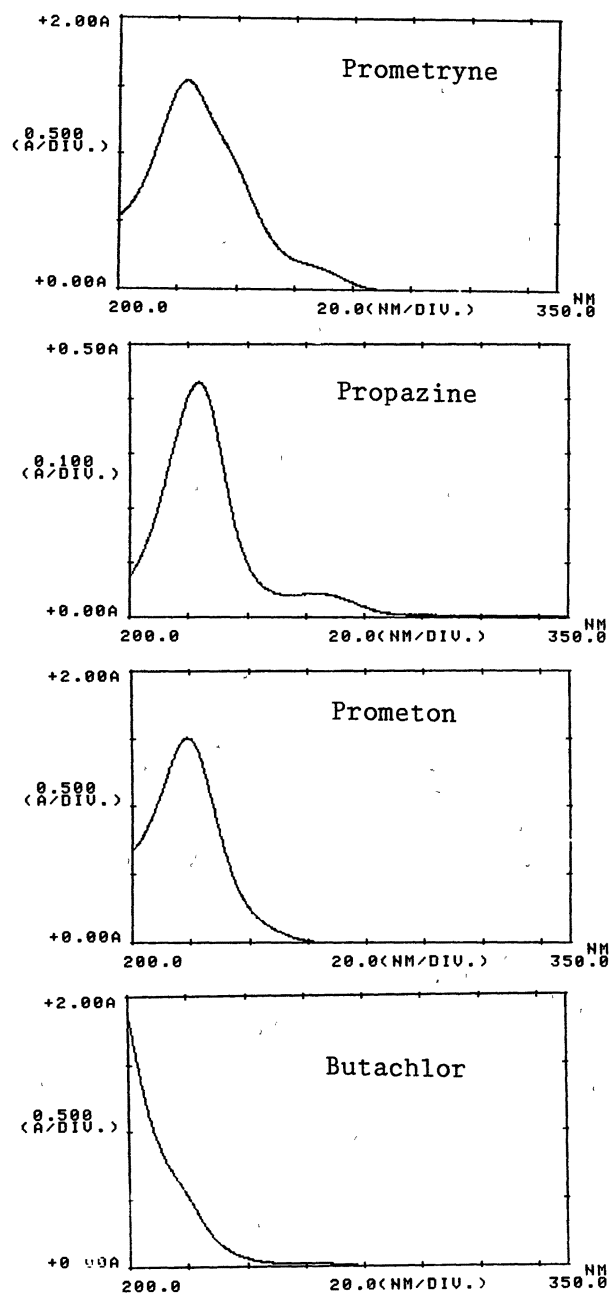


Figure 11 UV Spectra of the Herbicides

solution was filtered and refrigerated in a closed vial. In order to accurately determine the concentration of each stock solution, calibration curves were made for each herbicide from standards prepared by dissolving the herbicides in water-acetonitrile solutions. This allowed the preparation of standard solutions of accurate concentrations. The calibration curves were obtained by CZE using 10 mM phosphate buffer, pH 6.0. For the preparation of samples of propazine and butachlor, the herbicides were dissolved in the running electrolyte (micellar solution). The concentration of these stock solutions were determined in the same way as that of prometon and prometryne. The running electrolyte was prepared by dissolving proper amount of sodium borate, octylglucoside, and adjusting the pH to the desired value. The solutions were degased in an ultrasonic bath.

Mode of Injection. Both electromigration and hydrodynamic sample injection modes were used in this study. In the case of electromigration mode, the injection voltage which was the same as the separation voltage was applied for 5 to 10 seconds. This mode was used for the samples dissolved in water. The herbicides used in this study are electrically neutral and since they migrate with the bulk flow, injection by electromigration would not introduce discrimination. When the analytes were dissolved in the electrolyte containing the micelles, they associated with the charged micelles, which imparted them different negative charge densities due to the difference in the dissociation constants for the various herbicides with the micelles. In this case, gravity-driven flow (hydrodynamic mode) was used for sample injection, whereby sample reservoir was raised to a height of 20 cm above the outlet reservoir for 10 seconds.

Determination of t_{mc} and t_0 . The retention time of phenolphthalein, which is considered to be fully solubilized by the micelles, was considered as the retention time of the micelle, t_{mc} . The retention time of methanol was used as t_0 . Both

phenolphthalein and methanol were dissolved in the running electrolyte (*i.e.*, micellar solution).

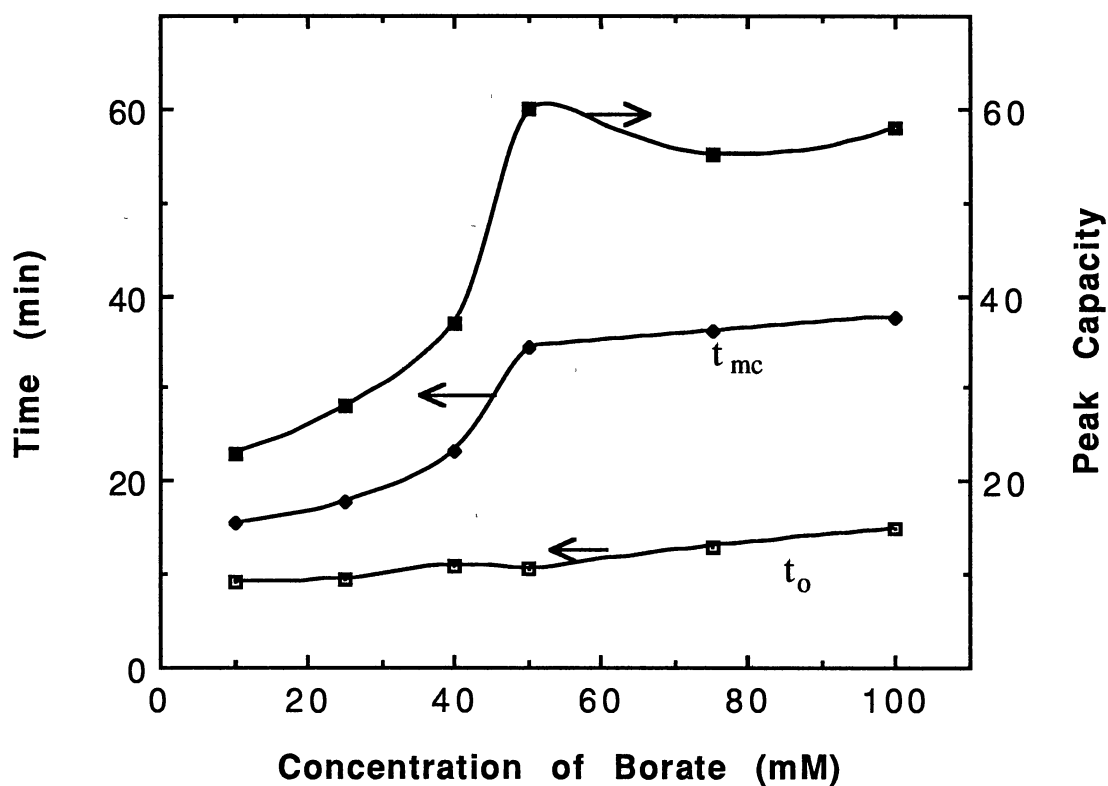
Results and Discussion

Effect of Operational Parameters

In order to evaluate the new micellar phase system, several operational parameters were studied using prometon and prometryne as model solutes. All the measurements were made at the same running voltage, and a separation distance of 50 cm (*i.e.*, from the injection end to the detection point).

Borate Concentration. To examine the effect of borate concentration on the separation properties of octylglucoside-borate micelles, the electrophoretic measurements were made with running electrolytes containing 40 mM octylglucoside, pH 10, at various concentrations of borate. Under these conditions, the amount of octylglucoside is well above its CMC, which has been reported to be 25 mM in pure water (75).

Figure 12 illustrates the effect of borate concentration in the running electrolyte on the retention window and peak capacity of the MECC system. It can be seen that the retention window increased significantly at borate concentrations between 10 to 50 mM. The optimal value seems to span between 50 and 100 mM. This wide range of concentration is important as far as the separation reproducibility is concerned. Indeed, a change in borate concentration will not introduce any appreciable fluctuation in the "retention window", $t_{mc} - t_0$. Referring to Fig. 12, the retention time of the inert tracer increased slightly with the borate concentration. At pH 10, the surface silanols of the



Separation capillary: untreated fused-silica, 50 cm (to the detection point), 80 cm (total length) x 50 μ m I.D.; Running electrolyte: 40 mM octylglucoside, pH 10; Sample injection: hydrodynamic, 5 seconds; Running voltage: 15 kV; Tracers: phenolphthalein (for t_{mc}) and methanol (for t_o); Detection: 220 nm. The experimental data points are the average of two measurements.

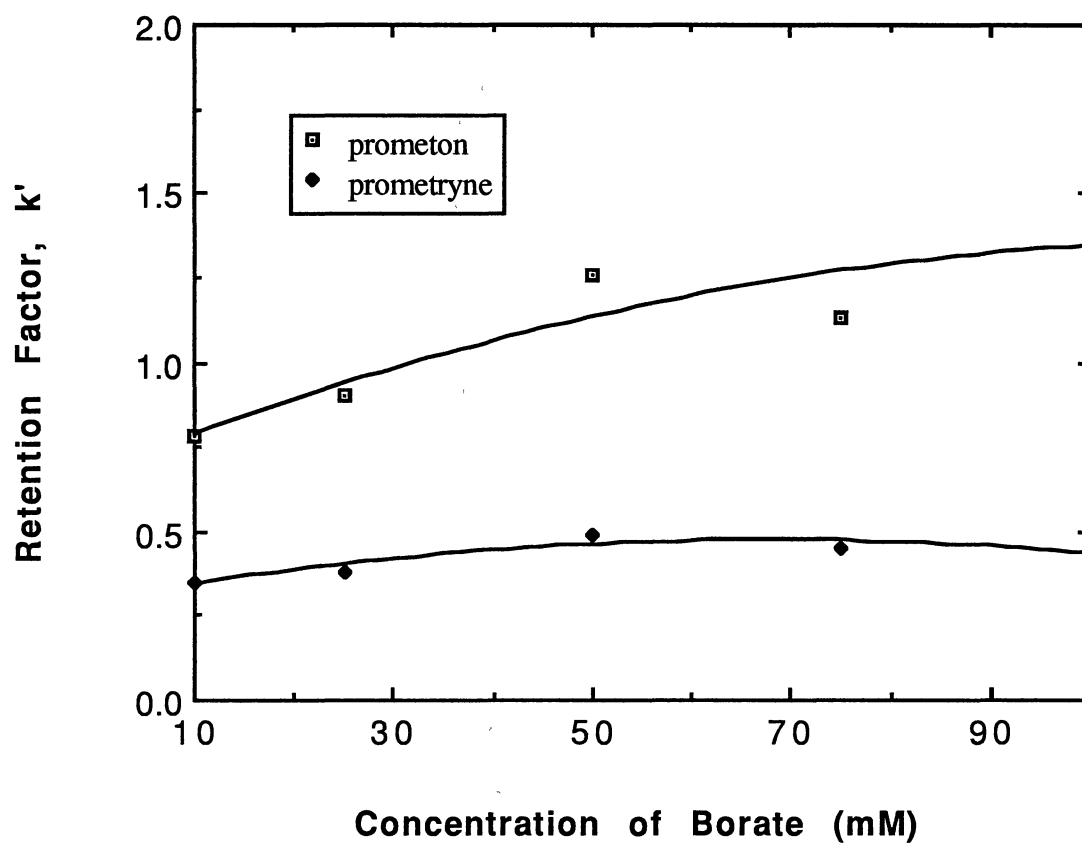
Figure 12 Effect of Borate Concentration on Retention Window and Peak Capacity

capillary are fully ionized and a constant electroosmotic flow is expected. However, increasing borate concentration leads to a decrease in the zeta potential (63), and in turn, the electroosmotic flow (see Eqn 2). This can explain the slight increase in the retention time of the inert tracer.

Unlike t_0 , the retention time of the micelles, t_{mc} , increased substantially at low concentrations of borate but remained constant at higher concentrations. The increase in the retention time of the micelles with borate concentration is due to an increase in the charge density of the micelles upon complexation between octylglucoside and borate ions. According to Eqn 37, if the concentrations of octylglucoside and hydroxide ions are kept constant, the magnitude of $[C_8\text{-Glc-Borate}]$ will increase with borate concentration. As a result, the overall charge density of the micelles, ρ_{mc} , will increase causing the electrophoretic mobility of the micelles, $\mu_{mc,e}$, to rise in the opposite direction to the electroosmotic flow. Since the electroosmotic flow was almost unchanged in the range of borate concentration from 10 mM to 100 mM, the net result was a decrease in the net mobility of the micelles, which in turn led to an increase in the retention time of the micelles. Thus, the separation window was elongated.

According to Eqn 38, at elevated borate concentrations, $[C_8\text{-Glc}]$ approaches zero, and therefore, $\rho_{mc} = \rho_{\text{complex}}$. As can be seen in Fig.12, upon exceeding a certain borate concentration, a saturation stage was reached. At this point, further increase in the concentration of borate did not bring about significant increase in the overall charge density of the micelles. The saturation stage was obtained at borate concentration around 50 mM, see Fig.12.

The retention factors, k' , of prometon and prometryne, were determined using Eqn 18. Figure 13 portrays the relationship between k' and the borate concentration. The retention factors of prometon and prometryne first increased at low borate concentrations, and then remained relatively unchanged at borate concentrations above



Sample: prometon and prometryne; Sample injection: electromigration, 10 seconds; Other experimental conditions are as in Fig.12. The experimental data points are the average of two measurements.

Figure 13 Effect of Borate Concentration on Retention Factor of Herbicides

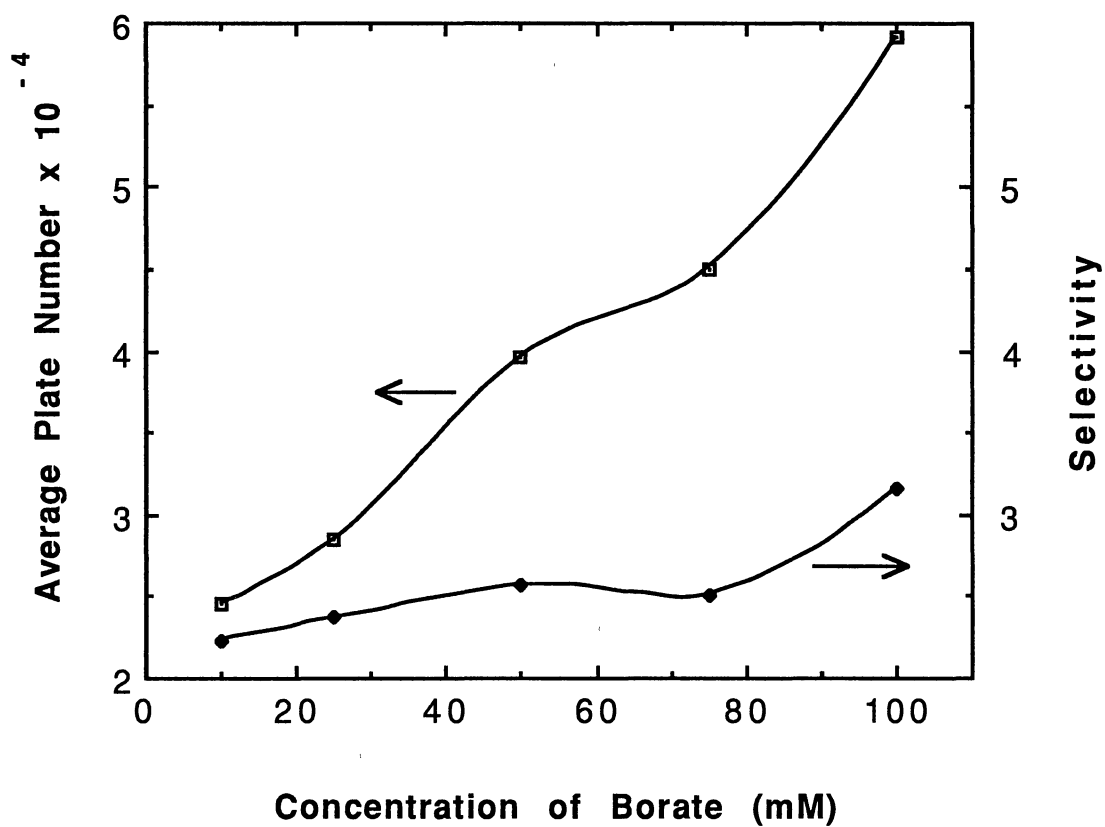
50 mM. This trend is analogous to that obtained with the retention time of the micelles and the explanation of the k' -borate concentration dependency follows the same reasoning.

The separation efficiencies, N , and the selectivity, α , were calculated using Eqns 12 and 19, respectively. The results are depicted in Fig. 14 for the two model solutes, prometon and prometryne.

According to Fig. 14, N increased with borate concentration. This may be due to the following phenomena. In MECC, the micelles are so small that there is no mass transfer limitation (76). Under these conditions, longitudinal molecular diffusion in the moving electrolyte is the ultimate limitation and Eqn 11a applies. Since increasing the borate concentration slightly decreased the flow velocity, *i.e.*, from 0.091 to 0.056 cm/sec, the amount of longitudinal diffusion in this velocity range is virtually unchanged. On the other hand, the mole fraction of charged micelles increased with borate concentration, and as a result, the average intermicellar distance decreased. Smaller intermicellar diffusion distances improve the kinetic of mobile phase mass transfer (77). Therefore, for the same amount of longitudinal molecular diffusion and reduced resistance to mass transfer in the moving electrolyte, N would increase with increasing borate concentrations in the running electrolyte.

The selectivity of the two herbicides also increased with borate concentration. This observation may indicate that the association constants of prometon and prometryne with the uncharged micelles (not complexed with borate) and the charged micelles (complexed with borate) are different.

The values of peak capacity were calculated using Eqn 22, and the results are presented in Fig. 12. As can be seen, peak capacity increased with borate concentration, and follows the same profile as that of t_{mc} . When compared to that of the inert tracer, the retention time of micelles, t_{mc} , increased significantly with borate concentration, and



Experimental conditions are as in Fig. 13. The experimental data points are the average of two measurements.

Figure 14 Effect of Borate Concentration on Separation Efficiency and Selectivity

as a consequence, the ratio t_{mc}/t_0 increased. The combined increase in the values of t_{mc}/t_0 and that of N would therefore produce an increase in peak capacity, see Eqn 22.

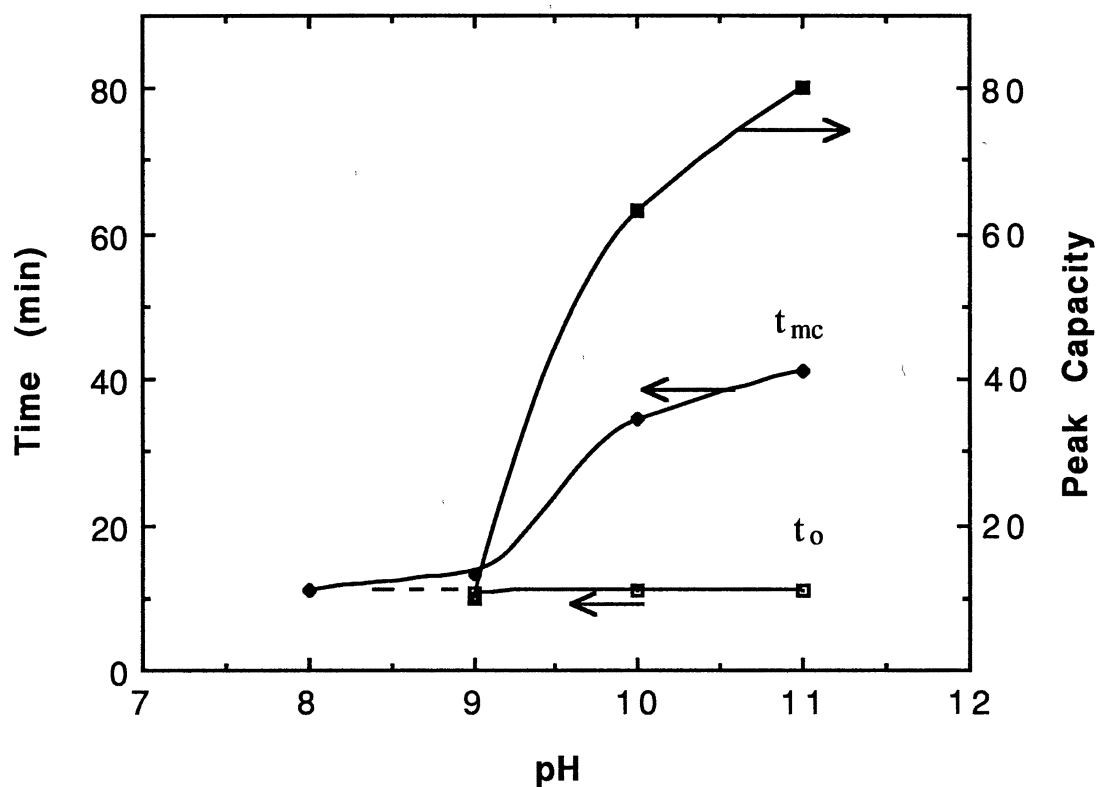
pH of the Running Buffer. To evaluate the effect of pH on the separation properties of the system under investigation, the electrophoretic experiments were carried out by running electrolytes containing 40 mM octylglucoside and 50 mM sodium borate at various pH.

Figure 15 illustrates the effect of pH on the "retention window", and peak capacity of the MECC system. The "retention window", $t_{mc} - t_0$, was greatly enlarged when the pH was raised from 9 to 11. Indeed, t_{mc} augmented significantly whereas t_0 remained relatively unchanged. The increase in t_{mc} with pH can be explained by Eqn 37. According to this equation, while keeping the concentrations of the octylglucoside and borate constant, any elevation in the concentration of hydroxide ions, $[OH^-]$, will lead to an increase in the concentration of octylglucoside-borate complex, with concomitant increase in the charge density of the micelles. On the other hand, t_0 remained constant in this pH range, because the silanol groups on the surface of the capillary are fully deprotonated above pH 8, and a further increase in pH will not produce more negative charge on the capillary surface. Therefore, the concentration of ionized surface silanols was unchanged, which resulted in a constant electroosmotic flow in this pH range.

As can be seen in Fig. 15, the peak capacity increased with electrolyte pH. This is due to the increase in N and the ratio t_{mc}/t_0 with increasing pH.

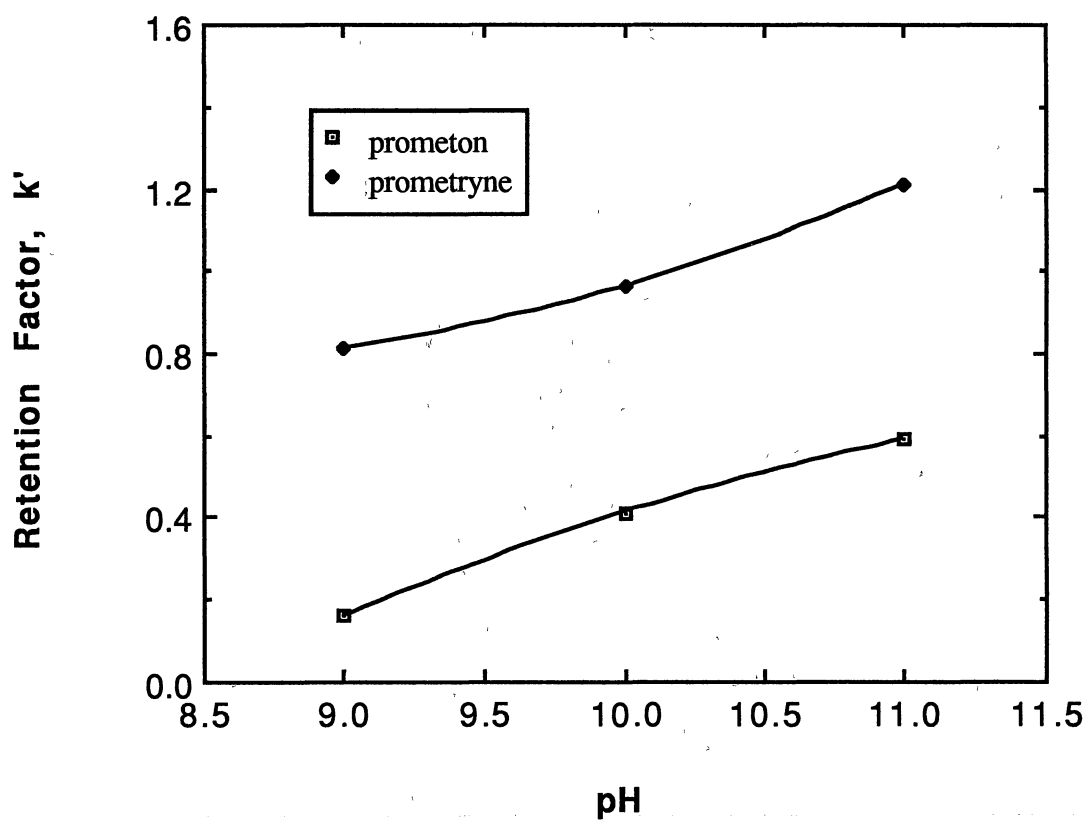
The plots of the retention factors of prometon and prometryne versus pH is shown in Fig. 16. The retention factors, k' , increased continuously in the pH range from 9 to 11; a trend similar to that of t_{mc} .

The separation efficiency and selectivity of prometon and prometryne were also pH dependent, as shown in Fig. 17. These results suggest that at higher pH, greater



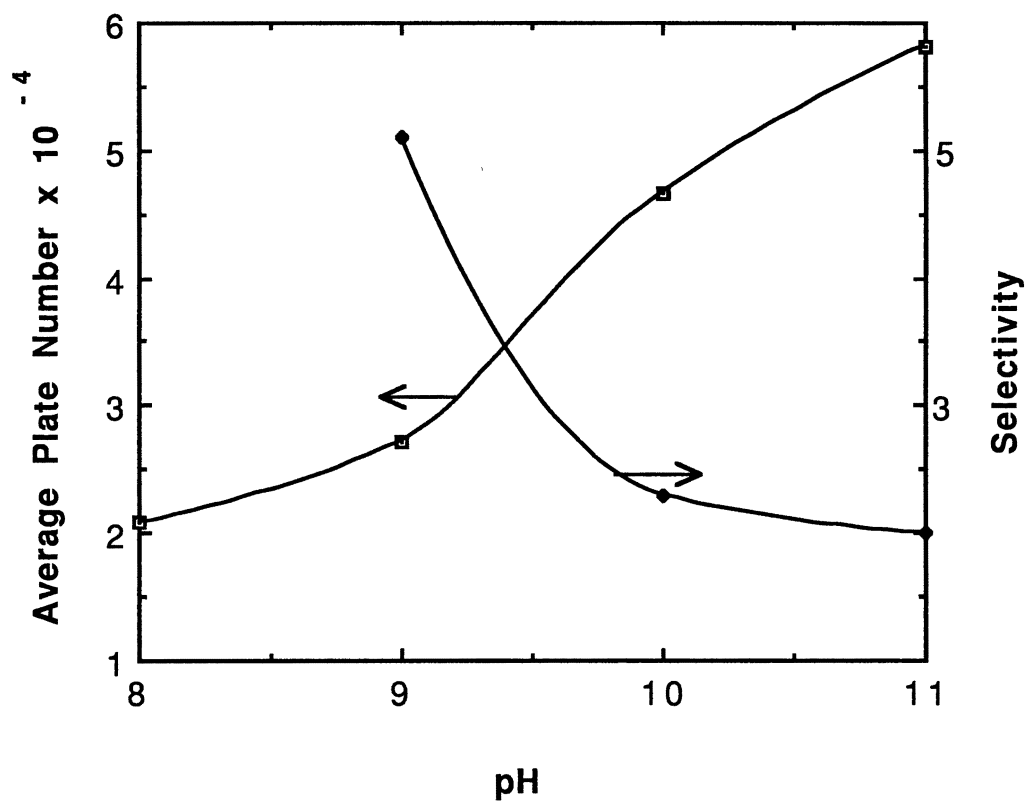
Running electrolyte: 40 mM octylglucoside, 50 mM sodium borate; Other experimental conditions are as in Fig. 12. The experimental data points are the average of two measurements.

Figure 15 Effect of pH on Retention Window and Peak Capacity



Samples: prometon and prometryne; Sample introduction: electromigration, 10 seconds; Other experimental conditions are as in Fig. 15. The experimental data points are the average of two measurements.

Figure 16 Effect of pH on Retention Factor



Experimental conditions are as in Fig. 16. The experimental data points are the average of two measurements.

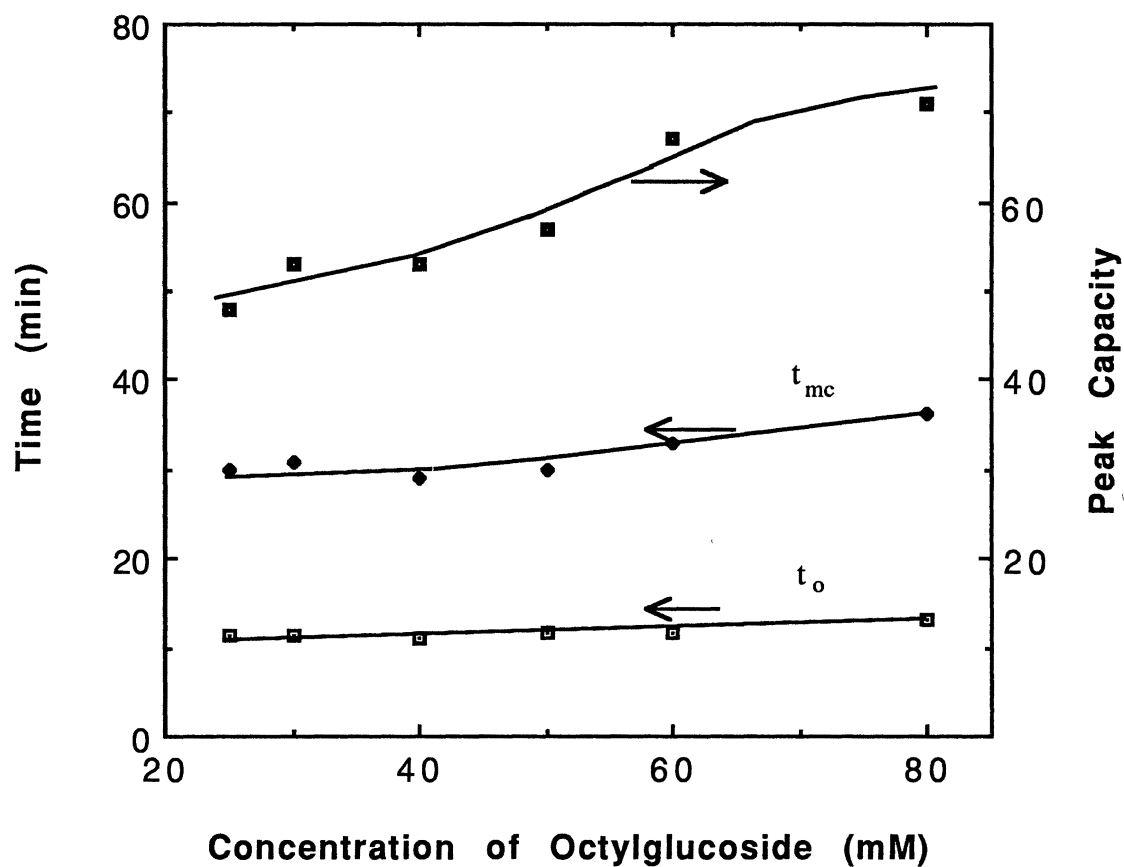
Figure 17 Effect of pH on Efficiency and Selectivity

separation efficiency can be obtained, may be due to the shorter intermicellar diffusion distance. The selectivity of the two herbicides decreased with increasing pH. This observation shows that the hydrophobicity of these two species is pH dependent.

Concentration of Octylglucoside. In order to study the effect of octylglucoside concentration on the effectiveness of the MECC system, the pH and the concentration of borate in the running electrolyte were kept constant. The running electrolyte was 50 mM sodium borate, pH 10, at various octylglucoside concentrations.

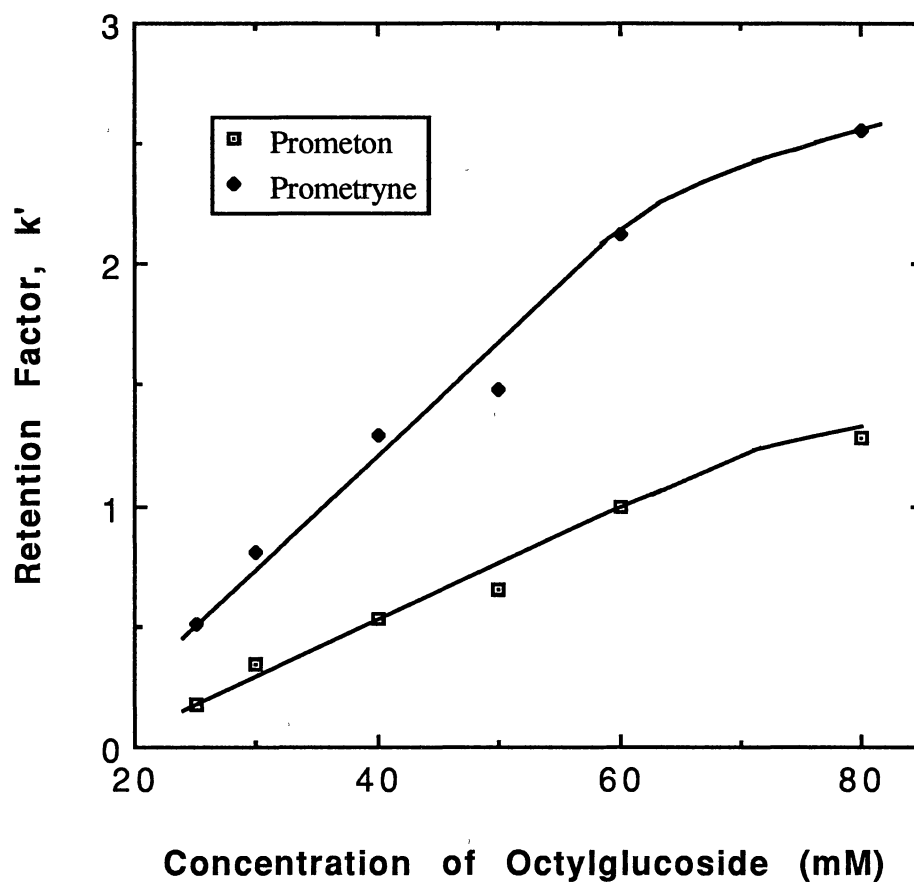
Plots of t_{mc} and t_0 versus octylglucoside concentration are shown in Fig. 18. As can be seen in Fig. 18, the retention window was kept almost constant regardless of the octylglucoside concentration. At constant borate and hydroxide ion concentrations, the increase in concentration of octylglucoside will lead to a higher concentration of octylglucoside-borate complex. However, this increase was not obvious since there was a relatively high concentration of borate (50 mM). As shown in Fig. 18, the retention time of the micelles, t_{mc} did not change significantly with increasing concentration of octylglucoside. The slight decrease in the electroosmotic flow was probably due to the increase in the viscosity of the running electrolyte as a result of high concentration of the surfactant. This is reflected by the increase in t_0 as shown in Fig. 18. The peak capacity of the MECC system also increased slightly in the range of octylglucoside concentration studied.

Increasing the octylglucoside concentration in the eluent corresponds to increasing the phase ratio, ϕ , which is defined as the ratio of volume of the pseudostationary phase to that of the mobile phase. The retention factor, k' , is related to ϕ and K through $k' = \phi K$. As can be seen in Fig. 19, plots of retention factor versus octylglucoside concentration are linear at low concentration of surfactant and leveled off at concentration greater than 60 mM.



Running electrolyte: 50 mM sodium borate, pH 10; Other experimental conditions are as in Fig. 12. The experimental data points are the average of two measurements.

Figure 18 Effect of Octylglucoside Concentration on Retention Window and Peak Capacity



Sample: prometon and prometryne; Sample introduction: electromigration, 10 seconds; Other experimental conditions are same as in Fig. 18. The experimental data points are the average of two measurements.

Figure 19 Effect of Octylglucoside Concentration on Retention Factor

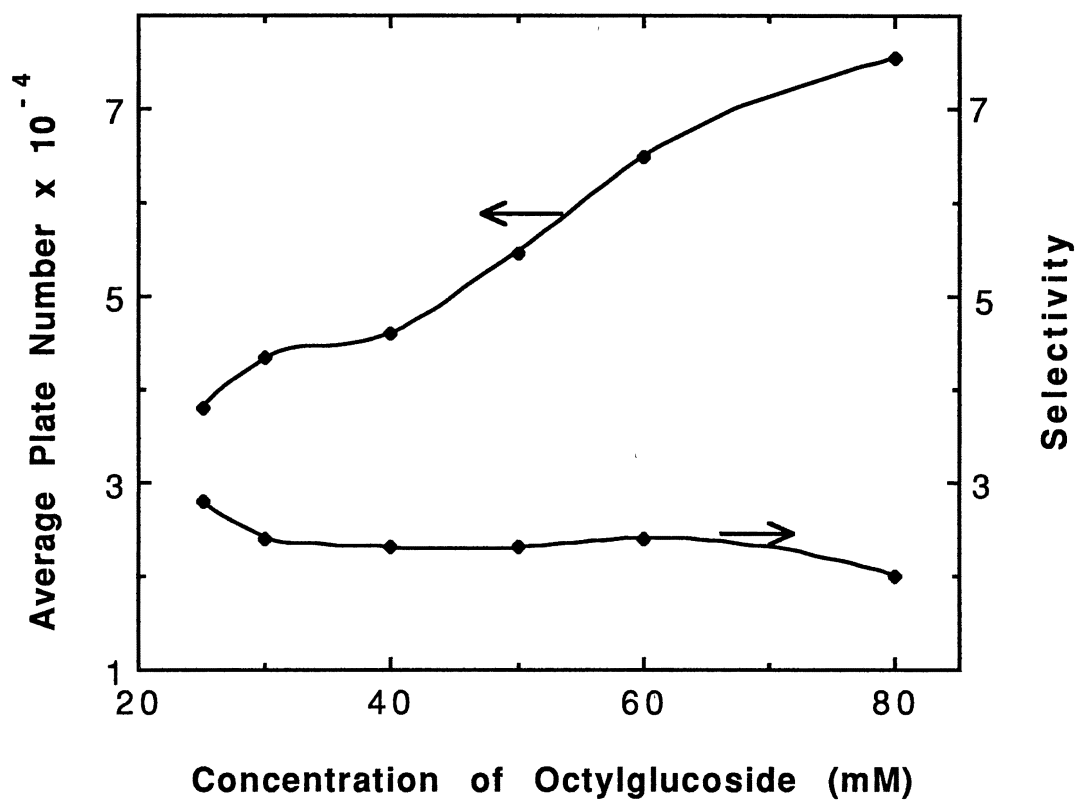
Plots of separation efficiencies, N , and selectivity, α , versus the concentration of octylglucoside are shown in Fig. 20. While the selectivity for the two herbicides was almost unchanged within the range of experimental errors, the average theoretical plate number increased with increasing concentration of octylglucoside. The higher separation efficiencies obtained at elevated octylglucoside concentration may be explained by the shorter diffusion distance between the micelles and concomitantly faster mass transfer in the mobile phase.

Typical Separation

Figure 21 is a typical electropherogram for the separation of the four herbicides, prometon, prometryne, propazine, and butachlor. The separation was carried out under the optimal condition, *i.e.*, in a buffer with 50 mM borate, and 40 mM octylglucoside, at pH 10. The four herbicides were completely resolved within 20 minutes. The structures of prometon, prometryne and propazine differ only by one functional group from each other (see page 48). All of them are non-ionic under the experimental conditions, and can not be separated by conventional capillary zone electrophoresis. This experiment shows the usefulness of MECC for the separation of electrically neutral compounds.

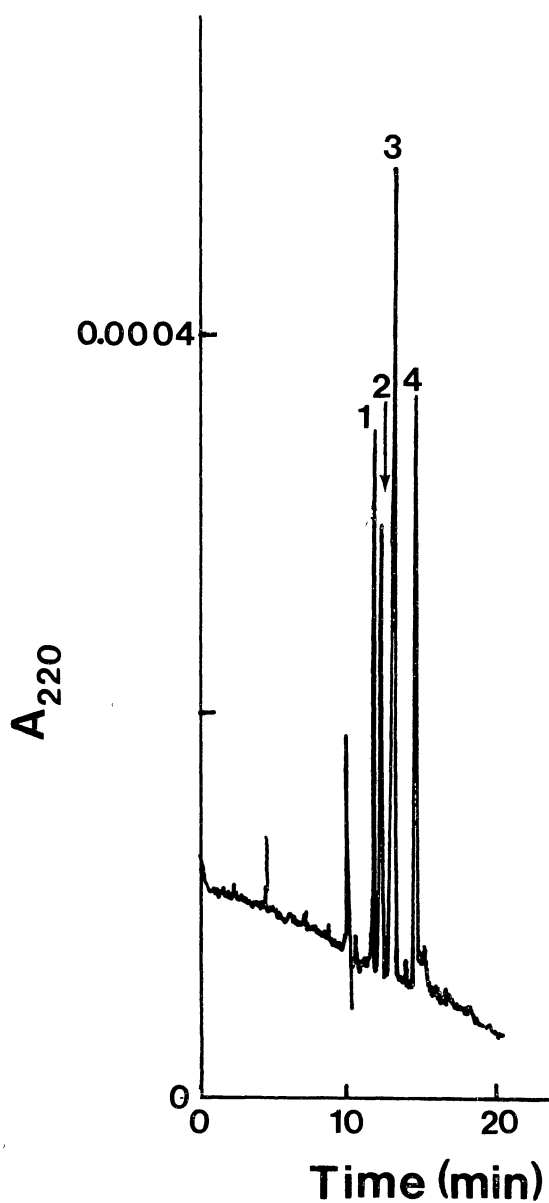
Limits of Detection

The limits of detection obtained in this work are listed in Table 5. The data were determined under conditions of Fig. 21, by injecting several dilutions of a relatively concentrated standard mixtures. The concentration limits correspond to a signal-to-noise ratio (S/N) of 3. The injected quantities were determined by Eqn 28. The detection limits show that as low as 1 $\mu\text{g/mL}$ (or a few micromolar) in terms of concentration or a few picograms in terms of absolute mass of solute injected can be determined.



Experimental conditions are as in Fig. 19. The experimental data points are the average of two measurements.

Figure 20 Effect of Octylglucoside Concentration on Efficiency and Selectivity



Separation capillary: same as in Fig. 12; Running electrolyte: 50 mM sodium borate, 40 mM sodium phosphate, pH 10; Injection: hydrodynamic, 10 seconds; Running voltage: 15 kV; Solutes: 1, 3.0 $\mu\text{g/mL}$ prometon; 2, 6.0 $\mu\text{g/mL}$ prometryne; 3, 2.0 $\mu\text{g/mL}$ propazine; 4, 8.0 $\mu\text{g/mL}$ butachlor; Detection: 220 nm.

Figure 21 Typical Electropherogram Illustrating the Separation of Neutral Herbicides

TABLE 5
LIMITS OF DETECTION

Sample solute	<u>Limit of Detection</u>			
	<u>Concentration</u> ($\mu\text{g/mL}$)	<u>Concentration</u> (μM)	<u>Injected Quantity</u> (pg)	<u>Injected Quantity</u> (femtomole)
Prometon	1.0	4.4	6.0	26.5
Prometryne	2.0	8.3	12	49.9
Propazine	0.7	3.0	4.2	18.0
Butachlor	2.7	8.7	16	52.3

Conclusions

Micellar electrokinetic capillary chromatography shows promise for the determination of neutral organics. The new MECC system with micelles of adjustable surface charge density allowed the control of the "retention window" by altering some of the operational parameters. The detection limits was quite promising.

However, as one of the techniques of capillary electrophoresis, MECC also suffers from its small sample loadability. Since the detection volumes are usually in the range of picoliters, further decrease in sample concentration is limited due to the detector sensitivity. To solve this problem, concentrating dilute samples prior to analysis is necessary. The next chapters provide solutions for the analysis of dilute samples.

CHAPTER IV

ON-LINE PRECONCENTRATION OF NEUTRAL SPECIES WITH TANDEM OCTADECYL CAPILLARIES- CAPILLARY ZONE ELECTROPHORESIS

Introduction

As described in the previous chapters, capillary electrophoresis employs high electric fields to yield rapid separations. In order to dissipate Joule heating resulting from the passage of current through the electrolyte inside the tube, capillaries of 25-100 μm I.D. are used. With such small diameter capillary tubes, the injection volume must be small (*i.e.*, 1-5 nL) in order to achieve high separation efficiencies. For this reason samples must be concentrated so that the thin plug injected would contain a detectable amount of the solutes. However, the requirement of concentrated samples is often difficult to meet, especially for environmental pollutants and biological samples.

Although this problem has been recognized since the introduction of capillary electrophoresis, little or no attention has focused on developing devices for sample concentration, especially on-line preconcentration. Recently, on-line preconcentration by isotachopheresis and electrophoresis were introduced (78-80). However, these techniques have some drawbacks. The isotachopheretic concentration mode is difficult to automate and is limited by the choice of electrophoresis buffers. Also, positive and negative analytes cannot be determined at the same time. The electrophoretic concentration method has a limited loadability, which means only small sample volume can be introduced.

In this regard, we have developed capillaries with interactive walls for on-line preconcentration of dilute samples. This chapter will discuss the performance of tandem octadecyl capillaries-capillary zone electrophoresis in concentrating neutral species of environmental interest.

In general, on-line preconcentration has several advantages over off-line preconcentration. With on-line preconcentration, sample contamination and decomposition can be effectively minimized. As will be demonstrated in this chapter and the following chapter, with interactive preconcentration open tubular capillaries, large amount of sample can be introduced without significant loss in separation efficiency, and consequently very low detection limit in terms of sample concentration can be achieved.

Principles

The accumulation of solutes on the capillary inner surface is an adsorption process, which can be represented as the reversible reaction of solute S in the liquid phase with an adsorption site A on the solid surface to form adsorbed S, *i.e.*, SA:



The distribution coefficient K_x of the above equilibrium is defined as

$$K_x = \frac{X_{SA}}{X_S X_A} \quad (39)$$

where X_{SA} , X_S , and X_A are mole fractions of SA, S, and A. K_x is considered as constant if the intermolecular interactions in each phase is assumed to be constant as X_{SA} and X_S vary. If the fractional coverage of sites by the adsorbed solute is defined as θ , then $X_{SA} = \theta$ and $X_A = 1 - \theta$. Substitution of X_{SA} and X_A into Eqn 39, yields the equation of Langmuir isotherm (81):

$$K_x = \frac{\theta}{X_S(1 - \theta)} \quad (40)$$

or

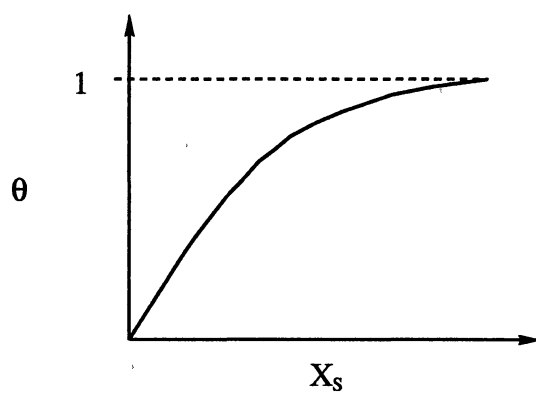
$$\theta = \frac{K_x X_S}{1 + K_x X_S} \quad (41)$$

A Langmuir isotherm, *i.e.*, a plot of θ versus the molar fraction of S in the nonadsorbed phase, X_S , is shown in Fig. 22a. At low solute concentrations, X_S is very small so that $K_x X_S \ll 1$, we have $\theta \approx K_x X_S$, and a linear isotherm is obtained. Also as illustrated in Fig. 22a, when the solute concentrations are large so that $K_x X_S \gg 1$, we have the limiting value of θ , $\theta \approx 1$, and the isotherm flattens out, *i.e.*, $K_x \approx 0$. This means that at high concentrations of solute, the adsorption sites become saturated with adsorbed solute molecules, and the concentration of solute in the adsorbed phase approaches a maximum value. The solute concentrations were relatively low in the on-line preconcentration studies. Therefore, linear isotherms were expected.

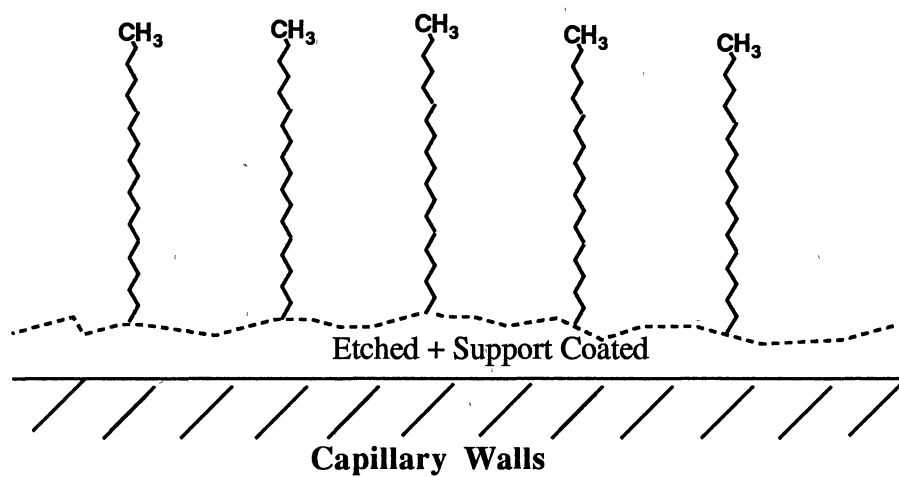
The capillary used in this study consisted of two sections connected with a Teflon tube having an inner diameter of the same size as the outer diameter of the two capillaries. The first part is a preconcentration capillary, *i.e.*, an open-tubular reversed-phase chromatography column with bonded octadecyl functions on the inner wall. The second part is a separation capillary, *i.e.*, a CZE capillary.

The on-line preconcentration with octadecyl capillaries exploits the principles of reversed-phase chromatography, in which the stationary phase is nonpolar with respect to the mobile phase. Figure 22b illustrates the structure of the inner surface of octadecyl capillaries used in this study.

As the sample is introduced, it first enters the preconcentration capillary, and is accumulated at the interactive walls. Samples are retained by the octadecyl groups by hydrophobic interaction. Since this type of interaction is non-selective, octadecyl



(a)



(b)

Figure 22. Typical Shape of Langmuir Isotherm (a), and Schematic Illustration of the Idealized Structure of Octadecyl Preconcentration Capillary (b)

capillaries can be applied for a wide variety of compounds provided that they have non-polar functions.

The on-line preconcentration process involves two consecutive steps: the accumulation of sample onto the walls of the preconcentration capillary, and the stripping of the accumulated solute from the capillary walls. The introduction of dilute samples should be carried out in the presence of a binding electrolyte (e.g. aqueous solution) that affords the strongest interactions between the analyte and the interactive walls. In the debinding step, the accumulated solutes on the walls of the preconcentration capillary should be stripped off the walls with a strong debinding electrolyte (e.g. hydro-organic solution) so that they enter the separation capillary as a thin plug whereby separation starts. The binding electrolytes used in this study were sodium phosphate solutions, whereas the debinding electrolytes were sodium phosphate solutions containing acetonitrile. Acetonitrile served as the debinding agent.

Experimental

Instruments

The instruments used in this study was the same as that described in the previous chapters except the modification in the capillary. The capillary used in this study composed of two capillaries connected in series. The first one was the preconcentration capillary, which had a length of 20 cm and an inner diameter of 50 μm . The second one was the separation capillary, which had a total length of 60 cm with 30 cm to the detection point. Untreated fused-silica capillary was used as the separation capillary.

Reagents and Materials

Colloidal silica, Ludox HS-40, was a gift from Du Pont (Willmington, DE).

Ammonium hydrogen bifluoride was from Fisher Scientific Company (Fair Lawn, NJ). Dimethyloctadecylchlorosilane and octadecyltrichlorosilane were from Petrarch Systems Inc (Bristol, PA). Naphthol was purchased from Aldrich (Milwaukee, WI). All the other chemicals and materials used in this study were the same as those described in the previous chapters.

Procedures

Capillary Surface Modification. The inner surface of the preconcentration capillaries were roughened before the bonding of the interactive functions (see Fig. 22b). The purpose of this treatment is to increase the specific surface area of the capillary wall and in turn the concentration of the interactive functions on the surface, so that larger amount of the analytes can be accumulated. This treatment involved etching, and in most cases, subsequent coating with colloidal silica.

In the etching process, the capillaries were filled with a 5% (w/v) solution of ammonium hydrogen bifluoride in methanol and allowed to stand for 1 hour before the solution was removed with a flow of nitrogen gas (82). The capillaries were then sealed in flame and heated at 250 °C or 300 °C for 5 hours. At high temperature, ammonium hydrogen bifluoride dissociates to produce gaseous hydrogen fluoride and ammonia (82). Thereafter, the capillaries were flushed with 0.01 M HCl, water and finally stored in HPLC grade methanol. Etching of fused-silica with hydrogen fluoride has been shown to produce pits of different diameters on the surface (83).

To prepare support coated capillaries, the etched tubes were filled with a 10% (w/v) colloidal silica solution and heated at 250 °C for 1 hr. This treatment was repeated 3 times and finally the capillaries were stored in HPLC grade methanol.

The preparation of capillaries with surface-bound octadecyl functions was carried out as follows: the etched and/or support coated capillaries were filled with a

solution of 0.2 g/mL octadecylmonochloro- or trichlorosilane in toluene, and heated at 110 °C for 1 hour. This treatment was repeated twice. After this treatment, the capillaries were flushed with acetone and stored in HPLC grade methanol.

In this study, the capillary surface was either etched or etched and then coated with colloidal silica in order to increase the surface area available for the attachment of octadecyl functions. The octadecyl capillary tubes are denoted by ODS-monofunctional-Cap, or ODS-trifunctional-Cap, to distinguish between capillaries coated with octadecyldimethylchlorosilane or octadecyltrichlorosilane, respectively.

Chromatographic Measurement with Open-tubular Octadecyl columns. To determine the retentivity of the octadecyl preconcentration capillaries toward the pollutants under investigation, a gravity-driven flow was used for both sample injection and the measurement of retention time. The reservoir at one end was raised to 20 cm above the outlet reservoir. Sodium nitrate was used as the inert tracer, since it is not retained by the octadecyl preconcentration capillary and detects well in UV. The retention factor was calculated using the following equation:

$$k' = \frac{t_r - t_0}{t_0} \quad (42)$$

where t_r and t_0 are the retention time of the sample and the the inert tracer, respectively.

Binding and Debinding Processes. The running electrolytes were prepared in deionized water. Dilute samples were prepared in the binding electrolyte. All samples and electrolytes were filtered, as described in the previous chapter.

For all types of solutes, sample introduction (or feeding) was carried out by either electromigration or hydrodynamic flow at the anode end. When the electromigration mode was used for sample introduction, the injection voltage was the same as that for the separation. The debinding electrolyte was also introduced by

electromigration. When the hydrodynamic mode was used, sample reservoir was raised to a certain height above the outlet reservoir. The debinding electrolyte was allowed to flow under hydrodynamic flow for the same period of time as that for the sample introduction. Then the reservoir at the anode end was lowered to the same height as that of the outlet reservoir and the voltage was applied.

In both cases, the volume and the amount of sample introduced were determined by Eqn 27, and 28, respectively. Between runs, the capillaries were flushed successively with acetonitrile, water, and the binding electrolyte. Thereafter, the capillaries were allowed to equilibrate for 10 to 20 minutes with the binding electrolyte before the next run.

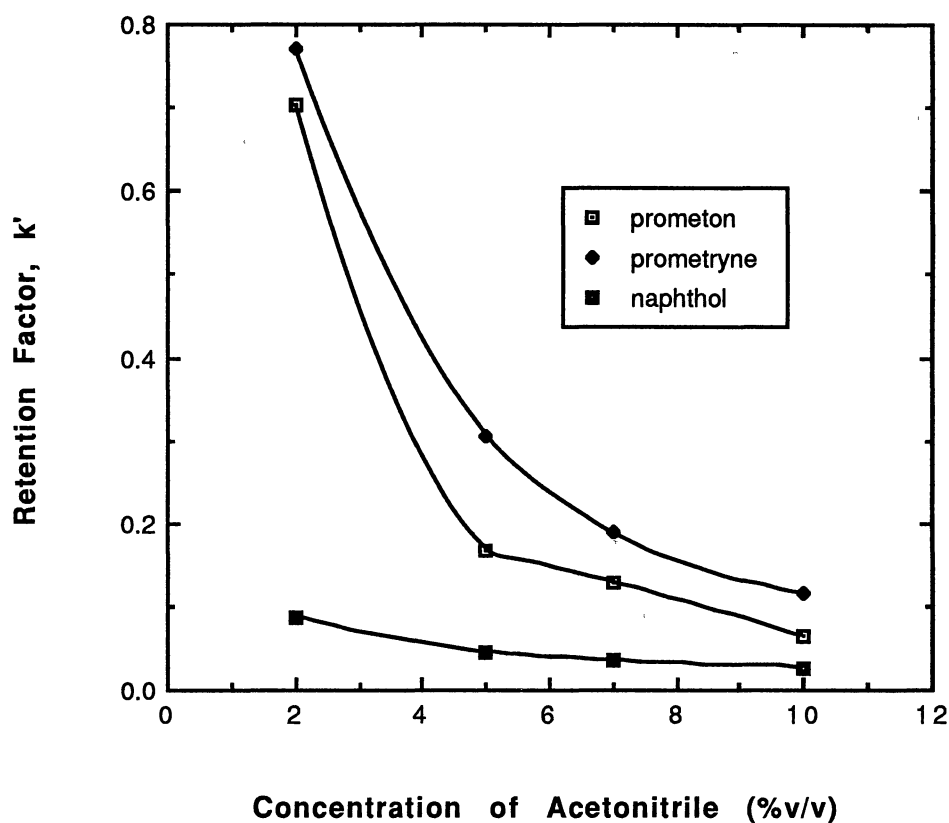
Results and Discussion

Normal Detection Limits with CZE

To evaluate the preconcentration approach under investigation, two herbicides, prometon and prometryne were chosen as neutral solutes to examine the detection limit with CZE alone. Under normal injection conditions, *i.e.*, the sample was introduced as a thin plug, the detection limits for both prometon and prometryne were 1 $\mu\text{g/mL}$ (*i.e.*, 4.4 and 8.3 micromolar for prometon and prometryne, respectively). To further decrease this detection limit, preconcentration is necessary.

Open-tubular Chromatography with Preconcentration Capillaries

The retention of octadecyl capillaries toward the solutes of interest was determined by elution chromatography with a gravity-driven flow (see experimental for detail). Figure 23 illustrates the results obtained with prometon, prometryne and naphthol by plots of retention factor, k' , versus percent acetonitrile (v/v) in the eluent.



Preconcentration capillary: ODS-trifunctional-Cap, etched at 300 °C, 20 cm x 50 μm I.D.; Separation capillary: untreated, 30 cm (to the detection point), 60 cm (total length) x 50 μm I.D.; Running electrolyte: 10 mM sodium phosphate, pH 6.0, at various percent acetonitrile (v/v); Sample injection: hydrodynamic, $\Delta h = 20$ cm, 10 seconds; Inert tracer: sodium nitrate; Detection: 220 nm. The experimental data points are the average of two measurements.

Figure 23. Retention Factor as a Function of Acetonitrile Concentration in the Mobile Phase

As shown in Fig. 23, these species were retained by the preconcentration capillaries to different extent. Prometon and prometryne were more retained than naphthol. This may due to their larger size (see the structures in chapter III) than that of naphthol. The presence of the two isopropyl groups in prometon and prometryne imparted to these solutes stronger hydrophobic interactions with the octadecyl functions of the preconcentration capillaries. Also, the unshared pairs of electrons on the nitrogen atoms in prometon and prometryne may form hydrogen bonds with the unreacted silanol groups of the surface of octadecyl capillaries surfaces, *i.e.*, silanophilic interaction (84). These may explain the higher retention for prometon and prometryne when compared with naphthol. The only difference in the structures of prometon and prometryne is that the methoxy group in prometon is replaced by a methylthio group in prometryne. Since oxygen is more electronegative than sulfur, the methoxy group is more polar than methylthio group. Therefore, prometryne is more hydrophobic than prometon. This may explain the slightly higher retention of prometryne. In all the cases, the retention factors decreased rapidly with increasing acetonitrile concentration in the mobile phase.

This experiment shows the ability of octadecyl preconcentration capillaries to retain neutral solutes when the mobile phase is pure aqueous buffer. It also shows that relatively high concentration of acetonitrile is needed to elute accumulated sample from the capillary wall.

Effect of Operational Parameters

In order to determine the optimum conditions for the preconcentration with octadecyl preconcentration capillaries, naphthol was chosen as a model solute to study the effects of various operational parameters. These parameters are the concentration of debinding agent, feeding time and capillary surface treatment .

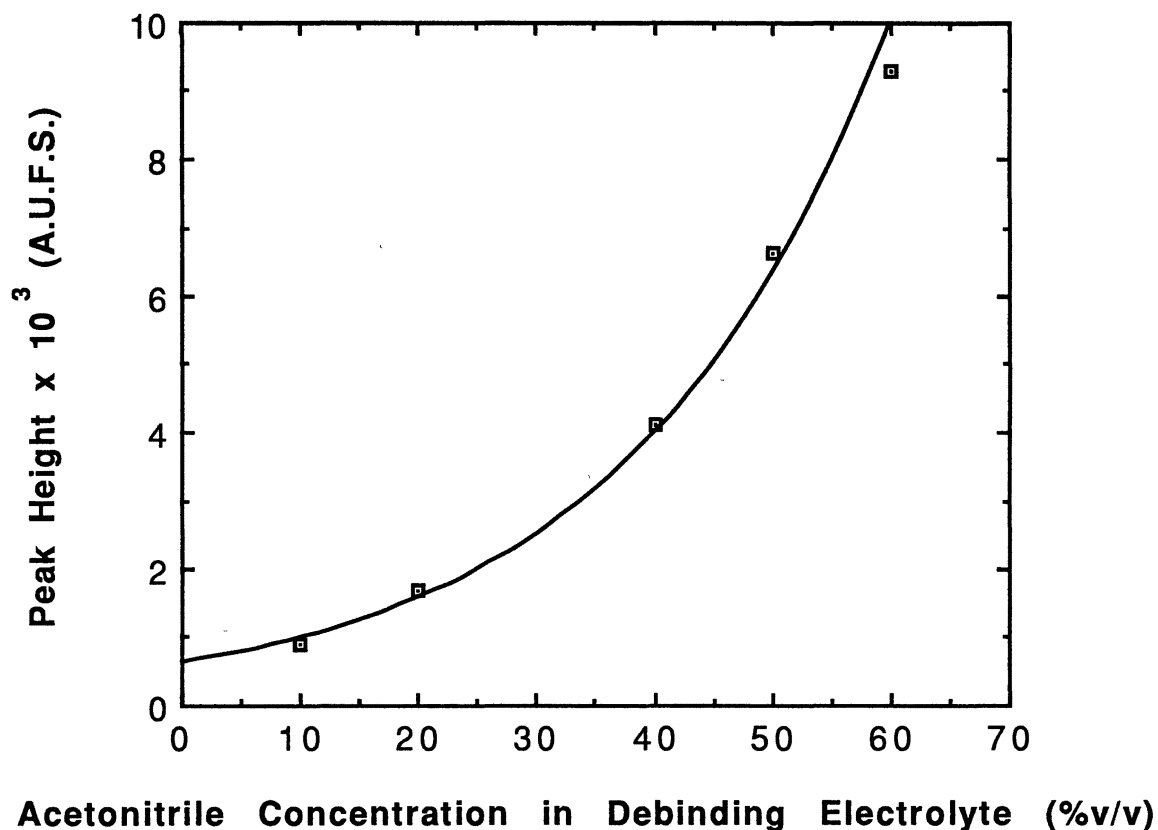
Concentration of Debinding Agent. In this study, acetonitrile was chosen as the

debinding agent. Figure 24 shows the effect of acetonitrile concentration in the debinding electrolyte on the peak height of desorbed naphthol. As expected, the signal increased with the concentration of acetonitrile. This means that high concentration of debinding agent can result in better recovery of the sample. However, high concentration of organic solvent led to a large breakthrough signal, which caused problem in the determination of very dilute samples.

Feeding Time. The effect of feeding time is shown in Fig. 25. As the feeding time increased the signal increased rapidly first and then leveled-off. This means that an adsorption equilibrium was reached between the feed and the inner surface of the preconcentration capillary, and further increase in feeding time did not lead to more accumulation of solute.

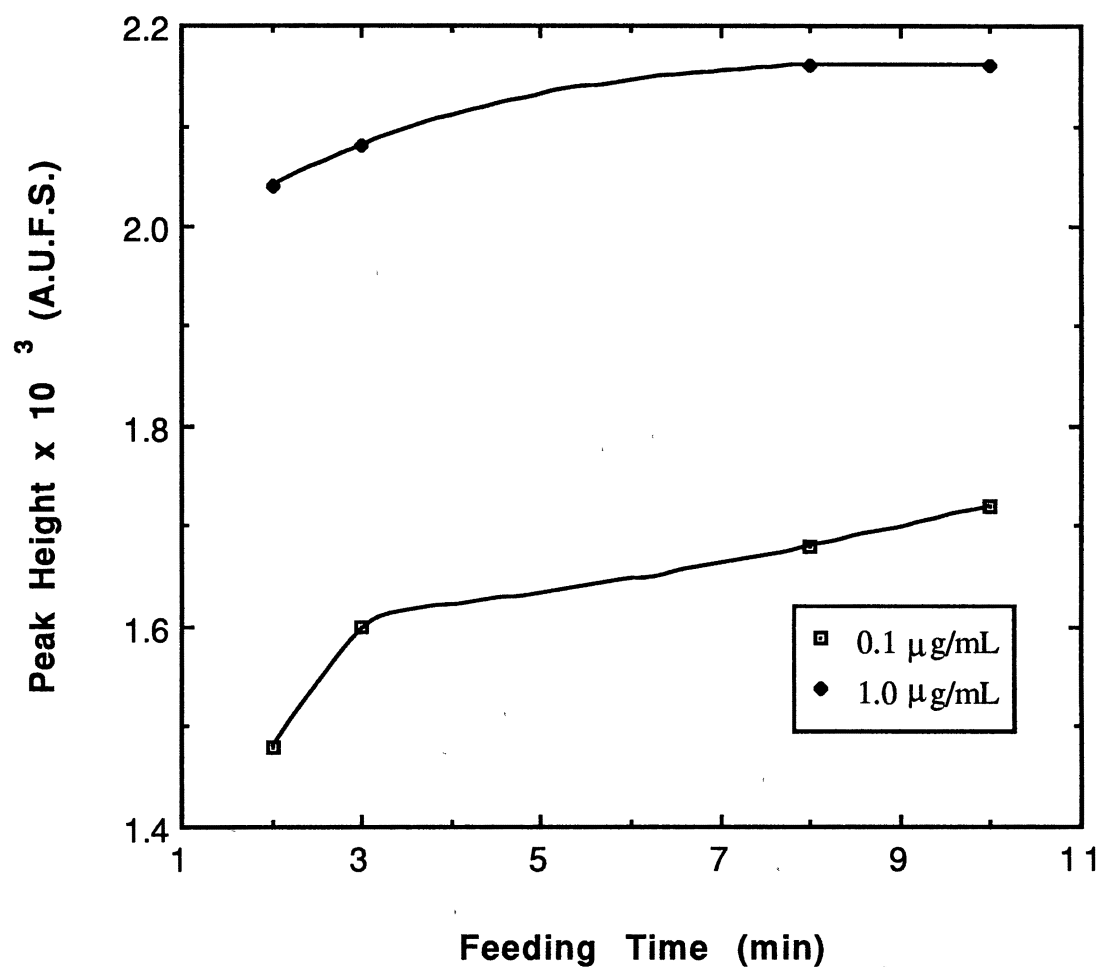
Capillary Treatment. The capillary inner surface treatment is critical for the quality of preconcentration. The effect of this treatment on the preconcentration process was studied by comparing several octadecyl capillaries whose inner surfaces were treated differently. The results are illustrated in Fig 26 in terms of peak height of naphthol versus sample concentration. For comparison, the result obtained by normal CZE (*i.e.*, without preconcentration) is also shown.

According to these plots, with the same sample concentration, the highest detector signal was obtained with the capillary whose inner surface was etched, support coated and bonded with trifunctional octadecyl silane. The signal obtained by normal CZE was much less than those obtained with on-line preconcentration. As shown in Fig. 26, with the use of octadecyl preconcentration capillaries, the detectability of CZE can be increased 40-50 times, when the surface coverage with octadecyl functions is high, curve 4 in Fig. 26.



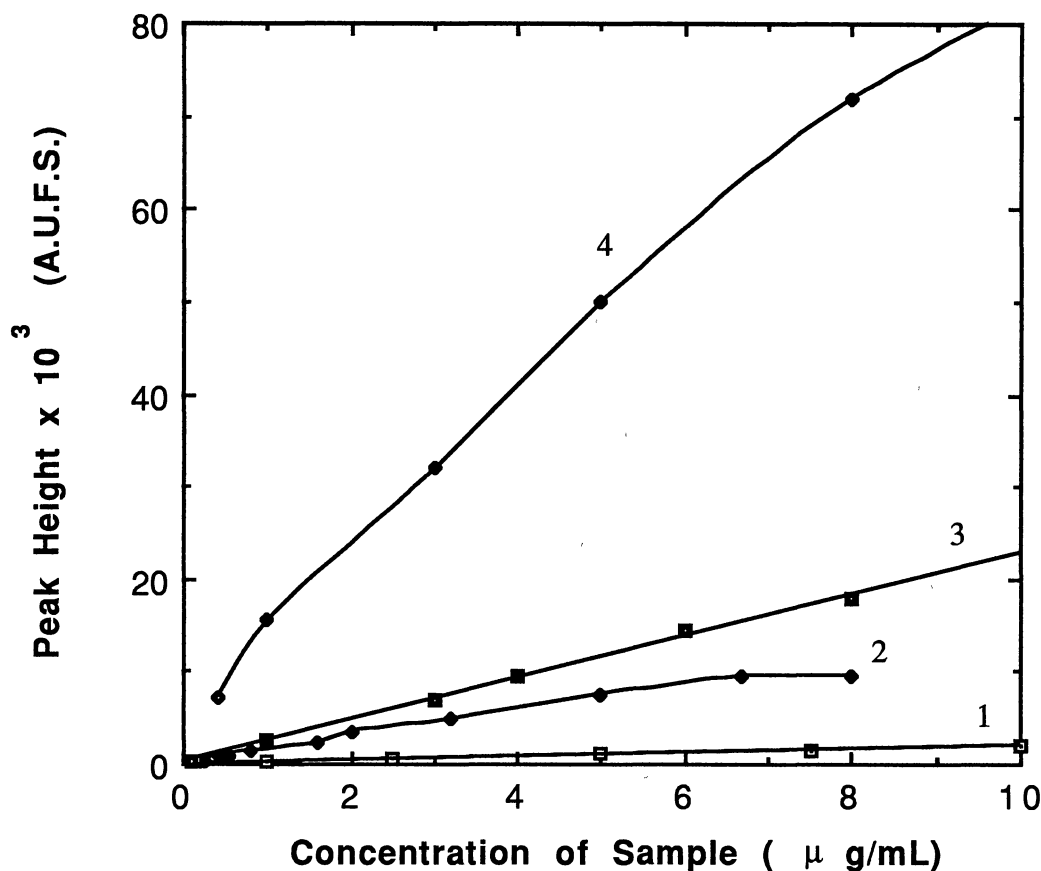
Preconcentration capillary: ODS-monofunctional-Cap, etched at 250 °C , 20 cm x 50 μm I.D.; Separation capillary: same as in Fig. 23; Binding electrolyte: 50 mM sodium phosphate, pH 6.5; Debinding electrolyte: acetonitrile in binding electrolyte; Sample: 1.3 $\mu\text{g/mL}$ naphthol; Sample introduction: electromigration, 5 min; Running voltage: 15 kV; Detection: 226 nm. The experimental data points are the average of two measurements.

Figure 24. Effect of Acetonitrile Concentration in the Debinding Electrolyte



Debinding electrolyte: 50% (v/v) acetonitrile in binding electrolyte; Sample: naphthol; other experimental conditions are as in Fig. 24.

Figure 25 Effect of Feeding Time



Sample: naphthol; Running voltage: 15 kV; Detection: 226 nm.

1: Normal injection; separation capillary are as in Fig 23; Sample injection: electromigration, 10 seconds;

2, 3,4: Preconcentration capillaries: 20 cm x 50 μm I.D., (2) ODS-monofunctional-Cap, etched at 250 °C , (3) ODS-trifunctional-Cap, etched at 250 °C , (4) ODS-trifunctional-Cap, etched at 250 °C, support coated; Separation capillaries: same as in Fig. 23. Binding and debinding electrolytes are as in Fig. 25; Sample injection: electromigration: 5 min.

The experimental data points are the average of two measurements.

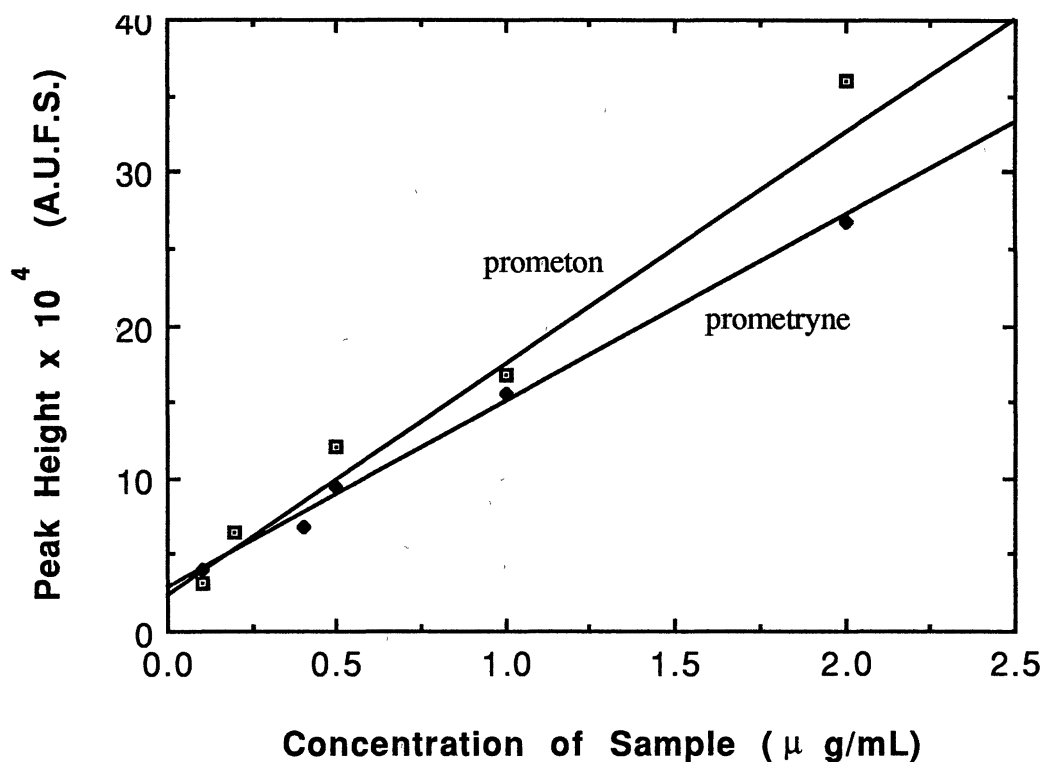
Figure 26 Effect of Capillary Surface Concentration in Octadecyl Functions

Quantitative Determination of Dilute Samples with Octadecyl Preconcentration Capillaries

To examine the usefulness of tandem octadecyl capillary-->CZE in the quantitative determination from dilute samples, and to assess the detection limit in terms of concentrations using the tandem format, prometon and prometryne were employed as model solutes. The results are depicted in Fig. 27 by plots of peak height versus sample concentration. As can be seen in Fig. 27, peak height increased linearly with sample concentration in the range studied. The detection limit for both prometon and prometryne were approximately 0.1 µg/mL (*i.e.*, 0.44 and 0.83 micromolar for prometon and prometryne, respectively), which is 10 folds lower than that of normal CZE, under otherwise the same experimental conditions.

Conclusion

With the on-line preconcentration technique, the minimum detectable concentrations were 10-50 fold lower than normally handled by CZE alone with concentration sensitive detectors. The octadecyl preconcentration capillary requires small amount of the sample and permits continuous sample loading, *i.e.*, large sample volume can be introduced and consequently low detection limit in terms of concentration can be obtained. Furthermore, with preconcentration capillaries plots of peak height versus sample concentration are linear over a wide range, which allow the quantitative determination of dilute samples. Moreover, the on-line preconcentration with interactive capillaries involves small amounts of interactants, and requires simple instrumentation that are customarily used in CZE. These features make the on-line preconcentration technique developed in this work potentially useful in the area of analytical chemistry.



Preconcentration capillary: ODS-trifunctional-Cap, etched at 300 °C, 20 cm x 50 μm I.D.; Separation capillary: same as in Fig. 23; Binding electrolyte: 10 mM sodium phosphate, pH 6.0; Debinding electrolyte: 50% (v/v) acetonitrile in binding electrolyte; Sample introduction: hydrodynamic, 5 min; Running voltage: 15 kV; Detection: 220 nm.

Fig. 27 Quantitative Determination of Dilute Sample with Octadecyl Preconcentration Capillaries

CHAPTER V

ON-LINE PRECONCENTRATION OF PROTEINS IN TANDEM METAL CHELATE CAPILLARIES-CAPILLARY ZONE ELECTROPHORESIS

Introduction

In the previous chapter, we introduced octadecyl capillaries for sample preconcentration by hydrophobic interaction. Since this type of interaction is non-selective, the octadecyl capillaries can be used for various species. However, polar and moderately polar compounds can not be retained by octadecyl capillaries. In addition, most often one or two components in a mixture are the analytes of interest, and therefore, a preconcentration step based on selective isolation will be preferred.

The development of life sciences and biotechnologies have engendered the need for new and capable separation methods based on biospecific interactions not only for the determination of the analytes of interest but also for their characterization. Many biological substances and in particular proteins lack in their structures a center for their sensitive detection, which limits their determination at low levels.

To overcome these impediments and to render capillary electrophoresis suitable for the determination of proteins from dilute samples, we introduced metal chelate capillaries, *i.e.*, capillaries having surface-bound metal chelating functions. The preconcentration with metal chelate capillaries is based on the affinity between proteins and the immobilized metal chelates on the capillary walls. Since this type of interaction is selective, only the proteins having affinity for the chelated metal can be retained.

Indeed, with tandem metal chelate capillaries-capillary zone electrophoresis, the selective preconcentration and subsequent separation of dilute protein samples were accomplished.

Principles

In metal chelate capillaries, the metal is immobilized *via* chelating ligands chemically bonded to the capillary wall. Iminodiacetic acid (IDA) was used as the metal chelate stationary phase. Similar to metal interaction chromatography, proteins are retained by the immobilized metal through interaction with electron donor side chain groups situated on the protein surface. These groups are histidine, cysteine, and to a lesser extent tryptophan residues (85). Therefore, metal chelate capillaries would allow selective preconcentration of a protein or a group of proteins having affinity to the metal chelate walls.

As described in the previous chapter, the on-line preconcentration involves two steps, the accumulation followed by the desorption of the solutes, in which binding and debinding electrolytes are used successively. The accumulation of solute on the wall can be described by the adsorption model introduced in chapter IV. Since the accumulated solute on the inner walls should be stripped of the walls and introduced in the separation capillary as a thin plug, the debinding electrolyte should contain a strong competing agent that desorbs the metal and the protein from the binding sites on the surface of the metal chelate capillary. In this regard, EDTA is an excellent candidate since it forms stronger complex with metals than the covalently attached IDA functions on the surface of the capillaries. Thus, the binding electrolytes used in this study were sodium phosphate solutions, whereas the debinding electrolytes were sodium phosphate containing EDTA. Besides that, the concentration of the debinding agent is also very

important to ensure a fast desorption kinetic and minimize band broadening during the process of debinding.

Experimental

Instruments

The instruments used in this study was the same as that described in chapter IV, except that the preconcentration capillaries used in this study were open-tubular metal interaction chromatography capillaries, *i.e.*, fused-silica capillaries of 50 or 75 μm I.D. with immobilized IDA functions on the inner walls. The separation capillaries consisted of fused-silica capillaries of 50 μm I.D. with interlocked polyether coatings prepared in our laboratory as described earlier (10). The hydrophilic coatings were essential to minimize solute-wall interactions during solutes differential migration.

Reagents and Materials

Albumin and iron-free transferrin from human, and carbonic anhydrase from bovine erythrocytes were purchased from Sigma (St. Louis, MO, U.S.A.). γ -Glycidyloxypropyltrimethoxysilane (Z-6040) was a gift from Dow Corning (Midland, MI, U.S.A.). Iminodiacetic acid was donated by Hampshire (Nashua, NH, USA). Reagent grade ethylenediaminetetracetic acid disodium salt (EDTA) was from Fisher Scientific (Pittsburgh, PA, U.S.A.). Deionized water was used to prepare the running electrolyte. All solutions were filtered. Other chemicals and materials used in this study were the same as those described in the previous chapters.

Procedures

Capillary Surface Modification. Similar to the octadecyl capillaries, the inner

surface of the metal chelate preconcentration capillaries were also treated before the bonding of the interactive functions. The procedures for the etching and coating of the capillaries were the same as those described in chapter IV.

To prepare capillaries with surface-bound metal chelating functions, the following procedures were applied: the etched and/or support coated capillary was filled with a solution of γ -glycidoxypolytrimethoxysilane and heated at 100 °C for 30 min. This treatment was repeated twice. Subsequently, the epoxy activated capillaries were allowed to react with a 10% (w/v) solution of iminodiacetic acid at 65 °C in an oven. This treatment was repeated twice. Finally, the capillaries were flushed with water and then stored in HPLC grade methanol.

Figure 28 depicts the idealized structure of the metal chelate capillaries used in this study. The capillary surface was either etched or etched and then coated with colloidal silica. As can be seen in Fig. 28, a hydrophilic coating was introduced in order to shield the modified surface toward proteins and minimize protein adsorption by non specific interactions. Iminodiacetic acid functions (IDA) were covalently attached to this hydrophilic coating to serve as metal chelating ligands. In all the studies, Zn(II) was immobilized on the capillary surface, and the corresponding metal chelate capillary tubes are denoted by Zn(II)-IDA-Cap.

Binding and Debinding Processes. Proteins were dissolved in the binding electrolyte. All the samples were freshly prepared for each set of experiments. The binding and debinding processes were carried out by either electromigration or hydrodynamic flow, *i.e.*, gravity-driven flow, following the same procedures as that described in chapter IV.

Before each run, the capillaries were flushed successively with debinding electrolyte containing 30 mM EDTA, water, 0.2 M ZnCl₂ solution, water again and then

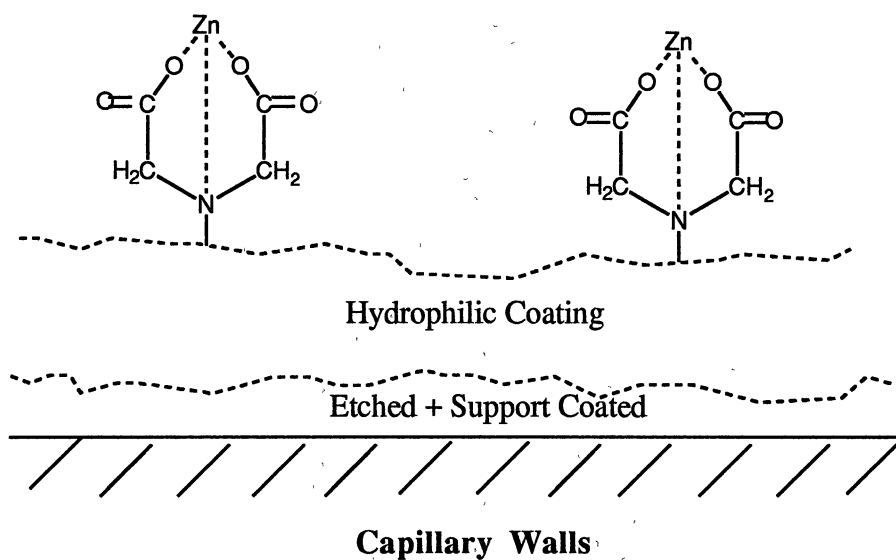


Figure. 28. Schematic Illustration of the Idealized Structure of the Inner Surface of Metal Chelate Preconcentration Capillary

the binding electrolyte. Finally, the capillaries were allowed to equilibrate for 10 to 20 minutes with the binding electrolyte.

Results and Discussion

Human albumin, human transferrin and bovine carbonic anhydrase were selected as model proteins to illustrate the principles of on-line preconcentration using tandem metal chelate capillaries-capillary zone electrophoresis. These proteins are known for their interactions with Zn(II)-IDA sorbents (86, 87)

Electroosmotic Flow

In order to ascertain the influence of the preconcentration capillary and its surface content on the overall electroosmotic flow, the bulk flow through both capillaries was measured with phenol as the inert tracer under various electrolyte compositions and capillary surface content. The results are listed in Table 6.

TABLE 6
ELECTROOSMOTIC FLOW*

Status of Preconcentration Capillary	Electroosmotic flow (nL/min)
Without chelated Zn	68.5
With chelated Zn	54.4
With chelated Zn and adsorbed protein	54.2

* Preconcentration capillary: Zn(II)-IDA, 20 cm x 50 μ m I.D., etched at 300 °C;

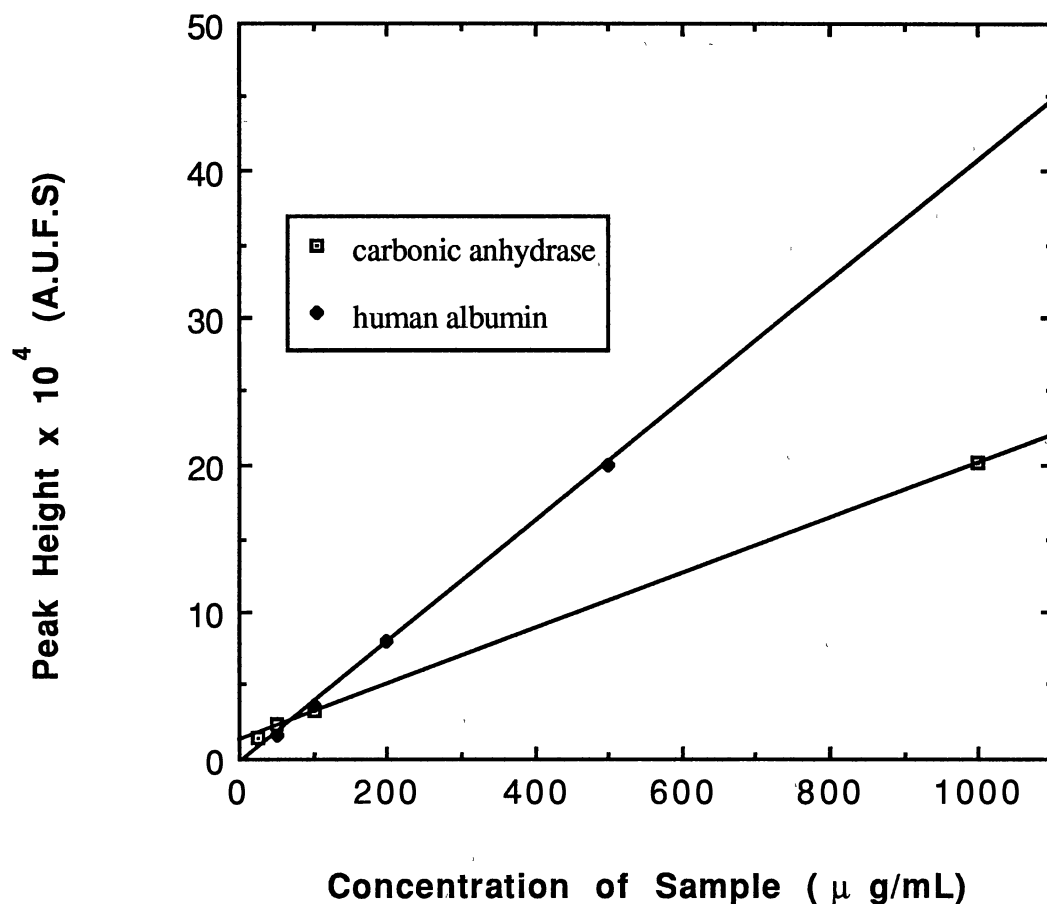
Separation capillary: interlocked polyether 200, 30 cm (to the detection point), 60 cm

(total length) x 50 μm ; Running voltage: 20 kV; Running electrolyte: 10 mM sodium phosphate, pH 6.0; Sample: human albumin 200 $\mu\text{g/mL}$; Sample injection: electromigration, 5 seconds; Detection: 210 nm.

As can be seen in table 5, the electroosmotic flow was higher in the absence than in the presence of the chelated metal on the capillary inner surface. This may be due to the negative zeta potential of the naked iminodiacetic acid capillary at pH 6.0. The decrease in electroosmotic flow in the presence of chelated zinc may be due to the fact that the metal neutralized the negative charge on the surface and therefore decreased the negative zeta potential. On the other hand, the presence of the adsorbed protein on the capillary surface did not change the magnitude of the flow when compared to that in the presence of chelated zinc. This can be explained by the ampholyte nature of the protein at this particular pH. Therefore, since the presence of adsorbed proteins and/or metal at the surface of the capillary resulted in a slight decrease in the overall electroosmotic flow, the elution and stripping of the protein of the capillary walls passing the detection point were readily achieved by electromigration.

Normal Detection Limit

To evaluate the effectiveness of the preconcentration approach under investigation, it was necessary to examine the potential of CZE alone in the analysis of dilute protein samples. Under normal injection conditions, plots of peak height versus sample concentration were linear in the concentration range studied, *i.e.*, for up to 1 mg/mL (see Fig. 29). However, the detection limits in terms of concentrations were 25 and 50 $\mu\text{g/mL}$ for carbonic anhydrase and albumin, respectively. This set of



Separation capillary: interlocked polyether 200, 50 cm (to the detection point), 80 cm (total length) \times 50 μm I.D.; Running electrolytes: 10 mM sodium phosphate for albumin, 100 mM sodium phosphate for carbonic anhydrase, pH 6.0; Running voltage, 20 kV; Sample injection: electromigration, 5 seconds; Detection: 200 nm. The experimental data points are the average of two measurements.

Figure 29 Normal Detection Limit of Albumin and Carbonic Anhydrase

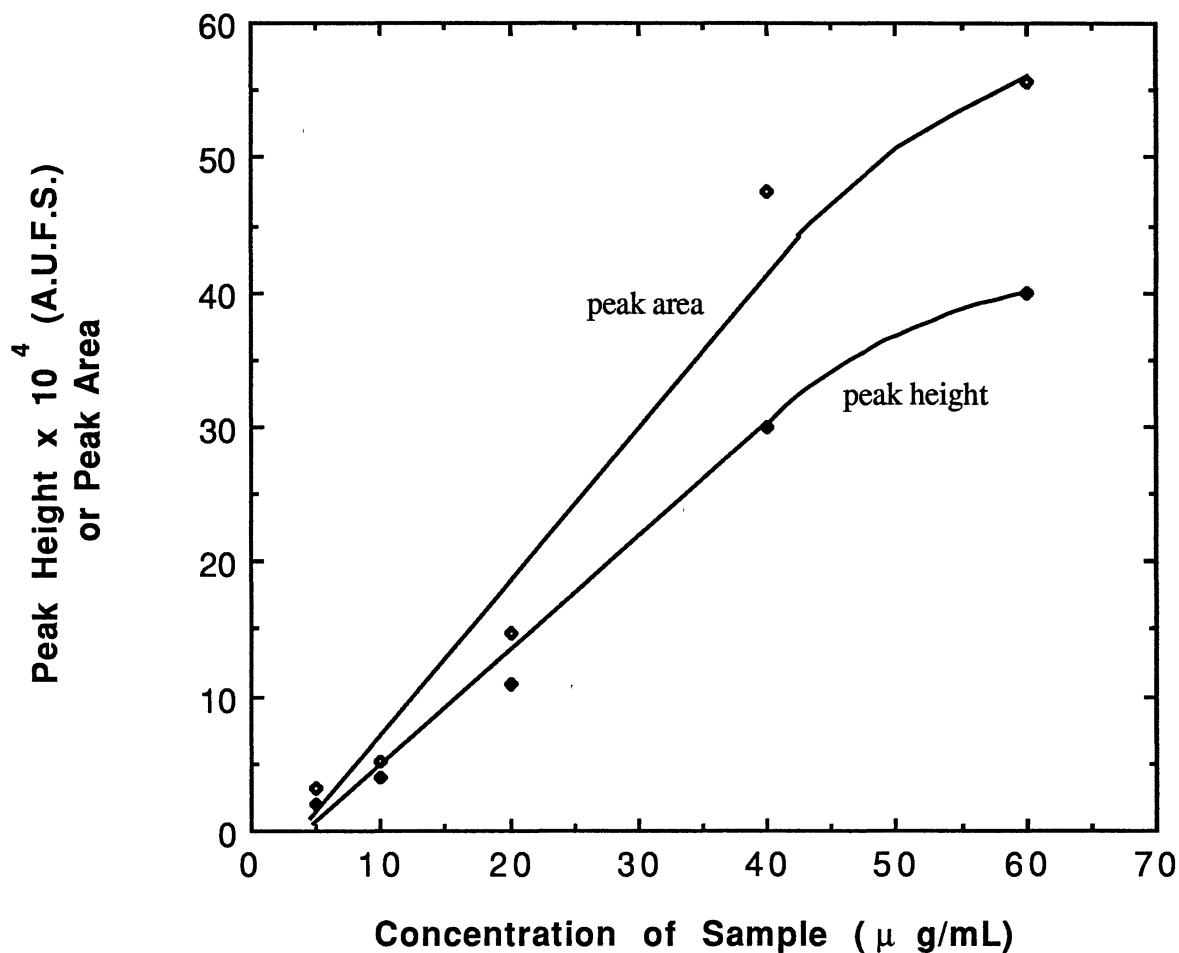
experiments shows that a means for preconcentration is necessary in order to analyze trace amounts of analyte in a given sample.

Quantitative Determination of Dilute Samples with Metal-Chelate Preconcentration Capillaries

To examine the usefulness of tandem Zn(II)-IDA-Cap.-->CZE in the quantitative determination of proteins from dilute samples, and to assess the detection limit in terms of concentrations using the tandem format, human albumin was employed as model solute. The results are depicted in Fig. 30 by plots of peak area and peak height versus sample concentration. As can be seen in Fig. 30, peak area and peak height increased linearly with sample concentration for up to 40-50 $\mu\text{g/mL}$. This concentration range was then used throughout the studies to evaluate the effects of operating parameters using metal chelate preconcentration capillaries. The detection limit for albumin was approximately 0.5 $\mu\text{g/mL}$ (*i.e.*, *ca* 7.0 nanomolar), which is 100 times lower than the detection limit with normal CZE, under otherwise the same detection conditions.

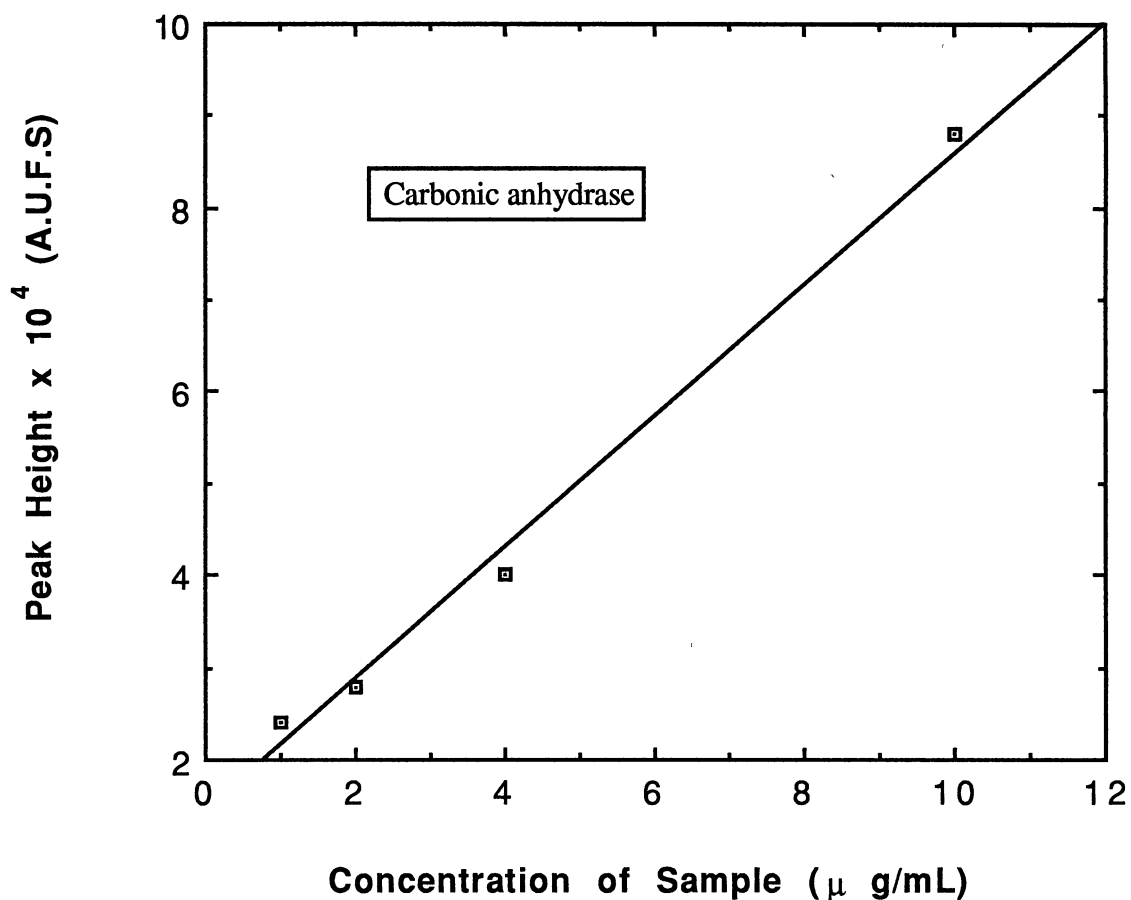
Quantitative determination of dilute samples by CZE with on-line metal chelate preconcentration capillaries can also be applied to other proteins having affinity toward the chelated zinc. Figure 31 shows the results for carbonic anhydrase, and a straight line was obtained over a relatively wide range of concentration. The detection limit was about 1 $\mu\text{g/mL}$. This represents a decrease in the detection limit by a factor of *ca.* 25 when compared to normal injection in CZE.

Figures 32 and 33 portray typical electropherograms for carbonic anhydrase and human albumin, respectively, obtained with tandem Zn(II)-IDA-Cap.-->CZE. Sharp peaks are obtained even though the sample volumes introduced were relatively large, *ca.* 120 nL. It has to be noted that in normal CZE, the maximum sample volume that can be introduced is about 5-10 nL. Above this amount, severe band broadening will result.



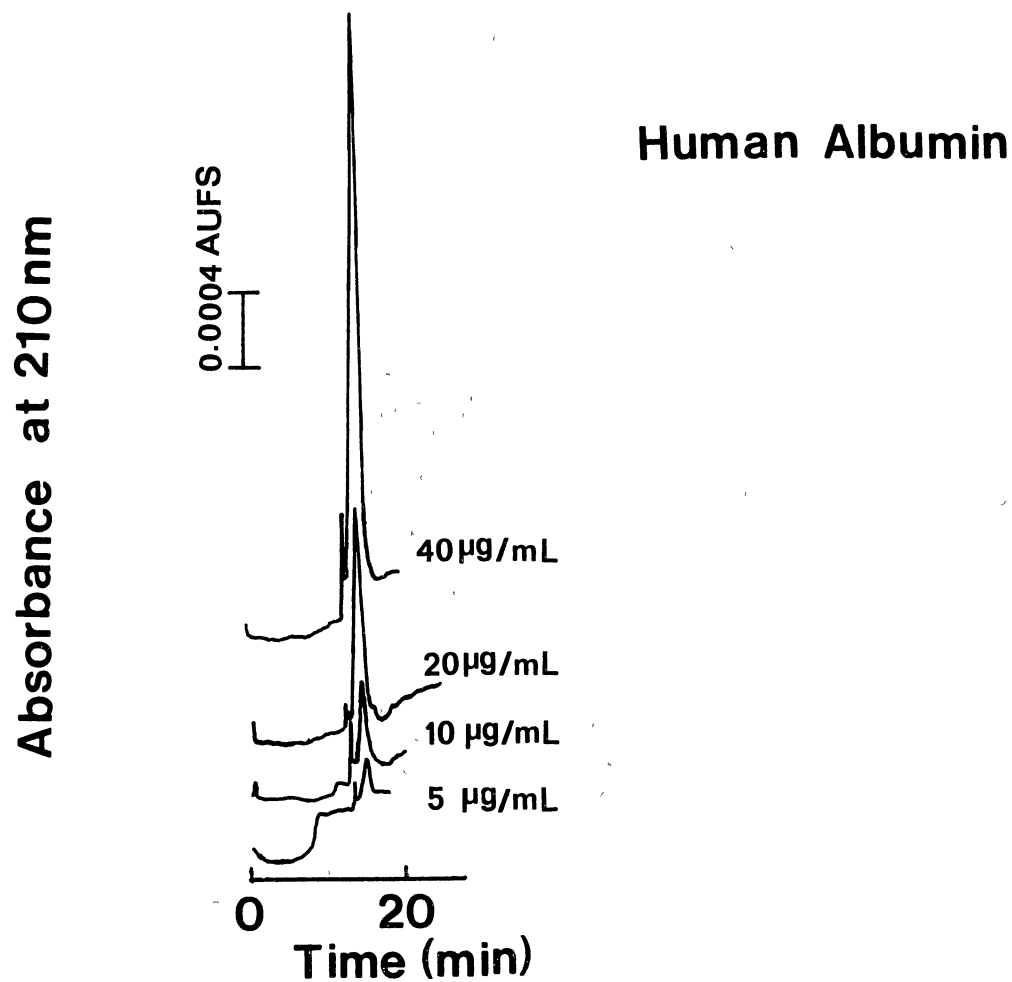
Preconcentration capillary: Zn(II)-IDA, etched at 250 °C, support coated with colloidal silica, 20 cm x 75 μm; Separation capillary: same as in Fig. 29; Binding electrolyte: 10 mM sodium phosphate, pH 6.0; Debinding electrolyte: 10 mM sodium phosphate, 30 mM EDTA, pH 3.8; Sample introduction: electromigration, 5 min; Running voltage 20 kV; Detection: 210 nm.

Figure 30 Preconcentration of Dilute Human Albumin



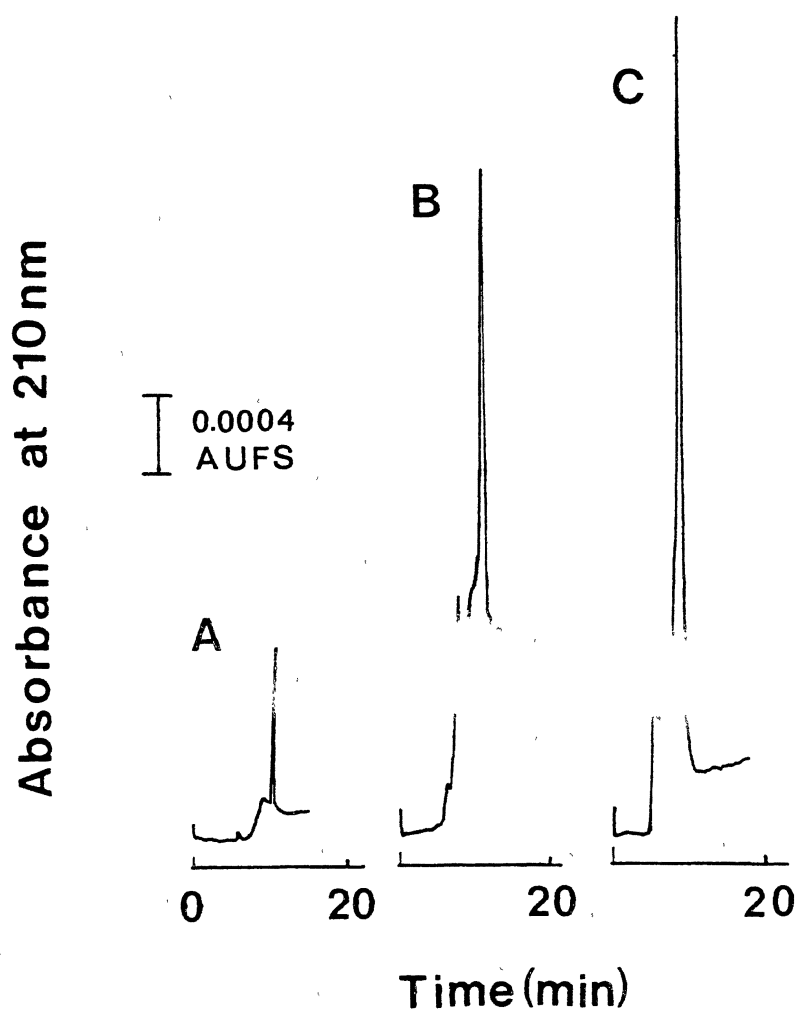
Preconcentration capillary: Zn(II)-IDA, etched at 300 °C, 20 cm x 50 μm I.D.;
 Separation capillary: same as in table 5; Binding electrolyte: 10 mM sodium phosphate,
 pH 6.0; Debinding electrolyte: 100 mM sodium phosphate, 30 mM EDTA, pH 3.8;
 Sample introduction: hydrodynamic, $\Delta h = 18$ cm, 5 min; Running voltage, 20 kV;
 Detection: 200 nm.

Figure 31 Preconcentration of Dilute Carbonic Anhydrase



Experimental conditions are as in Fig. 30.

Figure 32 Typical Electropherograms Illustrating the Preconcentration of Human Albumin with Zn(II)-IDA-Cap-->CZE



Debinding electrolyte: 100 mM phosphate containing 30 mM EDTA, pH 6.0;
 Other experimental conditions are as in Fig. 30; Sample concentration: (A) 10 $\mu\text{g/mL}$,
 (B) 40 $\mu\text{g/mL}$, (C) 100 $\mu\text{g/mL}$.

Figure 33 Typical Electropherograms Illustrating the Preconcentration of Carbonic Anhydrase with Zn(II)-IDA-Cap-->CZE

This illustrates the effectiveness of on-line preconcentration with metal chelate capillaries as far as the separation efficiencies and detection limit are concerned.

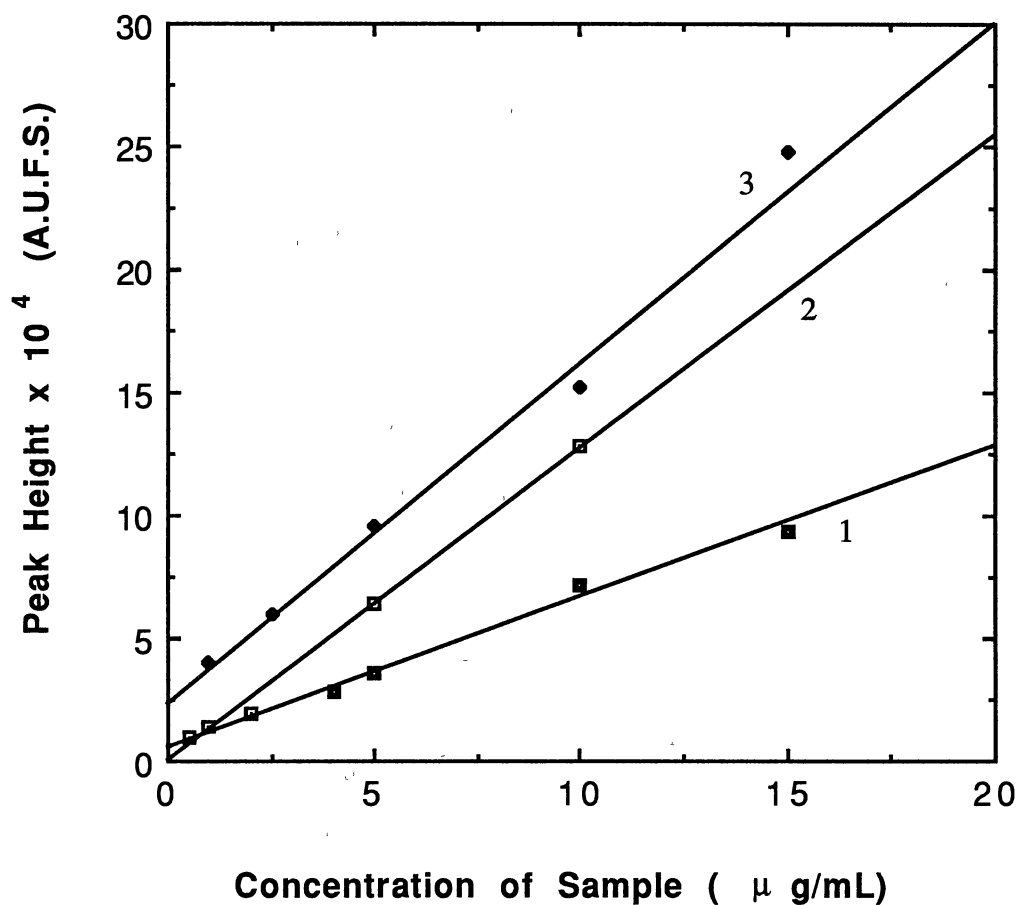
Effects of Operational Parameters

To determine the optimum conditions for on-line preconcentration, the effects of various operational parameters were investigated. These parameters include the capillary design, *i.e.*, capillary inner surface treatment, the composition of the binding and debinding electrolytes, and the mode and duration of sample introduction.

Capillary Design. An important operational parameter in on-line preconcentration with interactive capillary is the design of the preconcentration capillary. The linear capacity of the preconcentration capillary influences the amount of sample that can be accumulated on the inner walls. The higher the linear capacity of the capillary the lower the detection limit is. The linear capacity of the preconcentration capillary increases with increasing the concentration of metal chelating ligands attached to the capillary surface.

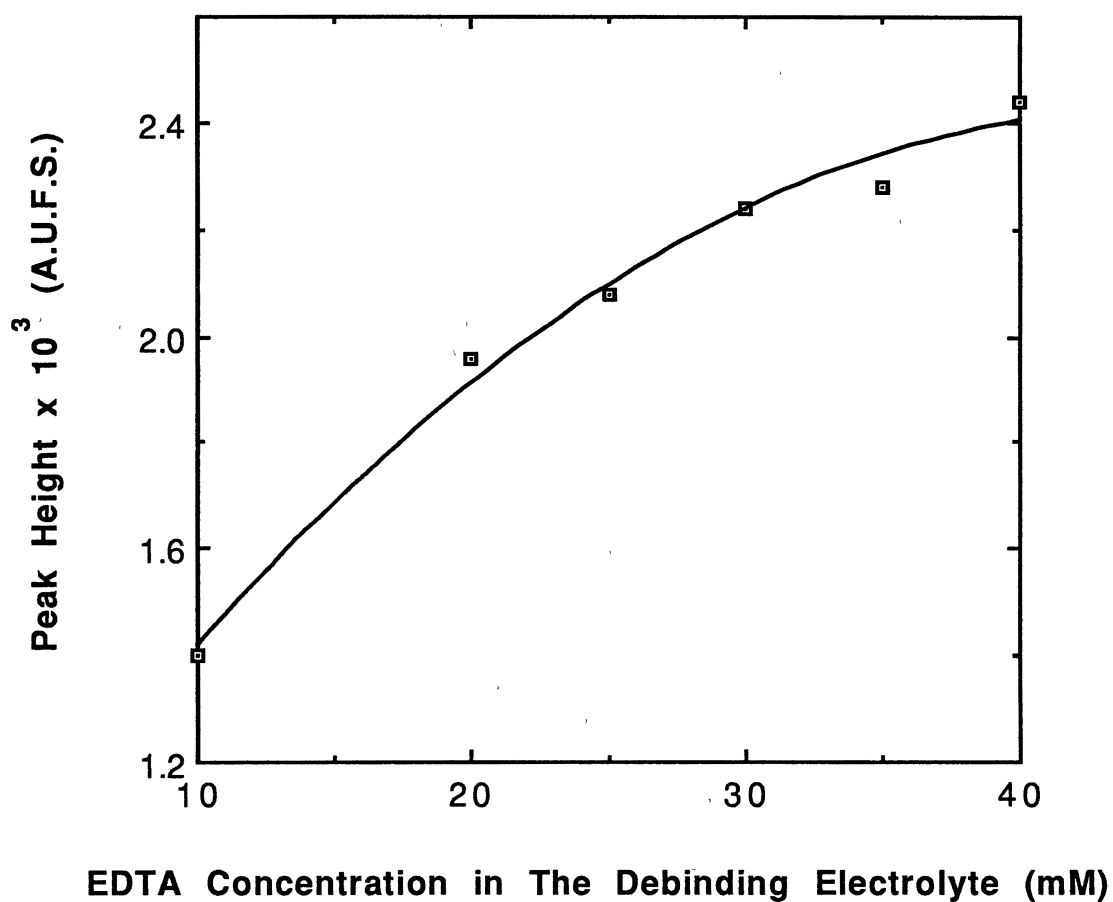
The inner surface of the preconcentration capillaries was increased by chemical and/or physical treatments before the metal chelating functions were attached. The surface roughening is described in the experimental section. The results are depicted in Fig. 34 in terms of peak height versus sample concentration. As can be seen in Fig. 34, the best results were obtained with the capillary that is etched at 300 °C and coated with colloidal silica. This means that it has the highest surface coverage with metal chelating functions.

Concentration of Debinding Agent. As mentioned earlier, the choice and the concentration of the debinding agent is very important in the preconcentration process. The graph in Fig. 35 shows that the detector signal increases with the concentration of



Preconcentration capillary: Zn(II)-IDA, etched and/or coated with colloidal silica, 20 cm x 50 μm I.D.; (1) etched at 250 °C; (2) etched at 300 °C, (3) etched at 300 °C and support coated with colloidal silica; Sample introduction: hydrodynamic, 5 min, Δh = 18 cm; Detection: 200 nm; Other experimental conditions are as in Fig. 30.

Figure 34 Effect of Capillary Design on the Effectiveness of On-line Preconcentration with Zn(II)-IDA-Cap-->CZE



Debinding electrolyte: 10 mM sodium phosphate containing different concentration of EDTA, pH 3.8; Sample: 30 $\mu\text{g/mL}$ albumin; Other experimental conditions are as in Fig. 30.

Figure 35 Effect of the Concentration of the Competing Agent in the Debinding Electrolyte

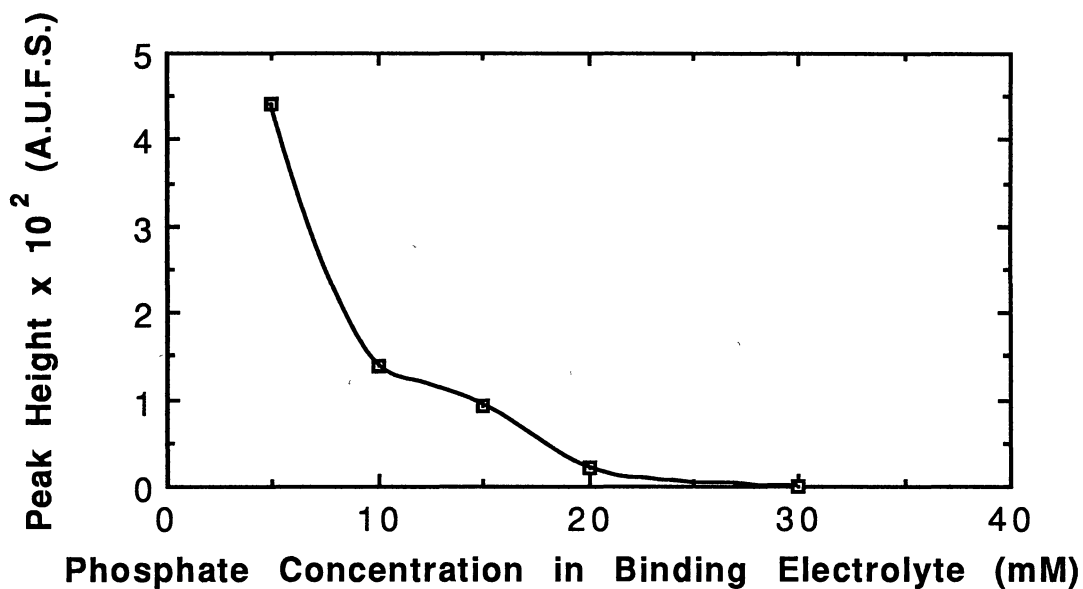
EDTA in the debinding electrolyte. An optimum concentration for the debinding process is about 30 mM, whereby the current is still in the range that does not lead to system overheating. At this optimum concentration of EDTA, a good recovery of the sample is achieved and fast desorption is obtained.

Ionic Strength of the Electrolyte. The effect of the ionic strength of the binding and debinding electrolytes was also investigated and the results are shown in Fig. 36 and table 7.

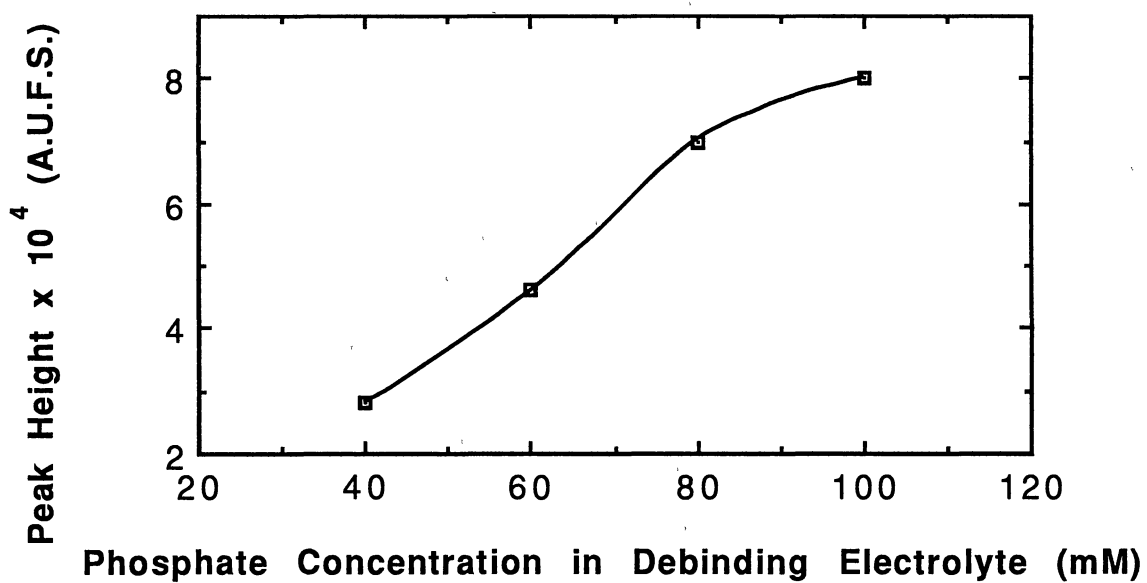
TABLE 7
EFFECT OF IONIC STRENGTH IN THE DEBINDING ELECTROLYTE*

Phosphate Concentration (mM)	Peak Height x 10 ³ (A.U.F.S.)
10	2.46
20	2.60
40	2.72
100	2.40

* Preconcentration capillary: Zn(II)-IDA, etched at 250 °C, 20 cm x 50 µm I.D.; Binding electrolyte: 10 mM sodium phosphate, pH 6.0; Debinding electrolyte: 30 mM EDTA containing different concentration of sodium phosphate, pH 6.0; Sample: 25 µg/mL albumin; Sample introduction: hydrodynamic, 5 min, $\Delta h = 18$ cm; Running voltage: 20 kV; Detection: 210 nm. The experimental data are the average of two measurements.



(a)



(b)

(a) Sample: 25 $\mu\text{g/mL}$ albumin; Other experimental conditions are as in Fig. 30.

(b) Preconcentration capillary: etched at 300 $^{\circ}\text{C}$, 20 cm x 50 μm I.D; Sample: 20 $\mu\text{g/mL}$ albumin; Other experimental conditions are as in Fig. 34.

Figure 36 Effect of Ionic Strength in Binding (a) and Debinding (b) Electrolytes

It can be seen in Fig. 36a that increasing the concentration of phosphate in the binding electrolyte decreases the peak height. When the concentration reaches 30 mM, the peak height drops to almost zero. This may reflect that phosphate behaves as a competing agent with the protein for the binding sites on the surface of the preconcentration capillary. As expected, without the debinding agent, *i.e.*, EDTA, increasing the ionic strength of the debinding electrolyte resulted in an increase in the peak height, as shown in Fig. 36b.

It seems that phosphate can also be used as debinding agent. However, as far as the efficiency and the peak height are concerned, phosphate were not as good as EDTA in terms of the protein recovery from the surface and the desorption kinetics. If phosphate salt is used as debinding agent, high concentration is necessary in order to strip the accumulated proteins of the capillary wall as a narrow plug. But high ionic strength is undesirable in CZE, because excessive Joule heating will be generated which will cause band broadening.

On the other hand, with constant concentration of EDTA (30 mM), the concentration of phosphate concentration in the debinding electrolyte did not affect the peak height within the concentration range studied, as shown in table 7. This is manifested by the drop in peak height when phosphate concentration increased from 40 mM to 100 mM, see Fig. 7. Increasing the phosphate concentration in the EDTA solution from 40 to 100 mM resulted in a significant drop in peak height, probably due to band broadening arising from excessive Joule heating at this high ionic strength. EDTA solutions containing low salt concentration are effective in bringing about complete desorption of the accumulated analyte from the inner walls.

pH of the Debinding Electrolyte. The effect of pH of the debinding electrolyte was studied and the results are listed in table 8. As shown in table 8, the peak height is constant in the pH range investigated. This is because EDTA was the major factor that

led to the desorption of the accumulated solutes from the preconcentration capillary inner surface.

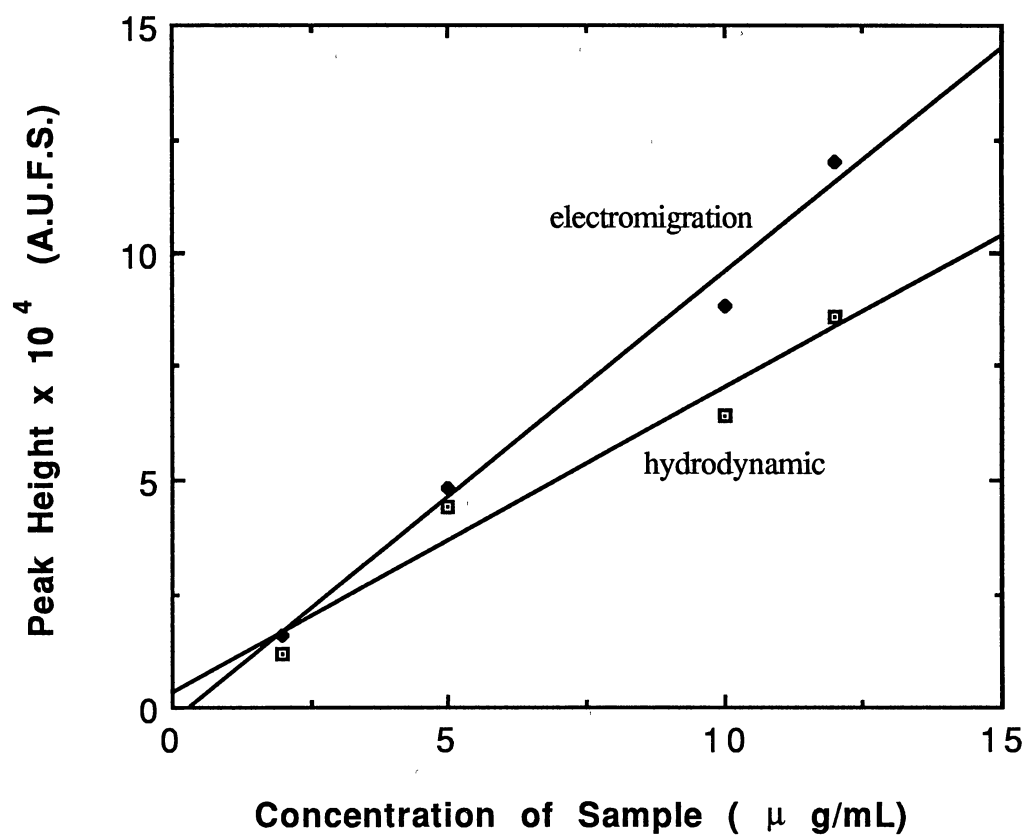
TABLE 8
EFFECT OF PH OF THE DEBINDING ELECTROLYTE*

pH	Peak Height x 10 ³ (A.U.F.S.)
3.3	1.72
3.8	1.88
5.0	1.88
6.0	1.76
7.0	1.88

* Debinding electrolyte: 10 mM sodium phosphate, 30 mM EDTA, at different pH;
Sample: 25 µg/mL albumin; Other experimental conditions same as in Fig. 30.

Mode of Sample Introduction. Dilute samples can be introduced by either hydrodynamic flow or eletromigration. The graph in Fig. 37 shows that both injection modes resulted in linear relationship between the peak height and the concentration of the sample. So either of them can be used in quantitative analysis of dilute protein samples.

The sample volumes introduced in this study are listed in table 9. The experimental data were determined by Eqn 27. The calculated value for hydrodynamic



Preconcentration capillary: etched at 300 °C, 20 cm x 50 μm I.D.; Sample introduction: same as in Fig. 31 for hydrodynamic, and same as in Fig 30 for electromigration; Other experimental conditions are as in Fig. 30.

Figure 37 Comparison of Sample Introduction by Hydrodynamic and Electromigration Modes

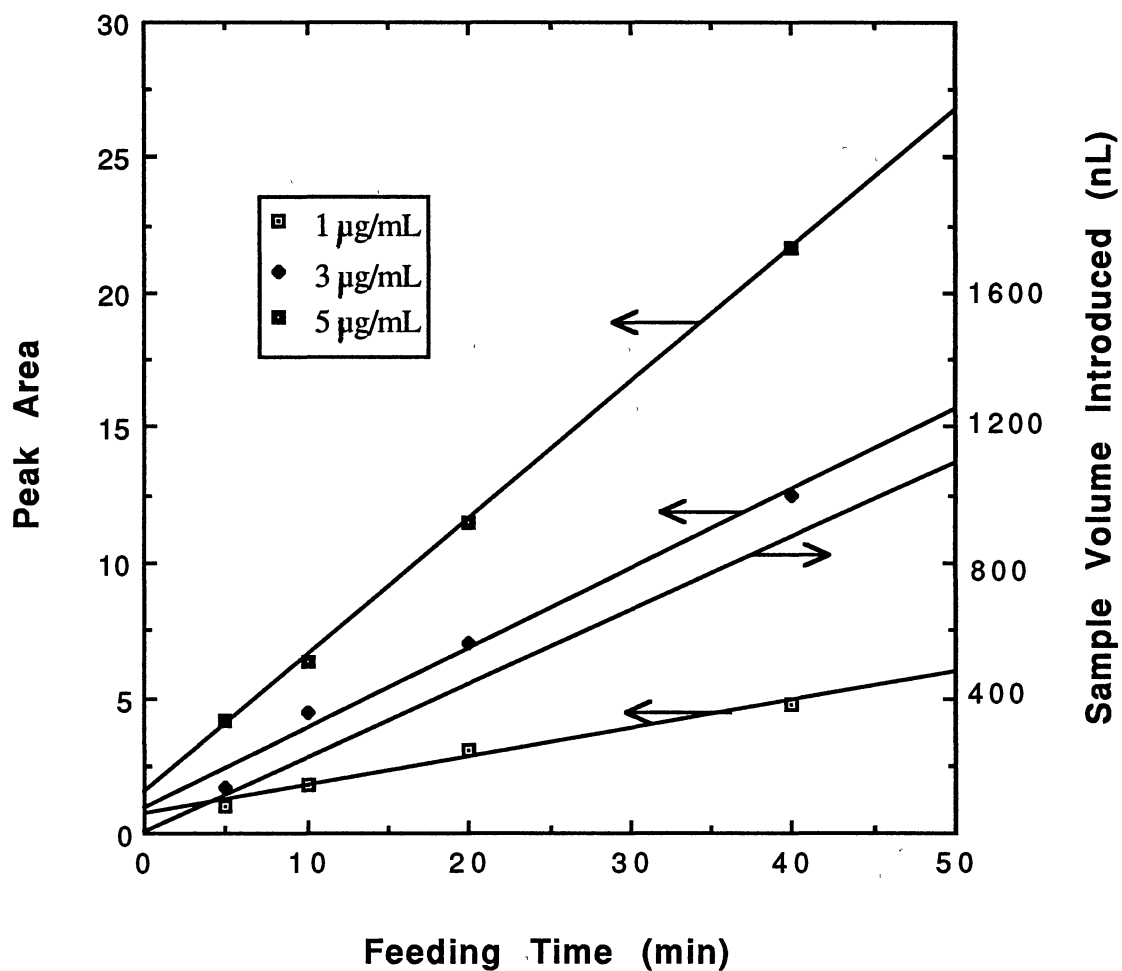
sample introduction was obtained using Poiseuille equation (Eqn 25). Since the ionic strength of the electrolyte was relatively low, η and ρ were taken as those of plain water at 25 °C. Because the volume introduced by electromigration is greater than that by hydrodynamic flow, the signal obtained in the first mode was higher than that obtained by the second mode.

TABLE 9
SAMPLE VOLUME INTRODUCED BY ELECTROMIGRATION
AND HYDRODYNAMIC FLOW*

Mode of sample introduction	Volume introduced (nL)	
	Experimental	Calculated
Hydrodynamic	110	98
Electromigration	121	---

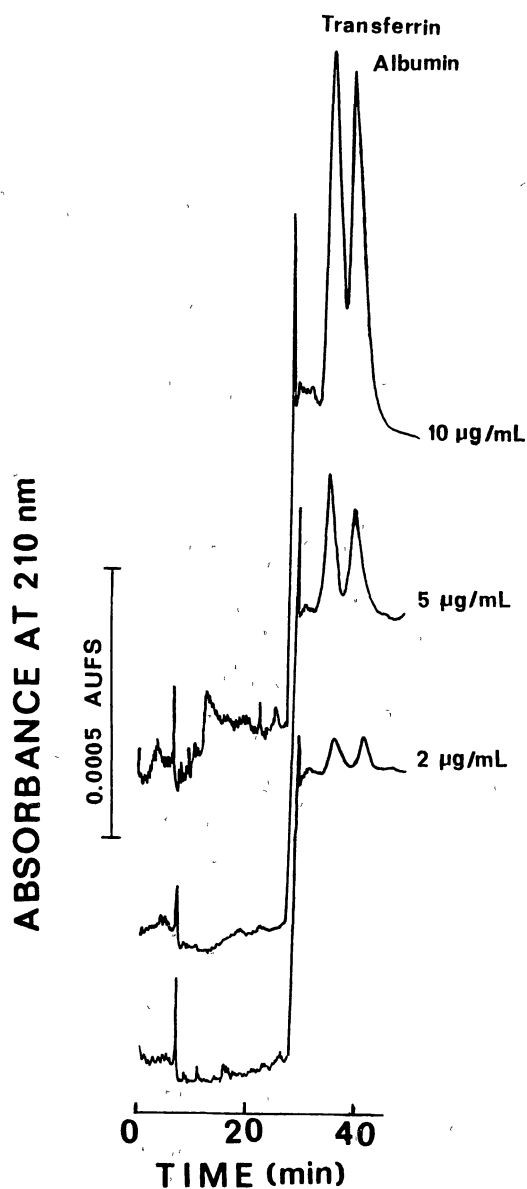
* Experimental conditions are as in Fig. 37.

Feeding time. The duration of sample introduction determines the volume introduced and consequently influence the amount accumulated on the walls from a given solution. The result of this study is shown in Fig. 38. The sample volume introduced as a function of time is also shown. In all cases the linear capacity of the capillary was not exceeded, and more accumulation on the wall can be expected. For samples of low concentration the amount accumulated increased slightly than with high concentrations as the time increased. This is expected since adsorption from dilute



Sample introduction: hydrodynamic, $\Delta h = 18$ cm; Other experimental conditions are as in Fig. 30.

Figure 38 Effect of Feeding Time on the Amount of Solute Accumulated



Preconcentration capillary: Zn(II)-IDA, etched at 300 °C, 20 cm x 50 µm I.D.;
 Separation capillary: as in Fig 2. Binding electrolyte: 10 mM phosphate, pH 6.0;
 Debinding electrolyte: 10 mM phosphate, 30 mM EDTA, pH 6.0; Sample introduction:
 hydrodynamic, 5 min, $\Delta h = 18$ cm; Detection: 210 nm.

Figure 39. Preconcentration and Subsequent Separation with
 Tandem Zn(II)-IDA Cap--> CZE

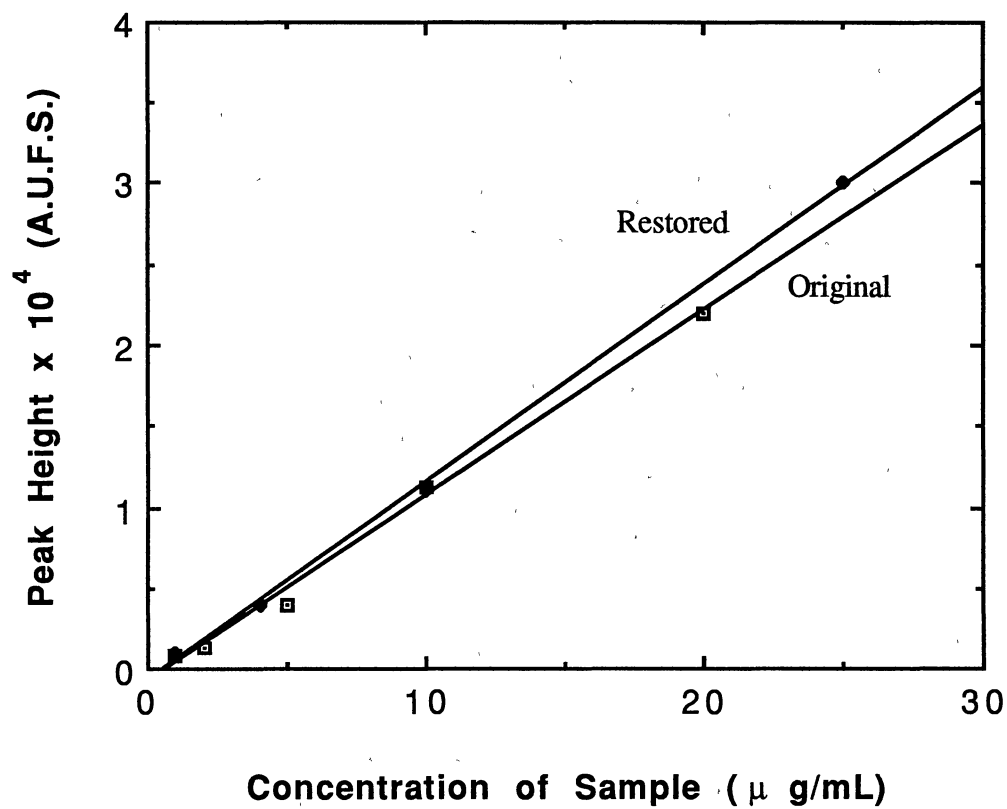
solution occurs at a slower rate than with relatively concentrated sample; a diffusion controlled process.

Preconcentration and Separation of Proteins

Metal chelate capillary has the virtue of allowing the selective concentration of a protein or a group of proteins from dilute samples. Indeed, metal chelate sorbents exhibit affinity toward proteins having electron donor groups on their surfaces. Figure 39 shows the preconcentration of two zinc binding proteins, albumin and carbonic anhydrase, and subsequent separation at different concentration of both analytes. It is seen that both proteins can be concentrated and separated with relatively short time. Although large sample volume was introduced, the peaks are relatively narrow. The preconcentration of a group of proteins is accompanied by a competing process during which the protein that has the strongest affinity to the chelated metal will accumulate to a greater extent. Therefore, it is also possible to accumulate preferentially a given protein from a mixture containing other proteins.

Restoration of Capillary Coating

Although, preconcentration capillaries can perform constantly for few days, after prolonged use the capillary will lose some of its interactive coatings by hydrolytic degradation, and consequently its capacity for preconcentration will decrease. These capillaries can be restored by first removing the remained coating from the walls and then recoating of the surface as previously described (10). As can be seen in Fig. 40, the performance of the capillary can be restored to its original state by this procedure. This is another advantage of the preconcentration capillaries.



Preconcentration capillary: Zn(II)-IDA, etched at 300 °C, 20 cm x 50 μm I.D.;
Detection: 200 nm; Other experimental conditions are as in Fig. 30.

Figure 40. Restoration of Capillaries After Prolonged Use

Conclusions

The on-line preconcentration method described here with capillary having metallic walls offers a means by which dilute sample of proteins can be analyzed by CZE. The metal chelate capillaries were very effective in the selective accumulation of detectable amounts of proteins from dilute samples. The coupled format , Zn(II)-IDA-Cap.--> CZE, permitted the detection of 50 to 100 folds less concentrated sample than by CZE alone with concentration sensitive detectors. It also allowed simultaneous preconcentration and separation.

As a means for on-line preconcentration, the metal chelate capillaries have many advantages, such as small sample requirement, continuous sample loading and the ability for quantitative analysis from dilute samples. The capillaries can be reused, since the restoration of a deteriorated metallic tube can be easily and reproducibly performed and do not involve an extensive labor.

BIBLIOGRAPHY

1. Hjerten, S. *Chromatogr. Rev.* **1967**, *9*, 122.
2. Virtanen, R. *Acta Polytech. Scand.* **1974**, *1*, 123.
3. Mikkers, F.; Everaerts, F.; Verheggen, T. *J. Chromatogr.* **1979**, *11*, 169.
4. Jorgenson, J.; Lukacs, K. *Anal. Chem.* **1981**, *53*, 1298.
5. Jorgenson, J.; Lukacs, K. *Science* **1983**, *222*, 266.
6. Hjerten, S. *J. Chromatogr.* **1983**, *270*, 1.
7. Tsuda, T.; Nomura, K.; Nakagawa, G. *J. Chromatogr.* **1982**, *248*, 241.
8. Lauer, H.; McManigill, D. *Trends Anal. Chem.* **1986**, *5*, 11.
9. Hjerten, S.; Zhu, M.; *J. Chromatogr.* **1985**, *327*, 157.
10. W. Nashabeh and Z. El Rassi, *J. Chromatogr.*, in press.
11. W. Nashabeh and Z. El Rassi, *J. Chromatogr.*, **1990**, *57*, 514.
12. W. Nashabeh and Z. El Rassi, *J. Chromatogr.*, **1991**, *31*, 536.
13. Terabe, S.; Otsuka, K.; Ichikama, K.; Tsuchiya, A.; Ando, T. *Anal. Chem.* **1984**, *56*, 111.
14. Terabe, S.; Utsumi, H.; Otsuka, T.; Ando, T.; Inomata, T.; Kuze, S.; Hanaoka, Y. *J. High Res. Chromatogr.* **1986**, *9*, 666.
15. Hjerten, S.; Liao, J.; Yao, K. *J. Chromatogr.* **1987**, *387*, 127.
16. Everaerts, F.; Beckers, J.; Verheggen, T. *Isotachophoresis: Theory, Instrumentation and Applications*; Elsevier: Amsterdam, 1976.
17. Guttman, A.; Paulus, A.; Cohen, A.; Grinberg, N.; Karger, B. *J. Chromatogr.* **1988**, *448*, 41.
18. Cohen, A.; Nagarian, D.; Paulus, A.; Gurrman, A.; Smith, J.; Karger, B. *Proc. Natl. Acad. Sci., U.S.A.* **1988**, *85*, 9660.
19. Cohen, A.; Karger, B. *J. Chromatogr.* **1987**, *397*, 409.
20. Wallingford, R.; Ewing, A. *Anal. Chem.* **1988**, *60*, 1972.

21. Rose, D.; Jorgenson, J. *J. Chromatogr.* **1988**, 438, 23.
22. Roach, M.; Gozel, P.; Zare, R. *J. Chromatogr.* **1988**, 426, 129.
23. Pentoney, S.; Zare, R.; Quint, J. *Anal. Chem.* **1989**, 61, 1642.
24. Olivares, J.; Nguyen, N.; Yonker, C.; Smith, R. *Anal. Chem.* **1987**, 59, 1230.
25. Cohen, A.; Paulus, A.; Karger, B. *Chromatographia* **1987**, 24, 14.
26. Nickerson, B.; Jorgenson, J. *J. High Res. Chromatogr. Chromatogr. Comm.* **1988**, 11, 533.
27. Yeung, E. *Acc. Chem. Res.* **1989**, 22(4), 125.
28. Hjerten, S.; Zhu, M. *J. Chromatogr.*, **1985**, 346, 265.
29. Kilar, F.; Hjerten, S. *Electrophoresis* **1989**, 10, 23.
30. Lauer, H.; McManigill, D. *Anal. Chem.* **1986**, 58, 166.
31. McCormick, R. *Anal. Chem.* **1988**, 60, 2322.
32. Grassman, P.; Wilson, K.; Petrie, G.; Lauer, H. *Anal. Biochem.* **1988**, 173, 265.
33. Ludi, H.; Gassmann, E.; Grossenbacher, H.; Marki, W. *Anal. Chim. Acta* **1988**, 213, 215.
34. Walbroehl, Y.; Jorgenson, J. *J. Microcol. Sep.* **1989**, 1, 41.
35. Green, J.; Jorgenson, J. *J. Chromatogr.* **1989**, 478, 63.
36. Hjerten, S. *J. Chromatogr.* **1985**, 347, 191.
37. Cobb, K.; Dolnik, V.; Novotry, M. *Anal. Chem.* **1990**, 62, 2478.
38. Lee, E.; Muck, W.; Henion, J.; Covey, T. *J. Chromatogr.* **1988**, 458, 313.
39. Andrew, A. *Electrophoresis: Theory, Techniques, and Biochemical and Clinical Applications*; Clarendon Press: Oxford, U. K., 1981; Chapters 4 and 5.
40. Terabe, S.; Otsuka, K.; Ando, T. *Anal. Chem.* **1985**, 57, 834.
41. Burton, D.; Sepaniak, M.; Maskarinec, M. *J. Chromatogr. Sci.* **1987**, 25, 514.
42. Terabe, S.; Otsuka, K.; Ando, T. *Anal. Chem.* **1985**, 57, 834.
43. Gassmann, E.; Kou, J.; Zare, R. *Science* **1985**, 230, 813.
44. Nishi, H.; et al. *J. Chromatogr.* **1989**, 477, 259.
45. Otsuka, K.; Terabe, S.; Ando, T. *J. Chromatogr.* **1985**, 332, 219.

46. Burton, D.; Sepaniak, M.; Maskarinec, M. *J. Chromatogr. Sci.* **1986**, *24*, 347.
47. Tsuda, T. *J. High Res. Chromatogr., Chrom. Commun.* **1987**, *10*, 622.
48. Terabe, S.; Ozaki, H.; Otsuka, K.; Ando, T. *J. Chromatogr.* **1985**, *332*, 211.
49. Burton, D.; Sepaniak, M.; Maskarinec, M. *Chromatographia* **1986**, *21*, 583.
50. Gozel, P.; GAssmann, E.; Michelsen, H.; Zare, R. *Anal. Chem.* **1987**, *59*, 44.
51. Tran, A.; Blanc, T.; Leopold, E. *J. Chromatogr.* **1990**, *516*, 241.
52. Nishi, H.; Fukayamn, T.; Matsuo, M.; Terabe, S. *J. Microcol. Sep.* **1989**, *1*, 234.
53. Dobasi, A.; Ono, T.; Harn, S. *Anal. Chem.* **1989**, *61*, 1984.
54. Fanali, S. *J. Chromatogr.* **1989**, *474*, 441.
55. Cohen, A.; Terabe, S.; Smith, J.; Karger, B. *Anal. Chem.* **1987**, *59*, 1021.
56. Dolnik, V.; Liu, J.; Banks, J.; Novotny, M.; Bocek, P. *J. Chromatogr.* **1989**, *480*, 321.
57. Terabe, S.; Isemura, T. *Anal. Chem.* **1990**, *62*, 650.
58. Terabe, S. *Trends Anal. Chem.* **1989**, *8*, 129.
59. Adamson, A. *Physical Chemistry of Surfaces, 2nd ed.*; Interscience: New York, 1967, Chapter 4.
60. Martin, M.; Guiochon, G.; Walbroehl, Y.; Jorgenson, J. *Anal. Chem.* **1985**, *57*, 559.
61. Hiemenz, P. *Principles of Colloid and Surface Chemistry*; Dekker: New York, 1977, Chapter 11.
62. Karger, B.; Cohen, A.; Guttman, A. *J. Chromatogr.* **1989**, *492*, 585.
63. Giddings, J. C. *Separ. Sci.* **1969**, *4*, 181.
64. Giddings, J. C. *Anal. Chem.* **1967**, *39*, 1027.
65. O'Brrien, M.; Prendeville, G. *Weed Research* **1978**, *18*, 301.
66. Vacik, J. in Deyl, Z. Ed. *Electrophoresis, Part A*; Elsevier: Amsterdam, NY. 1979, page 3.
67. Block, R.; Durrum, E.; Zweig, G. *A manual of Paper Chromatography and Paper Electrophoresis*; Academic Press: NY, 1955, page 340.
68. Laubereau, P. in Bjorseth, A.; Angeletti, G. Eds. *Organic Micropollutants in the*

Aquatic Environment; D. Reidel Publishing Company: Dordrecht, Holland, 1986, page 40.

69. Martell, A.; Smith, R. *Critical Stability Constants, Vol. 2*; Plenum Press: New York, NY, 1975.
70. Balchunas, A.; Sepaniak, M. *Anal. Chem.* **1987**, *59*, 1466.
71. Gorse, J.; Balchunas, A.; Swaile, D.; Sepaniak, M. *J. High Res. Chromatogr. Chromatogr. Comm.* **1988**, *11*, 554.
72. Terabe, S.; Utsumi, H.; Otsuka, K.; Ando, T.; Inomata, T.; Kuze, S.; Hanaoka, Y. *J. High Res. Chromatogr.* **1986**, *9*, 667.
73. Lux, J.; Yin, H.; Schomburg, G. *J. High Res. Chromatogr.* **1990**, *13*, 145.
74. Balchunas, A.; Swaile, D.; Powell, A.; Sepaniak, M. *Sep. Sci. Technol.* **1988**, *23*, 1891.
75. Hjelmeland, L.; Crambuch, A. *Meth. Enzymol.* **1984**, *104*, 305.
76. Terabe, S.; Otsuda, K.; Ando, T. *Anal. Chem.* **1989**, *61*, 251.
77. Sepaniak, M.; Cole, R. *Anal. Chem.* **1987**, *59*, 472.
78. Foret, F.; Sustacek, V.; Bocek, P. *J. Microcol. Sep.* **1990**, *2*, 229.
79. Aebersold, R.; Morrison, H. *J. Chromatogr.* **1990**, *516*, 79.
80. Dolnik, V.; Cobb, K.; Novotny, M. *J. Microcol. Sep.* **1990**, *2*, 127.
81. Karger, B.; Snyder, L.; Horvath, C. *An Introduction to Separation Science*; John Wiley & Sons: New York, 1973, chapter 2.
82. Lee, M.; Wright, B. *J. Chromatogr.* **1980**, *184*, 235.
83. Liang, D.; Readey, D. *J. Am. Ceram. Soc.*, **1987**, *70*, 570.
84. Nahum, A.; Horvath, C. *J. Chromatogr.* **1981**, *203*, 53.
85. Porath, J.; Garlsson, J.; Osson, I.; Belfrage, G. *Nature*, **1975**, *258*, 598.
86. Hasson, H.; Kagedal, L. *J. Chromatogr.* **1981**, *215*, 333.
87. Kato, Y.; Nakamura, K.; Hashimoto, T. *J. Chromatogr.* **1986**, *354*, 511.

VITA

Jianyi Cai

Candidate for the Degree of

Master of Science

Thesis: ON-LINE PRECONCENTRATION TECHNIQUES FOR CAPILLARY ELECTROPHORESIS OF DILUTE SAMPLES. FUNDAMENTAL AND PRACTICAL STUDIES WITH PROTEINS AND ENVIRONMENTAL POLLUTANTS

Major Field: Chemistry

Biographical:

Personal Data: Born in Shanghai, China, November 14, 1963.

Education: Received Bachelor of Science Degree in Physics from East China Institute of Chemical Technology in July, 1985; completed requirements for the Master of Science degree at Oklahoma State University in December, 1991.

Professional Experience: August, 1989 to present, graduate research and teaching assistant, Oklahoma State University. August, 1985 to July, 1989, research associate, Shanghai Institute of Ceramics, Chinese Academy of Sciences.